AN INCREMENTAL, NON-LINEAR DISPLACEMENT METHOD FOR THE ELASTIC ANALYSIS OF SPACE TRUSSES AND PLANE FRAMES

by

C.T. DITTMER

A thesis submitted in partial fulfilment
of the requirements for the degree
Master of Science in Engineering.

Department of Civil Engineering,
UNIVERSITY OF CAPE TOWN.

April 1975

DECLARATION OF CANDIDATE

I, Colin Dittmer, hereby declare that this thesis is my own work and that it has not been submitted for a degree at another university.

Signed by candidate

April 1975.

CONTENTS

SYNOPSIS

An incremental displacement method which takes account of finite deflections is developed for the elastic non-linear analysis of space trusses. In the incremental loading procedure the elastic critical load of a structure is determined by establishing the load at which the determinant of the stiffness matrix passes through zero. Chord shortening due to bowing of truss compression members which have an initial imperfection in straightness is included in the analysis by modifying the member axial stiffness term. Numerical examples of truss analyses are presented and comparisons made with published results. An incremental non-linear displacement method is then developed for plane frame analysis taking account of finite deflections and the effect of axial force on flexural stiffness, but ignoring member chord shortening due to flexure. Numerical examples of plane frame analyses are presented and comparisons made with published results.

ACKNOWLEDGEMENTS

The writer wishes to thank Professor J.B. Martin, who suggested the topic of this thesis, for his interest and guidance throughout the whole project, and in particular for his constructive remarks on the manuscript.

The writer is indebted to the Council for Scientific and Industrial Research for financial assistance during the project.

Thanks are also due to Bridget Spalding for an excellently typed manuscript, to Kevin Martin for annotating the diagrams, and to Charlie Basson for reproducing copies of this thesis.

LIST OF SYMBOLS

SPECIAL SYMBOLS

$\{\ \}$	a column vector
$\underline{T}$	the vector T
$[\ ]$	a matrix
t	superscript, the transpose of a matrix.

LOWER CASE CHARACTERS

a_o	departure from straightness at midlength point of imperfect truss member
d	increment in associated quantity after deformation from the i^{th} to the $(i+1)^{th}$ position
k	element of member stiffness matrix
l	length of member
n	integer
x, y, z	global axes.

UPPER CASE CHARACTERS

A	cross-sectional area
A, B	ends of member AB
C_i	$\underline{T}_i^t \underline{\delta} = \underline{\delta}^t \underline{T}_i$, a scalar
E	Young's modulus
G_i	$\underline{R}_i^t \underline{\delta} = \underline{\delta}^t \underline{R}_i$, a scalar
I	moment of inertia
K'	EA/L_o^2
L'	arc length of bowed member
M	moment
M'	$M_A + M_B$
N	axial force
N_c	Euler load
$\bar{N}$	N/N_c

S	flexural stiffness
V	shear force.

GREEK CHARACTERS

α, β, γ	angles between member chord and global axes x, y, z respectively
Δ	shortening of member chord due to bowing
ΔL_i	increase in member chord length after deformation from the i^{th} to the $(i+1)^{th}$ position
ϵ	axial strain
ϵ'	$L' - 1$
θ	angle between initial chord and tangent to elastic line
θ'	angle between current chord and tangent to elastic line.

MATRICES AND VECTORS

$[A]$	transformation matrix relating $\underline{P}$ to $\underline{F}$
$[B_i]$	$\underline{\delta}\ \underline{T}_i^t$
$\underline{D}$	vector of projected lengths
$\underline{\delta}$	$\underline{D}_{i+1} - \underline{D}_i$
$\underline{e}$	vector of axial extension and end rotations for a member of a plane frame
$\{\bar{e}\}$	vector of axial strain and end rotations relative to the current chord for a member of a plane frame
$\underline{F}$	vector of axial force and end moments associated with $\{\bar{e}\}$
$[H_i]$	$\underline{R}_i\ \underline{T}_i^t$
$[I]$	identity matrix
$[\bar{I}]$	$\begin{bmatrix} 0 & -1 \\ 1 & 0 \end{bmatrix}$
$[K]$	stiffness matrix
$\underline{P}$	vector of nodal forces
$[Q_i]$	$\underline{R}_i\ \underline{\delta}^t$
$\underline{R}$	unit vector $\begin{Bmatrix} -\sin\alpha \\ \cos\alpha \end{Bmatrix}$
$[\bar{R}_i]$	$\underline{R}_i\ \underline{R}_i^t$
$[S]$	matrix of member axial and flexural stiffnesses

$\underline{T}$	vector of direction cosines
$[\bar{T}_i]$	$\underline{T}_i \, \underline{T}_i^t$
$\underline{u}$	vector of nodal displacement parameters.

SUBSCRIPTS

A, B	end A, B of member AB
c	compression
i	i^{th} position
(i+1)	an increment in the i^{th} position
j	iteration count
L	linear
NL	non-linear
t	tension.

SUPERSCRIPTS

L	linear
NL	non-linear
*	system.

INTRODUCTION

Non-linearity in the analysis of structures can result from two separate and unrelated causes, namely material non-linearity and geometric non-linearity. Material non-linearity occurs if the stress-strain characteristic of the material of construction is non-linear, while should the deformation of the structure be such that it becomes necessary to consider equilibrium in its deformed position, then the structure is termed geometrically non-linear.

For most familiar types of structure it is sufficiently accurate to determine the forces and deflections by means of the well known linear analysis techniques. That is, assuming a linear material stress-strain relationship, and satisfying equilibrium by assuming that all forces involved in the final stressed state - both internal and external - act on the undeformed configuration of the structure, will result in linear governing equations.

With regard to material non-linearity, the linear elastic range, being the operational zone of most structures, is of greatest interest. For some materials, however, the stress-strain characteristics are non-linear elastic and may be considered approximately linear for very small strains only. Furthermore, in such cases, even with deformations in the structure which can still be considered small from the equilibrium point of view, the non-linear stress-strain relationship is reflected in the behaviour of the structure. Force-displacement characteristics of such structures are thus non-linear. For these cases, even though it is still legitimate to consider equilibrium with respect to the undeformed configuration of the structure, the resulting analysis is non-linear.

With regard to geometric non-linearity, even though the stress-strain relationship of the material of construction is linear, the structure deformations may not be small enough to allow consideration of equilibrium in the undeformed configuration to be a valid approximation. In such cases, satisfaction of equilibrium must be discussed with respect to the final deformed configuration of the structure. Again the associated analysis is non-linear. Examples of this class of structure are suspension bridges and guyed masts which are so flexible that when loaded they deform considerably,

thereby altering significantly the direction and position of the internal and external forces. For these geometrically non-linear structures the results of a linear analysis are often grossly erroneous and usually imply a greater load carrying capacity than actually exists.

Though material and geometric non-linearities are themselves unrelated, the possibility exists that the behaviour of a structure be non-linear as a consequence of both material and geometric non-linearities. While the view is advanced[16,22,29] that the force method is most suited to materially non-linear problems, and the displacement method is best suited for treating geometric non-linearities, Noor[22] has developed a mixed method with fundamental unknowns consisting of both force and displacement parameters, and a computational algorithm for the solution of pin-jointed space truss problems with combined material and geometric non-linearities.

The displacement method has been used by Williams[40] and Saafan[27] in the analysis of rigidly jointed frames where change of geometry effects are taken into account. The effects of geometric non-linearity on the analysis have been separated into three categories: (1) finite deflection of joints; (2) change of member flexural stiffness; and (3) change in member length due to bowing. The iteration technique is thus further complicated because the derivation of the member end moments is dependent on the axial load in the member which cannot itself be directly defined from the joint displacements. A further point is that, while modification to member flexural stiffness due to axial load is included, the modification of member axial stiffness due to bowing is not. Williams and Saafan's examples do show an important point: end shortening due to flexure may be of the same order of magnitude as the linear extensional term.

In this thesis only geometric non-linearities will be considered, and thus it is assumed that the material of which each member is composed behaves throughout in a linear elastic manner. It is further assumed that each member is of constant section and loaded only at its ends, and that deflections due to shear are negligible.

An incremental non-linear displacement method for ball-jointed space truss analysis will be developed in the following chapter, and later this method extended to rigid-jointed plane frame analysis. The development of this incremental non-linear displacement method so as to analyse rigid jointed space frames may be readily affected without limitation.

PART I

CHAPTER 1

AN INCREMENTAL, NON-LINEAR DISPLACEMENT METHOD FOR SPACE TRUSSES

In order to develop an incremental, non-linear displacement method consider a typical member firstly in the initial, undeformed state denoted by a zero subscript; secondly in some deformed position denoted by the subscript i; and thirdly an incremental change in this deformed position denoted by the subscript (i+1).

1.1 Geometry of a Typical Member

Consider the member AB as shown in fig. 1.1. In the undeformed position the member is of length L_o, and the orientation of $\overrightarrow{AB}$ relative to the global axis system x, y, z, is given by the direction cosines $\underline{T}_o$ [‡] where

$$\underline{T}_o = \begin{Bmatrix} \cos \alpha_o \\ \cos \beta_o \\ \cos \gamma_o \end{Bmatrix} \tag{1.1}$$

Defining $\underline{D}$ as the vector of projected lengths onto the global axes, then

$$\underline{D}_o = L_o \underline{T}_o \tag{1.2}$$

In the deformed position the displacements of the nodes of the member are $\underline{u}_{Ai}$ and $\underline{u}_{Bi}$ as shown in fig. 1.1. The six node displacement components of $\underline{u}_i$ define the deformed position:

$$\underline{u}_i = \begin{Bmatrix} \underline{u}_A \\ \underline{u}_B \end{Bmatrix}_i , \tag{1.3}$$

---

‡ $\underline{T}_o = \{T\}_o$ denoting T_o is a vector quantity

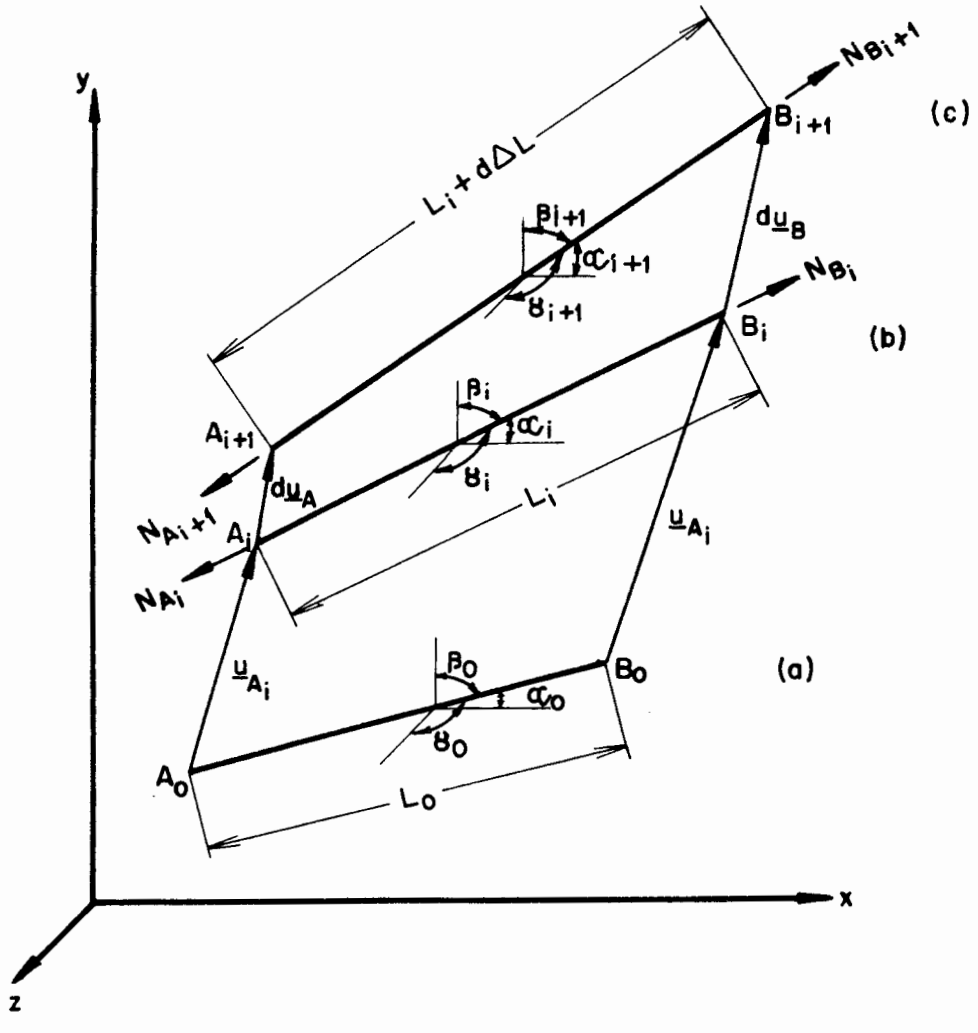

Fig. 1.1: (a) Initial position, (b) i^{th} position, (c) $(i+1)^{th}$ position

where

$$\underline{u}_{Ai} = \begin{Bmatrix} u_{Ax} \\ u_{Ay} \\ u_{Az} \end{Bmatrix}_i \quad \text{and} \quad \underline{u}_{Bi} = \begin{Bmatrix} u_{Bx} \\ u_{By} \\ u_{Bz} \end{Bmatrix}_i . \tag{1.4}$$

In this deformed position the length of the member is L_i. With the orientation of $\overrightarrow{AB}$ relative to the global axes now given by $\underline{T}_i$, where

$$\underline{T}_i = \begin{Bmatrix} \cos \alpha_i \\ \cos \beta_i \\ \cos \gamma_i \end{Bmatrix} , \tag{1.5}$$

the vector of projected lengths becomes

$$\underline{D}_i = L_i \, \underline{T}_i \tag{1.6}$$

where

$$L_i = L_o + \Delta L_i . \tag{1.7}$$

After an incremental change in configuration of the deformed position the member assumes the $(i+1)^{th}$ position, having undergone increments $d\underline{u}_A$ and $d\underline{u}_B$ in the displacements of its nodes. Thus

$$\underline{u}_{A_{i+1}} = \underline{u}_{A_i} + d\underline{u}_A$$

and (1.8)

$$\underline{u}_{B_{i+1}} = \underline{u}_{B_i} + d\underline{u}_B .$$

With the direction cosines of $\overrightarrow{AB}$ now given by

$$\underline{T}_{i+1} = \begin{Bmatrix} \cos \alpha_{i+1} \\ \cos \beta_{i+1} \\ \cos \gamma_{i+1} \end{Bmatrix} , \tag{1.9}$$

the vector of projected length is

$$\underline{D}_{i+1} = L_{i+1} \, \underline{T}_{i+1} , \tag{1.10}$$

where

$$L_{i+1} = L_i + d\Delta L$$
$$= L_o + \Delta L_i + d\Delta L. \qquad (1.11)$$

Furthermore it is convenient to define the vector

$$\underline{\delta} = d\underline{u}_B - d\underline{u}_A, \qquad (1.12)$$

and therefore

$$\underline{\delta} = \underline{D}_{i+1} - \underline{D}_i. \qquad (1.13)$$

1.2 The Change in Member Length

The length of the member in the $(i+1)^{th}$ position is given by

$$L_{i+1} = (\underline{D}_{i+1}^t \underline{D}_{i+1})^{\frac{1}{2}}. \qquad (1.14)$$

Since, from equation (1.13),

$$\underline{D}_{i+1} = \underline{D}_i + \underline{\delta},$$

this becomes

$$L_{i+1} = (\underline{D}_i^t \underline{D}_i + 2\,\underline{D}_i^t \underline{\delta} + \underline{\delta}^t \underline{\delta})^{\frac{1}{2}}.$$

Now,

$$L_i^2 = \underline{D}_i^t \underline{D}_i \quad \text{and} \quad \underline{D}_i^t = L_i \underline{T}_i^t,$$

therefore

$$L_{i+1} = L_i\left(1 + \frac{2\,\underline{T}_i^t \underline{\delta}}{L_i} + \frac{\underline{\delta}^t \underline{\delta}}{L_i^2}\right)^{\frac{1}{2}}. \qquad (1.15)$$

Using the binomial expansion $(1 + t)^{\frac{1}{2}} = 1 + \frac{1}{2}t - \frac{1}{8}t^2 + \ldots.$ and neglecting terms of third and higher order, yields

$$L_{i+1} = L_i\left(1 + \frac{\underline{T}_i^t \underline{\delta}}{L_i} + \frac{\underline{\delta}^t \underline{\delta}}{2\,L_i^2} - \frac{(\underline{T}_i^t \underline{\delta})^2}{2\,L_i^2}\right),$$

and, since

$$d\Delta L = L_{i+1} - L_i ,$$

then

$$d\Delta L = \underline{T}_i^t \underline{\delta} + \frac{\underline{\delta}^t \underline{\delta}}{2 L_i} - \frac{(\underline{T}_i^t \underline{\delta})^2}{2 L_i} . \qquad (1.16)$$

The term $\underline{T}_i^t \underline{\delta}$ in equation (1.16) is the usual first-order expression for the change in member length, while the remaining terms represent the second-order effect of increase in member length due to end displacements normal to the member axis. The sum of these non-linear terms must always be greater than, or equal to, zero since transverse displacements can only extend the member.

1.3 The Change in Direction Cosines

From equation (1.10)

$$\underline{T}_{i+1} = \frac{\underline{D}_{i+1}}{L_{i+1}} ,$$

and substituting equations (1.13) and (1.15) this becomes

$$\underline{T}_{i+1} = (\underline{D}_i + \underline{\delta}) \frac{1}{L_i} \left(1 + \frac{2 \underline{T}_i^t \underline{\delta}}{L_i} + \frac{\underline{\delta}^t \underline{\delta}}{L_i^2}\right)^{-\frac{1}{2}} .$$

Using equation (1.6) and the binomial expansion $(1+t)^{-\frac{1}{2}} = 1 - \frac{1}{2}t + \frac{3}{8}t^2 + \ldots.$ yields

$$\underline{T}_{i+1} = \left(\underline{T}_i + \frac{\underline{\delta}}{L_i}\right) \left(1 - \frac{\underline{T}_i^t \underline{\delta}}{L_i} - \frac{\underline{\delta}^t \underline{\delta}}{2 L_i^2} + \frac{3(\underline{T}_i^t \underline{\delta})^2}{2 L_i^2} + \ldots..\right)$$

and thus, to second order of smallness,

$$\underline{T}_{i+1} = \underline{T}_i + \frac{\underline{\delta}}{L_i} - \frac{\underline{T}_i \underline{T}_i^t \underline{\delta}}{L_i} - \frac{\underline{\delta} \underline{T}_i^t \underline{\delta}}{L_i^2} - \frac{\underline{T}_i \underline{\delta}^t \underline{\delta}}{2 L_i^2} + \frac{3 \underline{T}_i (\underline{T}_i^t \underline{\delta})^2}{2 L_i^2} . \qquad (1.17)$$

This change in direction cosines has no counterpart in linear analysis, where the equilibrium equations are formulated in terms of the undeformed geometry only.

1.4 Member Equilibrium

For any position of equilibrium of the member

$$N_A = N_B = N, \text{ say.}$$

Resolving this axial force in the directions of the global axes gives the components of N applied to the nodes A and B:

$$\underline{P}_i = \begin{Bmatrix} \underline{P}_A \\ \underline{P}_B \end{Bmatrix}_i = \begin{Bmatrix} -\underline{T} \\ \underline{T} \end{Bmatrix}_i N_i, \tag{1.18}$$

where

$$P_{A_i} = \begin{Bmatrix} P_{xA} \\ P_{yA} \\ P_{zA} \end{Bmatrix}_i, \quad \text{and} \quad \underline{P}_{B_i} = \begin{Bmatrix} P_{xB} \\ P_{yB} \\ P_{zB} \end{Bmatrix}_i. \tag{1.19}$$

1.5 Internal Force-Deformation Relationship

Defining the strain in the i^{th} position as

$$\epsilon_i = \frac{L_i^2 - L_o^2}{2L_o^2}, \tag{1.20}$$

then in the $(i + 1)^{th}$ position the strain is

$$\epsilon_{i+1} = \frac{(L_i + d\Delta L)^2 - L_o^2}{2L_o^2}$$

$$= \frac{L_i^2 - L_o^2}{2L_o^2} + \frac{L_i\, d\Delta L}{L_o^2} + \frac{(d\Delta L)^2}{2L_o^2}.$$

Substituting the expansion for $d\Delta L$, viz. equation 1.16, and neglecting terms of third and higher order yields

$$\epsilon_{i+1} = \frac{L_i^2 - L_o^2}{2L_o^2} + \frac{L_i\, \underline{T}_i^t\, \underline{\delta}}{L_o^2} + \frac{\underline{\delta}^t\, \underline{\delta}}{2L_o^2}. \tag{1.21}$$

Assuming a linear stress-strain relationship for the material,

$$N = EA\epsilon, \tag{1.22}$$

where the stiffness EA in tension or compression is based on the original cross-sectional area A.

1.6 Incremental Force - Displacement Equations

Combining equations 1.18 and 1.22 yields

$$\underline{P} = EA \begin{Bmatrix} -\underline{T} \\ \underline{T} \end{Bmatrix} \epsilon. \tag{1.23}$$

Now

$$d\underline{P} = \underline{P}_{i+1} - \underline{P}_i$$

therefore, from equation 1.23,

$$d\underline{P}_A = \begin{Bmatrix} P_{xA} \\ P_{yA} \\ P_{zA} \end{Bmatrix} = - EA \left\{ \underline{T}_{i+1} \epsilon_{i+1} - \underline{T}_i \epsilon_i \right\}.$$

From equations 1.20 and 1.21 this becomes

$$d\underline{P}_A = - EA \left\{ \underline{T}_{i+1} \left(\frac{L_i^2 - L_o^2}{2L_o^2} + \frac{L_i \underline{T}_i^t \underline{\delta}}{L_o^2} + \frac{\underline{\delta}^t \underline{\delta}}{2L_o^2} \right) - \underline{T}_i \left(\frac{L_i^2 - L_o^2}{2L_o^2} \right) \right\}.$$

Substituting the expansion for $\underline{T}_{i+1}$ viz. equation 1.17, noting that

$$EA \left(\frac{L_i^2 - L_o^2}{2L_o^2} \right) = N_i,$$

and neglecting terms of third and higher order, leads to

$$d\underline{P}_A = - \left[(K'L_i - \frac{N_i}{L_i})[\bar{T}_i] + \frac{N_i}{L_i}[I] \right] \underline{\delta} - \left[(K' - \frac{N_i}{L_i^2}) \left[[B_i] + \tfrac{1}{2}[B_i]^t \right] - (K' - \frac{3}{2} \frac{N_i}{L_i^2}) C_i [\bar{T}_i] \right] \underline{\delta},^{\ddagger} \tag{1.24}$$

where

$$K' = \frac{EA}{L_o^2}, \qquad [\bar{T}_i] = \underline{T}_i \underline{T}_i^t,$$

$$[\bar{I}] = \begin{bmatrix} 1 & 0 \\ 0 & 1 \end{bmatrix} \qquad [B_i] = \underline{\delta} \underline{T}_i^t,$$

and $C_i = \underline{T}_i^t \underline{\delta} = \underline{\delta}^t \underline{T}_i$, a scalar.

---

‡ [ ] parentheses denote a matrix.

1.7 Incremental Member Stiffness Matrix

From equation 1.18

$$d\underline{P}_B = - d\underline{P}_A \tag{1.25}$$

and, since, from equation 1.12

$$\underline{\delta} = \begin{Bmatrix} du_{Bx} - du_{Ax} \\ du_{By} - du_{Ay} \\ du_{Bz} - du_{Az} \end{Bmatrix} , \tag{1.26}$$

equation 1.24 gives the incremental member stiffness matrix $[K]$ relating the increments in external forces and external displacements.

$$d\underline{P} = [K]\, d\underline{u}. \tag{1.27}$$

$[K]$ may be written

$$[K] = [K^L] + [K^{NL}] , \tag{1.28}$$

where $[K^L]$ is the linear portion of $[K]$, i.e. $[K^L]$ is independent of the increments in displacements $d\underline{u}$; and $[K^{NL}]$ is the non-linear portion of $[K]$.

Partitioning equation 1.27 into

$$d \begin{Bmatrix} \underline{P}_A \\ \underline{P}_B \end{Bmatrix} = \begin{bmatrix} k_{AA} & k_{AB} \\ k_{BA} & k_{BB} \end{bmatrix} d \begin{Bmatrix} \underline{u}_A \\ \underline{u}_B \end{Bmatrix} , \tag{1.29}$$

from equation 1.24,

$$\begin{aligned} [k^L_{AA}] &= \left[(K'L_i - \frac{N_i}{L_i})[\bar{T}_i] + \frac{N_i}{L_i} [I] \right] , \\ [k^{NL}_{AA}] &= \left[(K' - \frac{N_i}{L_i^2}) \left[[B_i] + \tfrac{1}{2}[B_i]^t \right] - (K' - \frac{3}{2} \frac{N_i}{L_i^2})\, C_i\, [\bar{T}_i] \right] , \\ [k_{BB}] &= [k_{AA}] , \text{ and } [k_{AB}] = [k_{BA}] = - [k_{AA}] . \end{aligned} \tag{1.30}$$

1.8 Method of Solution

In order to analyse an assemblage of members, the incremental member stiffness matrix $[K]$ obtained for each member from equation 1.27, is assembled in its appropriate position to form the incremental structure stiffness matrix $[K^*]$.

$$d\underline{P}^* = [K^*]\, d\underline{u}^*, \tag{1.31}$$

where

$$[K^*] = [K_L^*] + [K_{NL}^*]. \tag{1.32}$$

The non-linear portion $[K_{NL}^*]$ is considered a correction term to the linear portion $[K_L^*]$. Consequently a simple iterative method of solution is possible.

For the $(i+1)^{th}$ load increment, $[K_L^*]$ is evaluated for the geometric configuration and axial forces of the i^{th} position of the structure. For the first iteration $[K_{NL}^*] = 0$, while for the $(j+1)^{th}$ iteration $[K_{NL}^*]$ is evaluated using both the geometry and forces of the i^{th} position as well as the displacements obtained from the solution of the j^{th} iteration. Thus for the $(j+1)^{th}$ iteration of the $(i+1)^{th}$ load increment

$$d\underline{P} = [K_L^* + K_{NL_j}^*]\, d\underline{u}_{j+1}^*. \tag{1.33}$$

For any load increment this iterative procedure may be continued until $d\underline{u}^*$, obtained from successive iterations, converges to a desired degree. The geometry of the structure is then updated and the new values of axial forces computed from equations 1.20 and 1.22. The next load increment may then be applied.

In the computer programme developed by the writer the degree of convergence of $d\underline{u}^*$ obtained by iterating equation 1.33 was determined by summing the absolute value of each nodal deflection, i.e. summing the absolute values of each element in $d\underline{u}^*$. The iteration procedure was stopped when the value of this sum obtained from successive iterations differed by less than some pre-assigned value. In succeeding chapters this value is referred to as a 'summed iteration deflection convergence tolerance'.

1.9 Elastic Instability

For a single member elastic instability occurs when the slope of its load-deflection curve becomes zero, as shown in Fig. 1.2.

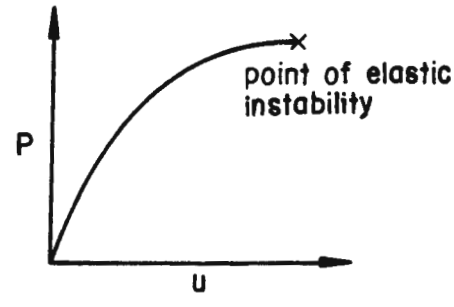

Fig. 1.2: Load-deflection curve for a single member

At this point

$$\frac{dP}{du} = 0,$$

therefore

$$dP = Kdu$$
$$= 0$$

requires that

$$K = 0$$

for elastic instability of a single member.

Generalizing this result to the load deflection matrix equation for the whole structure, viz. equation 1.31,

$$d\underline{P}^* = [K^*]\, d\underline{u}^*,$$

requires that

$$\left|K^*\right| = 0$$

for elastic instability of the structure.

In the computer programme developed by the writer, Gauss-reduction with back substitution was used to solve equation 1.31 for $d\underline{u}^*$, which reduces $[K^*]$ to a triangular matrix. Thus, for any iteration of a particular load increment, the determinant $|K^*|$ is readily evaluated as the product of the terms on the leading diagonal of the triangular matrix. Should the value of this determinant pass through zero then the point of elastic instability of the structure has been reached.

CHAPTER 2

THE BOWING SHORTENING OF A PINNED STRUT WHICH HAS AN INITIAL IMPERFECTION IN STRAIGHTNESS

2.1 The Relationship between Axial Force and Bowing Shortening

For a member that is not perfectly straight, or has some initial curvature, the end forces (taken as collinear) will produce bending moments along the member. If the end forces are compressive, the bending moment so caused will produce lateral deflection adding to the initial curvature, which in turn, shortens the chord length of the member.

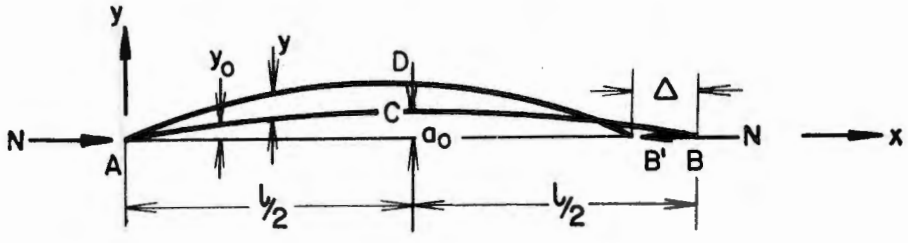

Fig. 2.1: Bowing shortening

Consider the member shown in Fig. 2.1. Let ACB be the initial stress free state. Suppose, for convenience, that this initial shape can be regarded as portion of a sine curve, so that the initial departure from straightness is given by

$$y_o = a_o \sin \frac{\pi x}{l} \qquad (2.1)$$

The quantity a_o is the maximum initial deflection of the member and occurs at its midlength point.

Under the action of the axial forces N, the member deflects to the position ADB'. The chord AB shortens by an amount Δ, that is

$$AB = AB' + \Delta.$$

The bending moment at any point on the axis is

$$M = N(y_o + y). \qquad (2.2)$$

Using the usual bending theory, the governing differential equation describing

the deflection y is

$$EI \frac{d^2y}{dx^2} = - M$$

$$= - N(y_o + y).$$

Substituting for y_o from equation 2.1 and writing $b^2 = N/EI$ yields

$$\frac{d^2y}{dx^2} + b^2y = - b^2 a_o \sin \frac{\pi x}{l} , \qquad (2.3)$$

the general solution of which is

$$y = C_1 \sin bx + C_2 \cos bx + \frac{1}{(\pi^2/b^2l^2) - 1} a_o \sin \frac{\pi x}{l} . \qquad (2.4)$$

Applying the boundary conditions

$$y = 0 \text{ when } x = 0,$$

and $y = 0$ when $x = l - \Delta \doteq l$,

yields $C_1 = C_2 = 0$,

and thus equation 2.4 reduces to

$$y = \frac{1}{(\pi^2/b^2l^2) - 1} a_o \sin \frac{\pi x}{l} \qquad (2.5)$$

With $N_c = \frac{EI \pi^2}{l^2}$, the Euler load; and $b^2 = \frac{N}{EI}$, it is convenient to write

$$\bar{N} = \frac{N}{N_c},$$

from which equation 2.5 becomes

$$y = \frac{\bar{N}}{1 - \bar{N}} a_o \sin \frac{\pi x}{l} ,$$

or in a dimensionless form (see Fig. 2.2)

$$\frac{y}{l} = \frac{\bar{N}}{1 - \bar{N}} \frac{a_o}{l} \sin \pi \frac{x}{l} . \qquad (2.6)$$

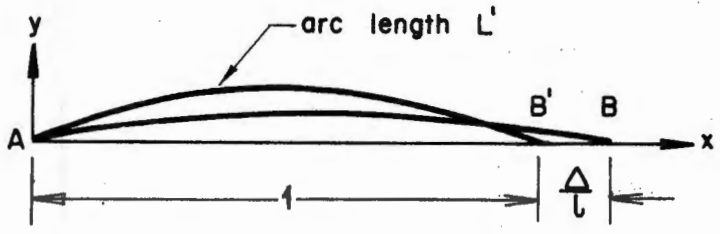

Fig. 2.2: Dimensionless configuration

With reference to Fig. 2.2, the arc length L' is given by

$$L' = \int_0^1 \sqrt{1 - \left(\frac{d(\frac{y}{l})}{d(\frac{x}{l})}\right)^2}\, d(\tfrac{x}{l}). \qquad (2.7)$$

Squaring the derivative of equation 2.6 and substituting into equation 2.7 yields

$$L' = \sqrt{1 + w^2} \int_0^1 \sqrt{1 - \frac{w^2}{1 + w^2} \sin^2 \pi \tfrac{x}{l}}\, d(\tfrac{x}{l}) , \qquad (2.8)$$

where

$$w = \frac{a_o \bar{N} \pi}{l(1 - \bar{N})} ;$$

and if

$$\theta = \pi \tfrac{x}{l} , \qquad (2.9)$$

then

$$L' = \frac{2}{\pi} \sqrt{1 + w^2} \int_0^{\pi/2} \sqrt{1 - \frac{w^2}{1 + w^2} \sin^2 \theta}\, d\theta, \qquad (2.10)$$

which is a complete elliptical integral of the second kind and may be evaluated[30] to any desired degree of accuracy by summing sufficient terms of its series expansion.

Hence,

$$L' = \sqrt{1 + w^2} \left\{1 - (\tfrac{1}{2})^2 \frac{m}{1} - (\frac{1.3}{2.4})^2 \frac{m^2}{3} - (\frac{1.3.5}{2.4.6})^2 \frac{m^3}{5} \ldots\right\}, \qquad (2.11)$$

where $m = \dfrac{w^2}{1 + w^2}$.

From Fig. 2.2, writing $\epsilon' = \Delta/l$ we have

$$\epsilon' \doteq L' - 1 . \qquad (2.12)$$

The order of magnitude of the initial imperfection as a fraction of the member length, that is a_o/l, must be estimated to reflect the accuracy and precision in fabrication and erection of the components of the particular structure under consideration.

To incorporate the effect of bowing shortening into the incremental displacement method as described in Chapter 1, equation 2.10 or 2.11 would be required in an incremental form, necessitating its differentiation with respect to N. The mathematical complexity of equations 2.10 or 2.11 prohibits this.

Curves of the form

$$\frac{\epsilon'}{\epsilon'_o} = \left(\frac{\bar{N}}{\bar{N}_o}\right)^n \qquad (2.13)$$

(where ϵ'_o, $\bar{N}_o$ and n are constants) have similar shape to those of ϵ' vs. $\bar{N}$ as evaluated from equation 2.12 (see Fig. 2.3); but are easily differentiated and evaluated.

For convenience ϵ'_o was chosen equal to 0,002, which is an approximate value of the elastic limit for most construction materials. For any chosen value of a_o/l and its associated true curve of ϵ' vs. $\bar{N}$ from equation 2.12, it is possible to obtain values for $\bar{N}_o$ and n in equation 2.13 so that a curve of this equation follows the true curve very closely. However, as only an approximate value of the magnitude of initial imperfection a_o/l is estimated for a particular structure, it will not introduce any further error if the approximate curve of equation 2.13 does not follow the true curve exactly.

In Fig. 2.3 curves of ϵ' vs. $\bar{N}$ for various values of $\bar{N}_o$ and n in equation 2.13 are shown together with true curves of equation 2.12 for various values of a_o/l. Note that the curves of equation 2.12 are asymptotic to the line $\bar{N} = 1$, i.e. $N = N_c$, the Euler load.

2.2 The Inclusion of Bowing Shortening in the Incremental Non-linear Displacement Method for Space Trusses

Recall from equation 1.18 that

$$\begin{Bmatrix} \underline{P}_A \\ \underline{P}_B \end{Bmatrix} = \begin{Bmatrix} -\underline{T} \\ \underline{T} \end{Bmatrix} N,$$

therefore

$$\underline{dP}_A = -\underline{T}_{i+1} N_{i+1} + \underline{T}_i N_i$$

$$= -\underline{T}_{i+1} (N_i + dN) + (\underline{T}_{i+1} - d\underline{T}) N_i,$$

and thus

$$\underline{dP}_A = -\underline{T}_{i+1} dN - d\underline{T} N_i. \qquad (2.14)$$

For a tension member any small initial imperfection in straightness will not affect the strain-displacement relationship significantly, and thus equation 1.22 still holds,

therefore $dN = EA\, d\varepsilon.$ (2.15)

However, the application of compressive collinear forces to the ends of a member that has an initial curvature will cause shortening of the chord length due to two causes, viz. the stress-strain characteristics of the constituent material, and bowing shortening as described in the preceding section.

If the bowing strain is given by equation 2.13 then the total strain-axial force relationship of a compression member becomes

$$\varepsilon = \frac{N}{EA} + \varepsilon'_o \left(\frac{\bar{N}}{\bar{N}_o}\right)^n. \qquad (2.16)$$

Thus in the $(i+1)^{th}$ position,

$$\varepsilon_{i+1} = \frac{(N_i + dN)}{EA} + \frac{\varepsilon'_o}{(\bar{N}_o\, N_c)^n} N_i^n \left(1 + \frac{dN}{N_i}\right)^n,$$

and using the first two terms of the binomial expansion for positive integral n

$$\epsilon_{i+1} = \frac{N_i + dN}{EA} + \lambda N_i^n + n \lambda N_i^{n-1} dN,$$

where

$$\lambda = \frac{\epsilon'_o}{(\bar{N}_o N_c)^n} \qquad (2.17)$$

Now,

$$d\epsilon = \epsilon_{i+1} - \epsilon_i \qquad (2.18)$$

therefore

$$d\epsilon = \left(\frac{1}{EA} + n \lambda N_i^{n-1}\right) dN$$

or

$$dN = \frac{1}{1/EA + n \lambda N_i^{n-1}} d\epsilon. \qquad (2.19)$$

Substituting equations 1.20 and 1.21 into equation 2.18 yields

$$d\epsilon = \frac{L_i \underline{T}_i^t \underline{\delta}}{L_o^2} + \frac{\underline{\delta}^t \underline{\delta}}{2L_o^2} \qquad (2.20)$$

For a tension member, using equations 2.14, 2.15, 2.20 and the expansion for $\underline{T}_{i+1}$ (viz. equation 1.17) will lead to equation 1.24. Thus, to include bowing shortening, it may be seen by comparing equations 2.15 and 2.19 that the only difference in both the linear and non-linear portions of the incremental member stiffness matrix of equation 1.27 will be the value of K':

for tension members, $K' = K'_t = \frac{EA}{L_o^2}$ (2.21)

and for compression members,

$$K' = K'_c = \frac{1/L_o^2}{1/EA + n \lambda N_i^{n-1}}. \qquad (2.22)$$

Thus the inclusion of bowing shortening into an incremental non-linear displacement method programme for space truss analysis is easily affected.

2.3 A Note on the Solution Procedure

If the effect of bowing shortening is included in the analysis, the structure stiffness matrix is assembled and evaluated using equations 2.21 or 2.22 accordingly for a tension or compression member; and the same iterative procedure described in section 1.8 employed to solve for the increment in deflection.

To evaluate the axial forces of the members once the $(i+1)^{th}$ increment in deflection has been obtained

$$\epsilon_{i+1} = \frac{L_{i+1}^2 - L_o^2}{2L_o^2} \quad \text{as before.}$$

If $\epsilon_{i+1} > 0$ the member is in tension, and the axial force is still given by

$$N_{i+1} = EA\, \epsilon_{i+1}. \tag{2.23}$$

However, for $\epsilon_{i+1} < 0$, the compressive force is obtained from the equation

$$\frac{N_{i+1}}{EA} + \lambda N_{i+1}^n = \epsilon_{i+1}. \tag{2.24}$$

In the programme developed by the writer, the desired root N_{i+1} of equation 2.24 was obtained by employing a Newton-Raphson iteration technique, with the initial estimate of the root given by equation 2.23. Convergence was rapid.

Note that for a compression member N is negative. Therefore if n is conveniently chosen as an odd integer, the term $n \lambda N_i^{n-1}$ in equation 2.22 is positive, and the term λN_{i+1}^n in equation 2.24 is negative, as desired. Choosing n as an even integer would necessitate a suitable correction to these terms to ensure their correct sign.

CHAPTER 3

SPACE TRUSS NUMERICAL EXAMPLES

Example 3.1:

To illustrate the use of the incremental non-linear displacement method to predict the behaviour of a particular structure, the problem of a simple two-bar truss will be considered. For convenience no elastic limit is assigned to the constituent material, and it is assumed that the two members are prevented from buckling.

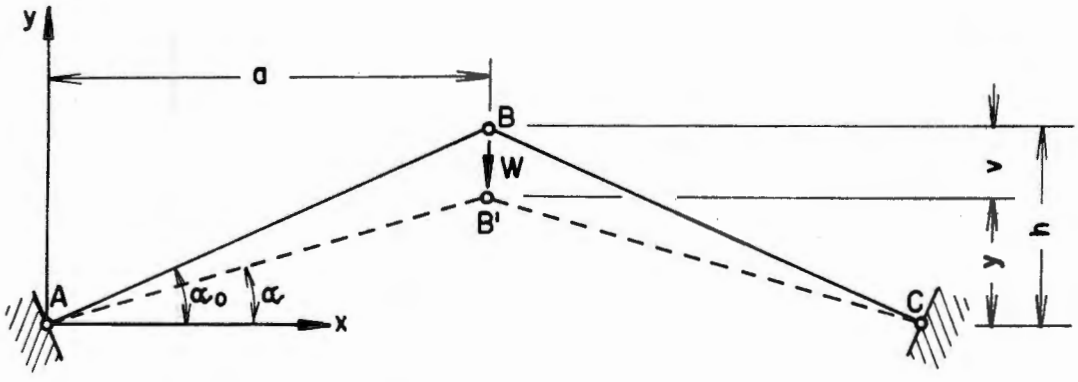

Fig. 3.1: Two-bar truss of Example 3.1

Because of the simplicity of this structure it is possible to verify results by means of a direct analytical approach. When a vertical load W is applied to node B it causes this node to deflect by an amount v, and the structure thus assumes the configuration AB'C, as shown in Fig. 3.1. For convenience the non-dimensional forms

$$\frac{v}{a} = x \qquad (3.1)$$

and $$\frac{W}{EA} = w$$

will be adopted and thus the deformation of the structure is governed completely by two parameters α_o and w, where α_o defines the initial geometry.

In the deformed position, with the axial strain given by

$$\epsilon = \frac{L^2 - L_o^2}{2L_o^2}$$

where $L_o = a \sec \alpha_o$

and $L = a \sec \alpha,$

the axial force N becomes

$$N = EA \frac{\sec^2 \alpha - \sec^2 \alpha_o}{2 \sec^2 \alpha_o}. \tag{3.2}$$

For equilibrium of node B

$$W = 2 N \sin \alpha$$

and therefore

$$w = \frac{\sin \alpha(\sec^2 \alpha - \sec^2 \alpha_o)}{\sec^2 \alpha_o} \tag{3.3}$$

Now, since

$$\tan \alpha = \tan \alpha_o - x, \tag{3.4}$$

for a chosen value of x the associated value of w may be obtained from equations 3.3 and 3.4. Differentiating equation 3.3 with respect to α and equating this to zero will yield α_c, the value of α corresponding to the elastic critical load of the structure:

$$\sec \alpha_c + 2 \sin^2 \alpha_c \sec^3 \alpha_c - \cos \alpha_c \sec^2 \alpha_o = 0 . \tag{3.5}$$

Employing a Newton-Raphson technique, with $\alpha_o = 30^o$, the critical value of α was found to be

$$\alpha_c = 0,31184,$$

thus

$$w_c = 0,05279$$

and

$$x_c = 0,25500.$$

In Figs. 3.2, 3.3, 3.4 and 3.5 load-deflection curves for the two-bar truss are shown for the case $\alpha_o = 30^o$. The curves labelled (a) are the

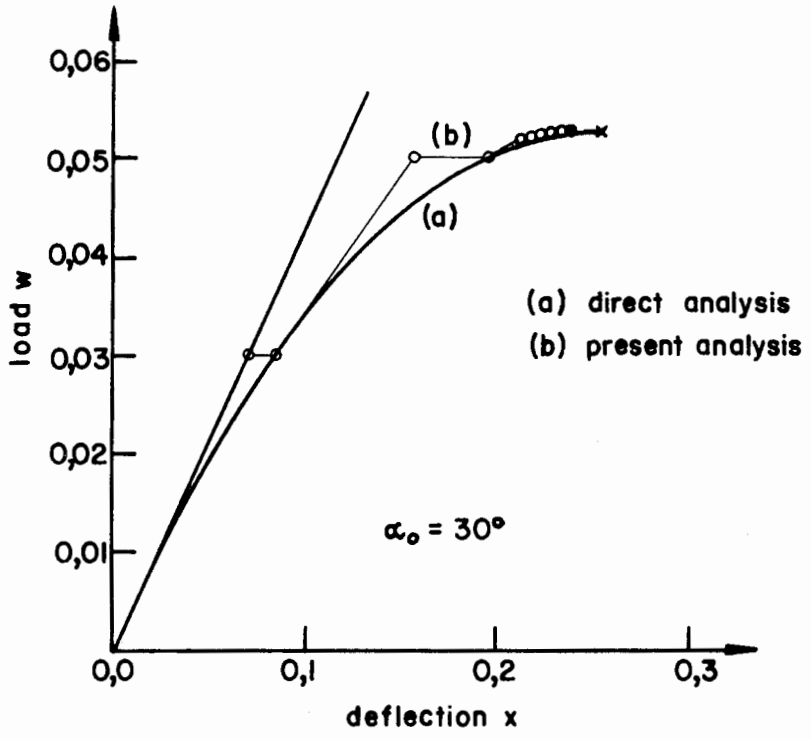

Fig. 3.2: Load-deflection curve of 2-bar truss

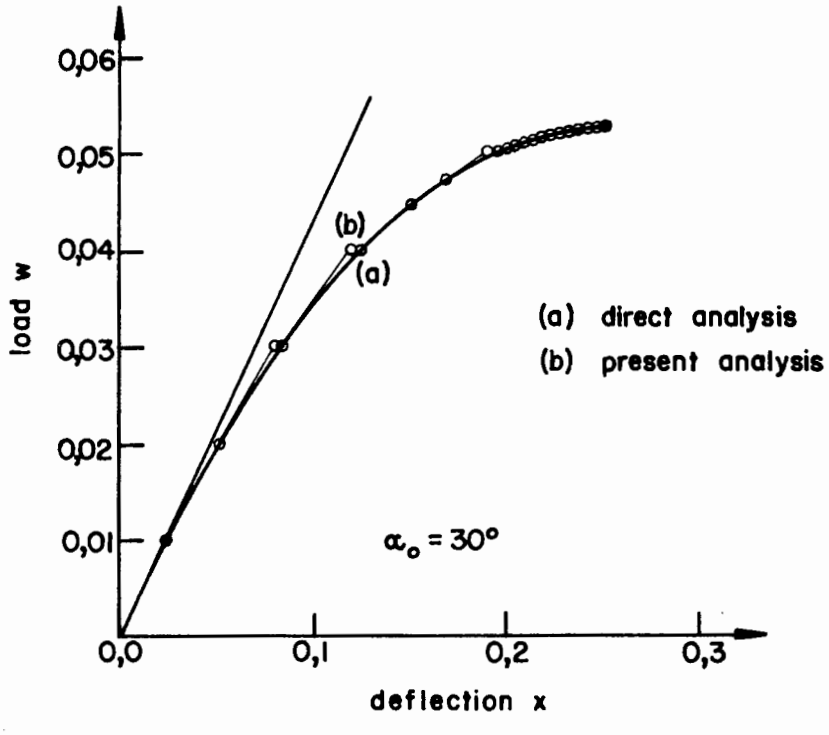

Fig. 3.3: Load-deflection curve of 2-bar truss

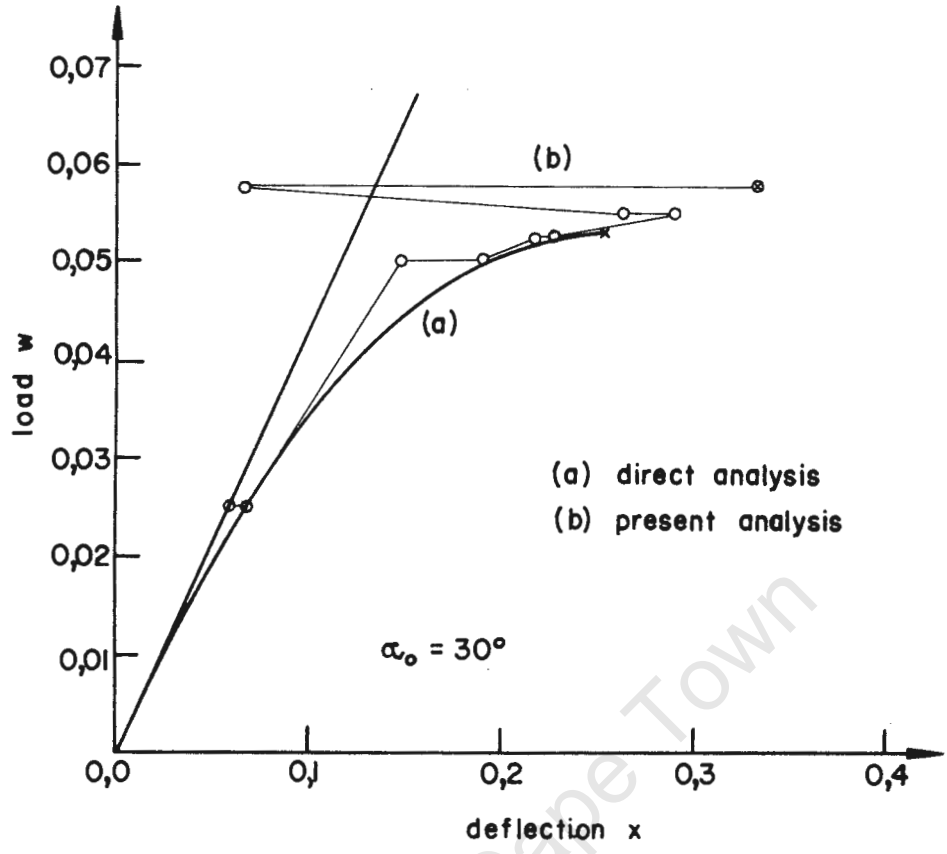

Fig. 3.4: Load-deflection curve of 2-bar truss

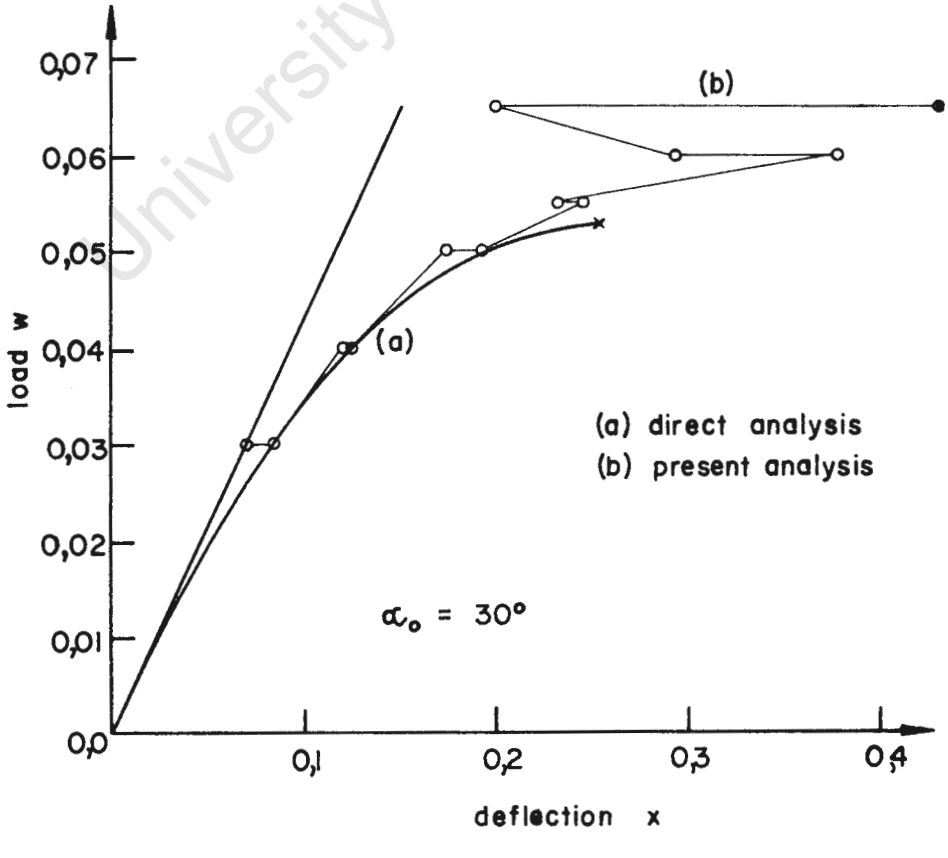

Fig. 3.5: Load-deflection curve of 2-bar truss

result of the direct analytical approach outlined above, those labelled (b) are the results of incremental non-linear displacement method analyses, while the straight line from the origin in each figure represents the linear solution. For the incremental non-linear displacement method analyses the summed iteration deflection convergence tolerance was 0,05. The horizontal portions of curves (b) are thus the change in deflection due to the iteration procedure.

It was found that substantially large load increments could be applied until the total load was within approximately 5 % of the elastic critical load after which it was necessary to reduce the size of the load increments drastically to avoid a grossly erroneous result, as shown in Figs. 3.4 and 3.5. As can be seen from Fig. 3.2, after applying only two load increments up to $w = 0,05$, the iterative procedure corrects the deflection to within 1,5 % of the correct value. The incremental non-linear displacement method result of Fig. 3.2 gives the elastic critical load of the structure as $w = 0,0528$ which is within 0,02 % of the correct value, although the associated deflection at the point of instability is 7 % in error. This result required a total of 21 iterations. It was found that reducing the permissible iteration convergence tolerance caused a substantial increase in the number of iterations without significant improvement in the value of deflection at the point of instability. A far more effective method of improving the accuracy of the solution was to decrease the magnitude of load increments especially as the point of instability was approached.

The load incrementing of Fig. 3.3 also produced a critical load of $w = 0,0528$ but the deflection at the point of instability was only 1,75 % in error. This result required a total of 48 iterations.

To compare the results obtained from the present analysis with those obtained by other methods, consider the two-bar truss in the initial position with α_o now equal to 0,1 radian and the load W applied in the opposite direction. Convergence patterns of the iterative procedures for the load cases $w = - 0,0005$ and $w = - 0,05$ are shown in Figs. 3.6 and 3.7 respectively. In both figures the true value of x is indicated as obtained from equations 3.3 and 3.4 of the direct analytical approach outlined above. The results of analyses performed by Turner et al[36] and Saafan[27] are also shown. The results obtained from the present analysis give some indication of the effect of load increment size on the accuracy of solution.

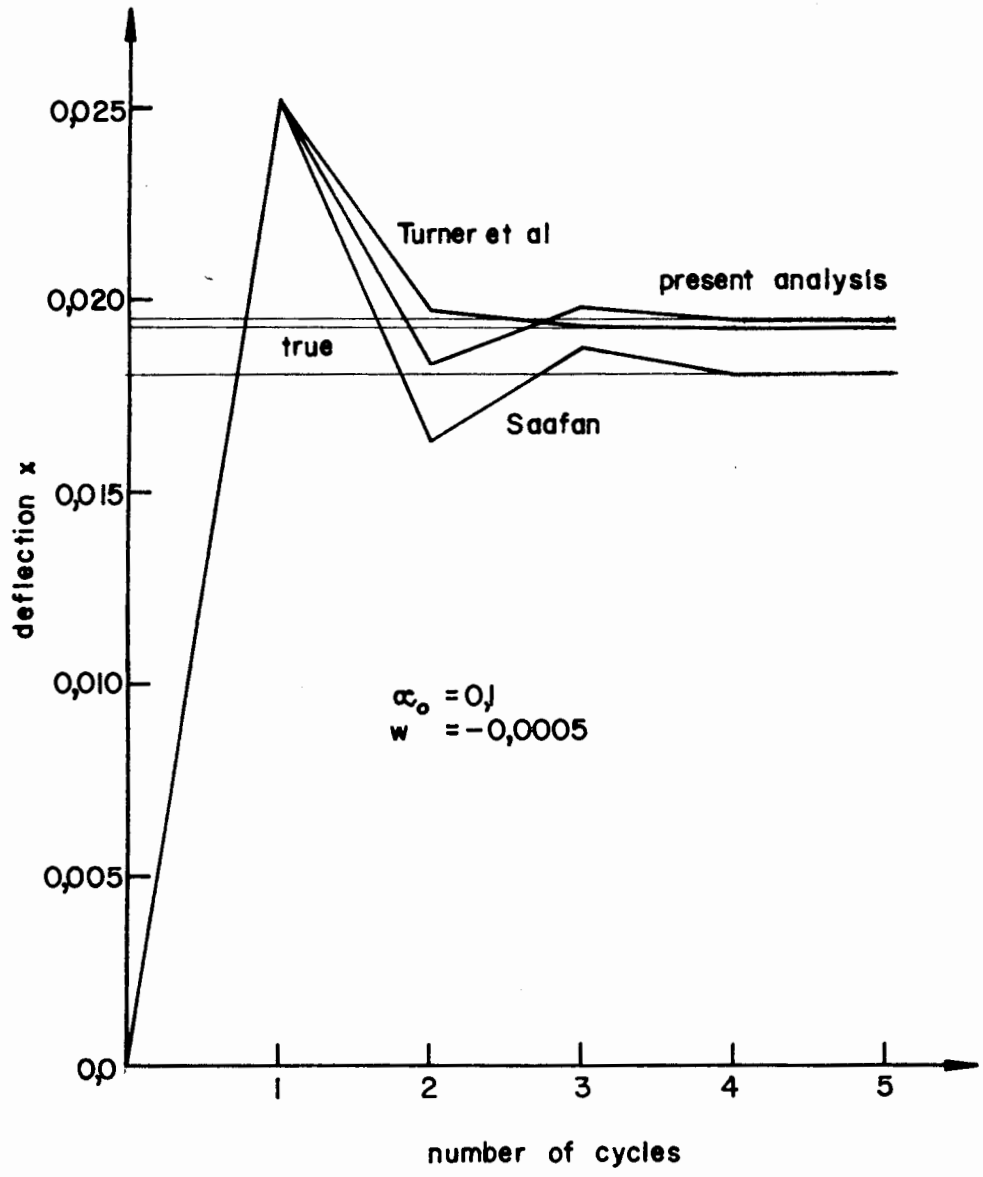

Fig. 3.6: Iterative convergence for w = - 0,0005

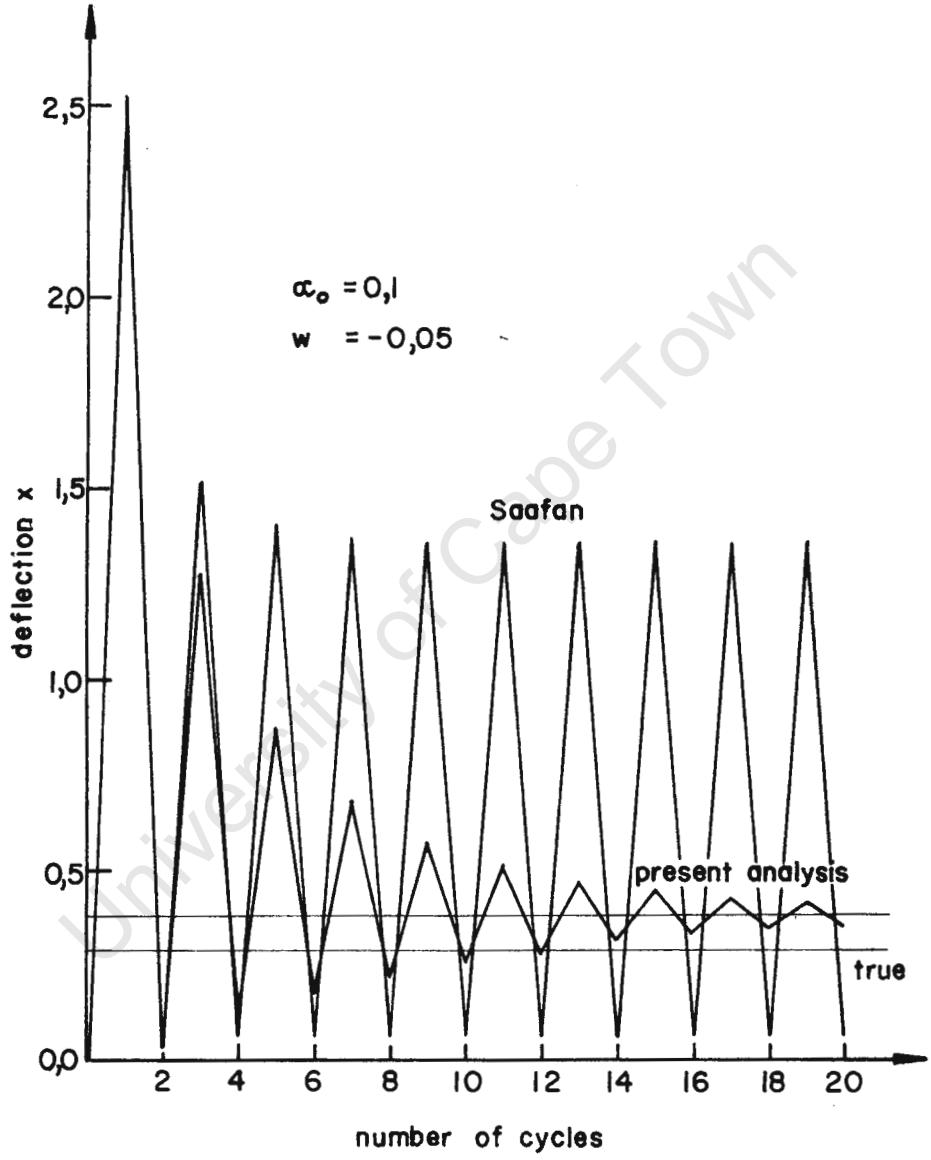

Fig. 3.7: Iterative convergence for w = - 0,05

For both load cases the full loads of - 0,0005 and - 0,05 were applied in a single load increment and the solutions iterated until convergence to four significant figures was obtained.

For the load case $w = - 0{,}0005$ the present analysis required six cycles to converge to a value which was 1 % in error of the true value, while a linear analysis produced a result 30 % in error. As can be seen from Fig. 3.6, the result of Saafan's analysis converges to a value more than 6 % in error, a consequence of approximations he introduces into his governing equations.

The second load case of $w = - 0{,}05$ is a single load increment 100 times the size of that considered above. With reference to Fig. 3.7 the present analysis converges to a value 32 % in error; the linear analysis produces a result 778 % in error; and Saafan's result oscillates ad infinitum between two limits. The fact that the incremental non-linear displacement method solution converges to a value 32 % in error indicates that because of the large value of load applied in a single increment, the third- and higher-order terms, neglected in the development of the analysis in Chapter 1, now become of numerical significance, and thus the second-order analysis is invalid for load increments that produce such large deformations.

Example 3.2:

The three-way grid dome shown in Fig. 3.8 has span 18 metres, radius 15 metres, rise 3 metres, and consists of 34 nodes and 60 members. The members are tubular steel of outer diameter 60,5 mm, and thickness 3,0 mm. The nodes were assumed to be ball-joints and those lying on the perimeter circle constrained against translation in any direction. The value of Young's modulus was taken to be 209 GPa. A uniform distributed load was applied to the whole structure in the minus-z direction, which was applied as nodal loads proportional to the plan area.

The results of sixteen analyses are summarized in table 3.1, where the values n and $\overline{N}_o$ in column six of the table are the bowing parameters of equations 2.17 and 2.22. For the non-linear analyses the magnitude of the load increments was 0,05 kPa.

If all the members of the dome are straight, and thus no bowing takes place under compressive axial load, the elastic critical load was found to be 9,35 kPa (analysis 16). Assuming that each member has an initial imperfection in straightness and accounting for bowing of members (all members of the dome are in compression), the elastic critical load was determined for the following values of bowing parameters n and $\overline{N}_o$: 7, 0,87; 11, 0,90; and 51, 0,98. (see Fig. 2.3). The values of the corresponding critical loads were found to be 1,55 kPa, 1,55 kPa and 1,75kPa respectively. (Closer approximations of these critical loads could be obtained by decreasing the magnitude of the load increments as the point of instability is approached).

Analyses 4 to 7 give the state of the structure one load increment before the point of instability was reached in analyses 13 and 14; analyses 8 to 10 one load increment before instability in analysis 15; and analyses 11 and 12 one load increment before instability in analysis 16. Column 8 of the table gives the maximum value of current axial force divided by Euler load occurring in any member of the structure, and thus it can be seen that the dome becomes elastically unstable as the Euler load is approached in at least one of the members. Analysis 6 of the table required 62 iterations while the next load increment (analysis 13) required the maximum number of 200 iterations, indicating lack of convergence in the iteration procedure at the point of instability.

By comparing analyses 1, 2 and 3, which correspond to the working load condition, it can be seen that there is little error in the linear analysis, and the introduction of bowing in analysis 3 does not affect the structure significantly at this load level.

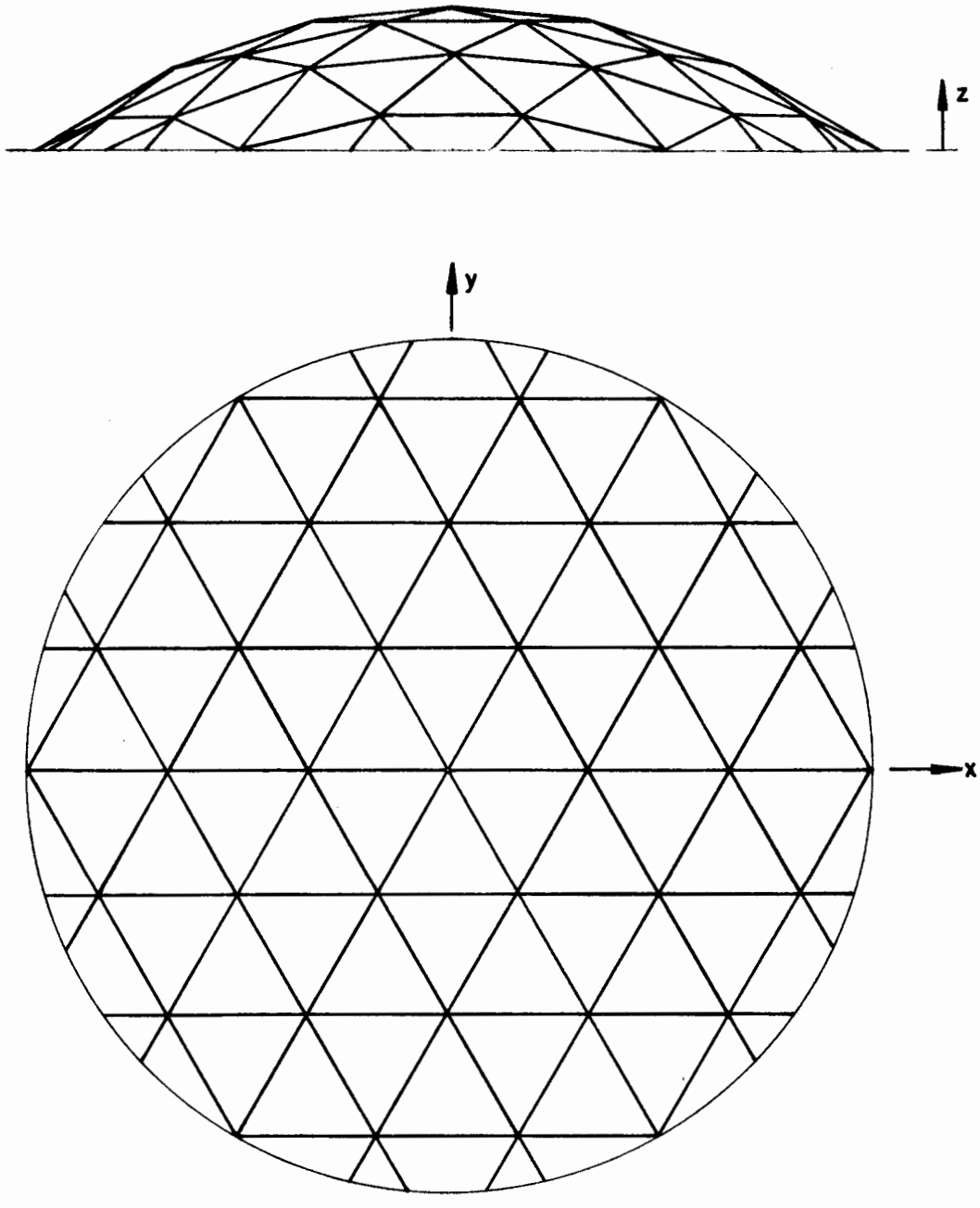

Fig. 3.8: Three-way grid dome

Analysis	Load (kPa)*	Type	SIDCT**	Bowing	n, $\overline{N}_o$	Vert. defl. of apex (mm)	Max $\frac{N}{N_c}$	Elastic crit. load (kPa)	no. of iterations	CPU time***
1	0,75	linear	-	-	-	3,806	0,434	-	1	0 : 03
2	0,75	non-linear	0,01	nil	-	3.806	0,434	-	30	0 : 33
3	0,75	non-linear	0,01	bowing	7; 0,87	4,006	0,428	-	30	0 : 35
4	1,50	linear	-	-	-	7.614	0,868	-	1	0 : 03
5	1,50	non-linear	0,01	nil	-	7,610	0,869	-	60	1 : 07
6	1,50	non-linear	0,01	bowing	7; 0,87	34,844	0,870	-	62	1 : 10
7	1,50	non-linear	0,01	bowing	11; 0,90	18,357	0,854	-	61	1 : 09
8	1,70	-	-	-	-	8,629	0,983	-	1	0 : 03
9	1,70	non-linear	0,01	nil	-	8,624	0,985	-	68	1 : 08
10	1,70	non-linear	0,01	bowing	51; 0,98	10,582	0,947	-	68	1 : 12
11	9,30	linear	-	-	-	47,205	5,379	-	1	0 : 03
12	9,30	non-linear	0,01	nil	-	45,207	5,420	-	372	6 : 05
13	loaded	non-linear	0,01	bowing	7; 0,87	-	-	1,55	262	4 : 23
14	to	non-linear	0,01	bowing	11; 0,90	-	-	1,55	64	4 : 34
15		non-linear	0,01	bowing	51; 0,98	-	-	1,75	73	1 : 22
16	instability	non-linear	0,01	nil	-	-	-	9,35	374	6 : 52

* for non-linear analyses load increment size = 0,05 kPa

** SIDCT = summed iteration deflection convergence tolerance

*** throughout this thesis computer CPU times refer to a UNIVAC 1106 computer

Table 3.1: Analyses of 3-way grid dome

PART II

CHAPTER 4

AN INCREMENTAL, NON-LINEAR DISPLACEMENT METHOD FOR PLANE FRAMES

Similar to the incremental, non-linear displacement method developed for a space truss in Part 1, consider a typical member of a plane frame firstly in the initial, undeformed state denoted by a zero subscript; secondly in some deformed position denoted by the subscript i; and thirdly an incremental change in this deformed position denoted by the subscript (i+1).

4.1 Geometry of a Typical Member

Consider the member AB as shown in Fig. 4.1. In the undeformed position the member is of length L_o. The orientation of $\overrightarrow{AB}$ is given by the angle α_o measured anti-clockwise from the positive direction of the x-axis.

In the deformed position the displacements of the nodes of the member are $\underline{u}_{A_i}$ and $\underline{u}_{B_i}$, as shown. The angle of orientation of the chord $\overrightarrow{AB}$ is now α_i. At end A, the tangent to the elastic line of the member makes an angle θ_{A_i} with the direction of the initial chord $\overrightarrow{AB}$, and an angle θ'_{A_i} with the current chord $\overrightarrow{A_iB_i}$. Similarly for end B. The six node displacement components of $\underline{u}_i$ define the deformed position:

$$\underline{u}_i = \begin{Bmatrix} u_{Ax} \\ u_{Ay} \\ \theta_A \\ u_{Bx} \\ u_{By} \\ \theta_B \end{Bmatrix}_i \qquad (4.1)$$

Also

$$\underline{u}_{A_i} = \begin{Bmatrix} u_{Ax} \\ u_{Ay} \end{Bmatrix}_i \quad \text{and} \quad \underline{u}_{B_i} = \begin{Bmatrix} u_{Bx} \\ u_{By} \end{Bmatrix}_i . \qquad (4.2)$$

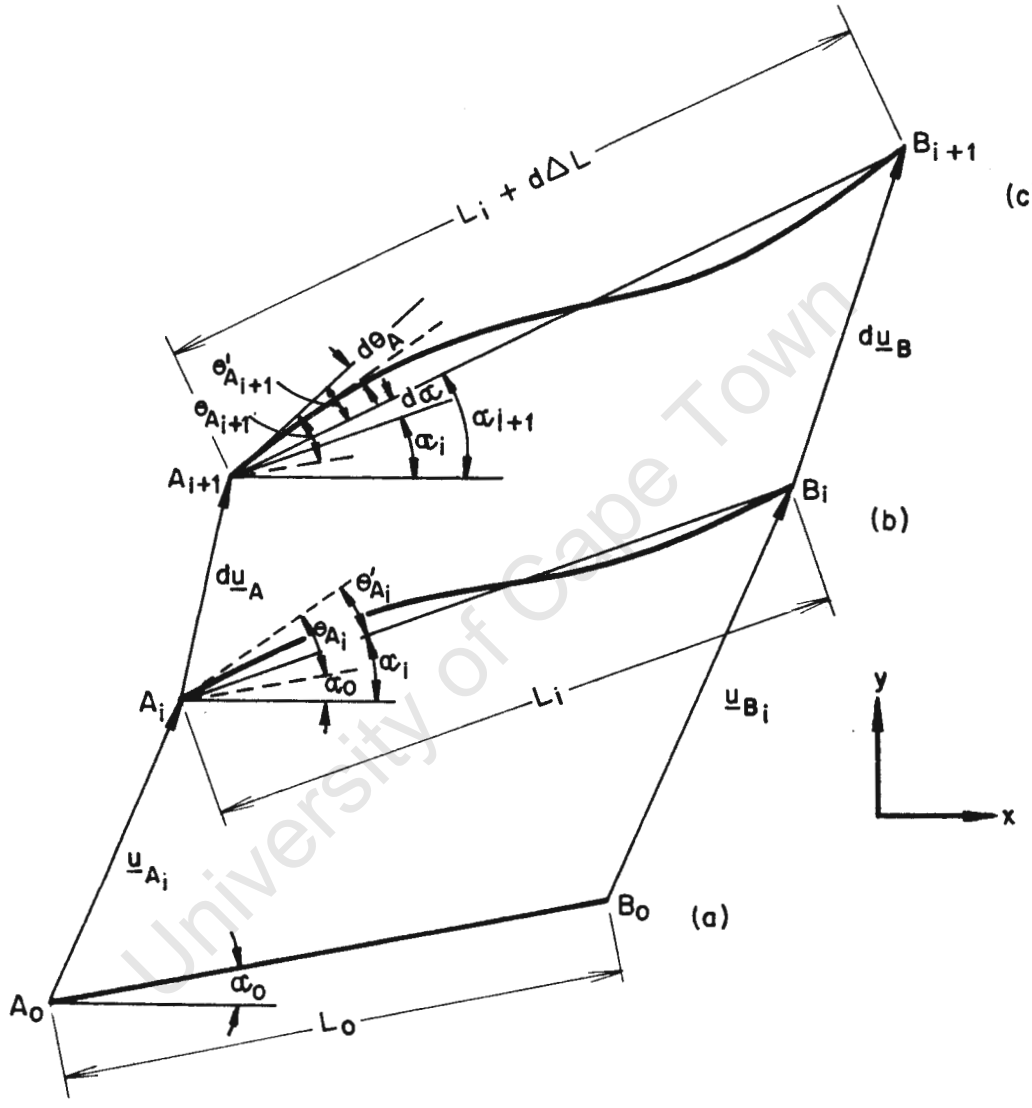

Fig. 4.1: (a) Initial position, (b) i^{th} position, (c) $(i+1)^{th}$ position

In this deformed position the length of the chord joining the displaced ends of the member is L_i, where

$$L_i = L_o + \Delta L_i, \quad \text{as for the space truss in Part 1.}$$

On defining the unit vector

$$\underline{T}_i = \begin{Bmatrix} \cos \alpha_i \\ \sin \alpha_i \end{Bmatrix}, \tag{4.3}$$

the vector of projected lengths of the current chord is

$$\underline{D}_i = \begin{Bmatrix} D_x \\ D_y \end{Bmatrix}_i = L_i \, \underline{T}_i. \tag{4.4}$$

In this deformed position the six internal forces acting on the member are defined by three independent quantities N_i, M'_{A_i} and M'_{B_i} - as shown in Fig. 4.2(a) -

$$\underline{F}_i = \begin{Bmatrix} N \\ M'_A \\ M'_B \end{Bmatrix}_i. \tag{4.5}$$

Note that the directions of the axial and shear forces are those associated with the chord joining the deflected nodes. Furthermore, the axial force N is computed on the basis of the new chord length of the member and the effect of change in member length due to flexure is disregarded.[16,27,34,40] The three internal deformations associated with the three independent internal forces are:

$$\underline{e}_i = \begin{Bmatrix} \Delta L \\ \theta'_A \\ \theta'_B \end{Bmatrix}_i, \tag{4.6}$$

After an incremental change in configuration of the deformed position the member assumes the $(i+1)^{th}$ position, having undergone increments $d\underline{u}_A$ and $d\underline{u}_B$ in the displacements of its ends, and an increment $d\alpha$ in the angle of

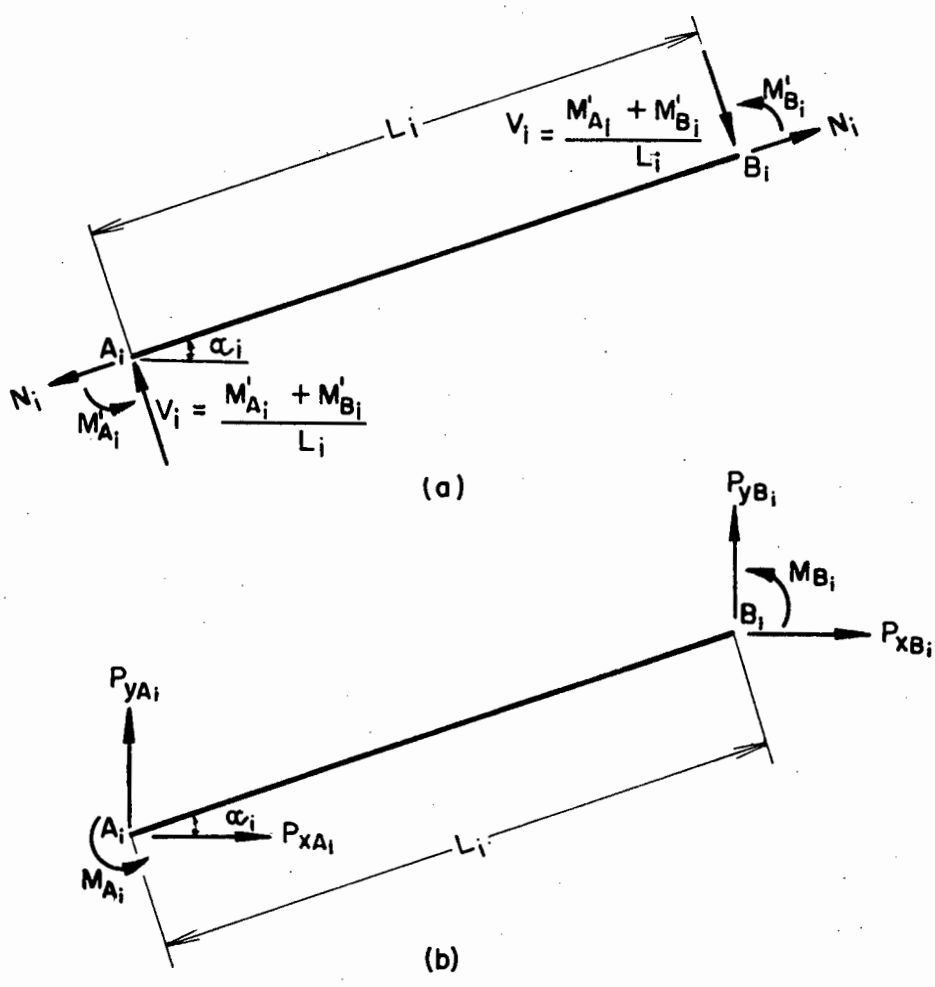

Fig. 4.2: (a) Internal forces, (b) external forces

orientation of the chord $\overrightarrow{AB}$. Furthermore, the tangents to the elastic line at ends A and B of the member rotate in an anti-clockwise (positive) direction by amounts $d\theta_A$ and $d\theta_B$ respectively (see Fig. 4.1).

Similar to the space truss of Part 1, for the $(i+1)^{th}$ position of the member of a plane frame we have:

the displacements

$$\begin{aligned} \underline{u}_{A_{i+1}} &= \underline{u}_{A_i} + d\underline{u}_A \\ \text{and } \underline{u}_{B_{i+1}} &= \underline{u}_{B_i} + d\underline{u}_B \ ; \end{aligned} \tag{4.7}$$

the unit vector

$$\underline{T}_{i+1} = \begin{Bmatrix} \cos \alpha_{i+1} \\ \sin \alpha_{i+1} \end{Bmatrix}; \tag{4.8}$$

the projected lengths of the current chord

$$\underline{D}_{i+1} = \begin{Bmatrix} D_x \\ D_y \end{Bmatrix}_{i+1} = L_{i+1}\, \underline{T}_{i+1} \ ; \tag{4.9}$$

the current chord length

$$\begin{aligned} L_{i+1} &= L_i + d\Delta L \\ &= L_o + \Delta L_i + d\Delta L \ ; \end{aligned} \tag{4.10}$$

the vector

$$\underline{\delta} = d\underline{u}_B - d\underline{u}_A = \begin{Bmatrix} du_x \\ du_y \end{Bmatrix}; \tag{4.11}$$

and therefore

$$\underline{\delta} = \underline{D}_{i+1} - \underline{D}_i . \tag{4.12}$$

The three internal deformations associated with the three independent internal forces of the $(i+1)^{th}$ position of the member are:

$$\underline{e}_{i+1} = \begin{Bmatrix} \Delta L_i + d\Delta L \\ \theta'_{A_i} + d\theta_A - d\alpha \\ \theta'_{B_i} + d\theta_B - d\alpha \end{Bmatrix} . \qquad (4.13)$$

4.2 The Change in Chord Length of a Member

With $\underline{\delta}$ and $\underline{T}$ redefined as in the preceding section, the second-order expression for the increment in chord length of a member when deforming from the i^{th} to the $(i+1)^{th}$ position is still given by equation 1.16, viz.

$$d\Delta L = \underline{T}_i^t \underline{\delta} + \frac{\underline{\delta}^t \underline{\delta}}{2L_i} - \frac{(\underline{T}_i^t \underline{\delta})^2}{2L_i} . \qquad (4.14)$$

4.3 The Change in Transformation Vector $\underline{T}$

Similarly, equation 1.17 still holds, viz.

$$\underline{T}_{i+1} = \underline{T}_i + \frac{\underline{\delta}}{L_i} - \frac{\underline{T}_i \underline{T}_i^t \underline{\delta}}{L_i} - \frac{\underline{\delta} \underline{T}_i^t \underline{\delta}}{L_i^2} - \frac{\underline{T}_i \underline{\delta}^t \underline{\delta}}{2L_i^2} + \frac{3\underline{T}_i (\underline{T}_i^t \underline{\delta})^2}{2L_i^2} . \qquad (4.15)$$

4.4 The Change in Angle of Orientation of $\overrightarrow{AB}$

$$\alpha_{i+1} = \alpha_i + d\alpha$$

and, with reference to Fig. 4.3,

$$d\alpha = \frac{DB_i}{L_i}$$

$$= \frac{CB_i}{L_i} - \frac{CD}{L_i}$$

$$= \frac{-du_x \sin\alpha_i + du_y \cos\alpha_i}{L_i} - \frac{(du_x \cos\alpha_i + du_y \sin\alpha_i) \tan d\alpha}{L_i}$$

Using the series expansion $\tan d\alpha = d\alpha + d\alpha^3/3! + \ldots\ldots$, and neglecting terms of third and higher order, yields

$$d\alpha = \frac{-du_x \sin\alpha_i + du_y \cos\alpha_i}{L_i} - \frac{(du_x \cos\alpha_i + du_y \sin\alpha_i)(-du_x \sin\alpha_i + du_y \cos\alpha_i)}{L_i^2} .$$

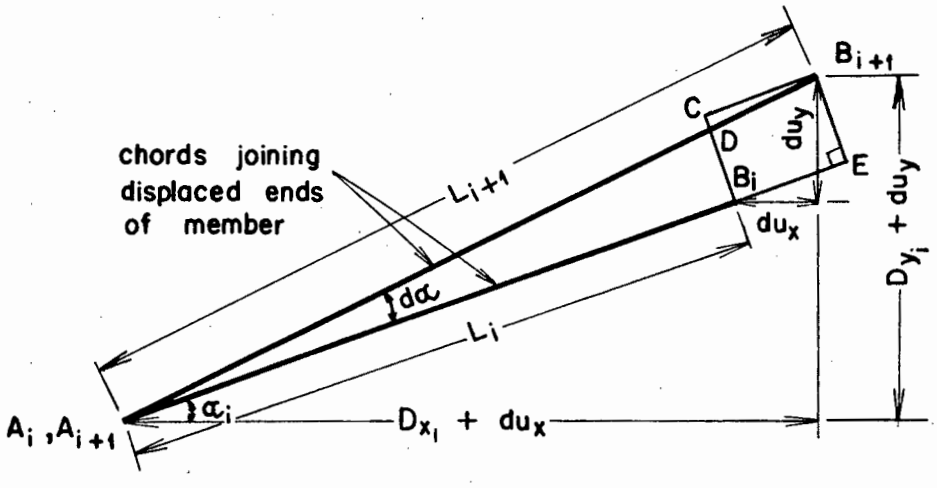

Fig. 4.3: Geometry in the i^{th} and $(i+1)^{th}$ positions

Defining a unit vector

$$\underline{R}_i = \begin{Bmatrix} -\sin \alpha_i \\ \cos \alpha_i \end{Bmatrix} \tag{4.16}$$

the second-order expression for $d\alpha$ becomes

$$d\alpha = \frac{\underline{R}_i^t \underline{\delta}}{L_i} - \frac{\underline{T}_i^t \underline{\delta}\, \underline{R}_i^t \underline{\delta}}{L_i^2} \tag{4.17}$$

The first term on the right hand side of equation 4.17 is the usual first-order expression for the rotation of the chord, while the second term gives the effect of increase in chord length serving to decrease chord rotation.

4.5 An Expression for $\underline{R}_{i+1}/L_{i+1}$

Under the stipulation that external forces are applied only at the nodes the shear force V is constant along the length AB of the member, and is of magnitude

$$V = \frac{M'_A + M'_B}{L}. \tag{4.18}$$

(See Fig. 4.2a)

Resolving this shear force in the directions of the global axes produces terms of the form

$$-\frac{\sin \alpha}{L}(M'_A + M'_B) \quad \text{and} \quad \frac{\cos \alpha}{L}(M'_A + M'_B),$$

and, when formulating the equations of member equilibrium in the following section (4.6), it will be seen that a second-order expression for

$$\frac{\underline{R}_{i+1}}{L_{i+1}} = \frac{1}{L_{i+1}} \begin{Bmatrix} -\sin \alpha \\ \cos \alpha \end{Bmatrix}_{i+1} \quad \text{will be required.}$$

From equations 4.8 and 4.9

$$\frac{\underline{R}_{i+1}}{L_{i+1}} = \frac{1}{L_{i+1}^2} \begin{Bmatrix} -D_y \\ D_x \end{Bmatrix}_{i+1},$$

and from equations 1.15, 4.11 and 4.12, this becomes

$$\frac{\underline{R}_{i+1}}{L_{i+1}} = \begin{Bmatrix} -D_{y_i} - du_y \\ D_{x_i} + du_x \end{Bmatrix} \frac{1}{L_i^2}\left(1 + \frac{2\,\underline{T}_i^t\,\underline{\delta}}{L_i} + \frac{\underline{\delta}^t\,\underline{\delta}}{L_i^2}\right)^{-1}.$$

Using the binomial expansion $(1 + t)^{-1} = 1 - t + t^2 + \ldots\ldots$ yields

$$\frac{\underline{R}_{i+1}}{L_{i+1}} = \left(\frac{\underline{R}_i}{L_i} + \frac{1}{L_i^2}\begin{Bmatrix} -du_y \\ du_x \end{Bmatrix}\right)\left(1 - \frac{2\,\underline{T}_i^t\,\underline{\delta}}{L_i} - \frac{\underline{\delta}^t\,\underline{\delta}}{L_i^2} + \frac{4(\underline{T}_i^t\,\underline{\delta})^2}{L_i^2} + \ldots\right),$$

and thus, to second-order of smallness,

$$\frac{\underline{R}_{i+1}}{L_{i+1}} = \frac{\underline{R}_i}{L_i} - \frac{2\underline{R}_i\,\underline{T}_i^t\,\underline{\delta}}{L_i^2} + \frac{1}{L_i^2}[\bar{I}]\,\underline{\delta} - \frac{2\underline{T}_i^t\,\underline{\delta}}{L_i^3}[\bar{I}]\,\underline{\delta} - \frac{\underline{R}_i\,\underline{\delta}^t\,\underline{\delta}}{L_i^3} + \frac{4\underline{R}_i(\underline{T}_i^t\,\underline{\delta})^2}{L_i^3}, \tag{4.19}$$

where $[\bar{I}] = \begin{bmatrix} 0 & -1 \\ 1 & 0 \end{bmatrix}$

4.6 Member Equilibrium

With reference to Fig. 4.2, the joint equations of equilibrium for the member in the i^{th} position can be described by the $[A]$ matrix as follows:

$$\underline{P}_i = [A]_i\,\underline{F}_i, \tag{4.20}$$

that is,

$$\begin{Bmatrix} P_{xA} \\ P_{yA} \\ M_A \\ P_{xB} \\ P_{yB} \\ M_B \end{Bmatrix}_i = \begin{bmatrix} -\cos\alpha & \frac{-\sin\alpha}{L} & \frac{-\sin\alpha}{L} \\ -\sin\alpha & \frac{\cos\alpha}{L} & \frac{\cos\alpha}{L} \\ 0 & 1 & 0 \\ \cos\alpha & \frac{\sin\alpha}{L} & \frac{\sin\alpha}{L} \\ \sin\alpha & \frac{-\cos\alpha}{L} & \frac{-\cos\alpha}{L} \\ 0 & 0 & 1 \end{bmatrix}_i \begin{Bmatrix} N \\ M'_A \\ M'_B \end{Bmatrix}_i. \tag{4.21}$$

Using equations 4.3 and 4.16 this may be written

$$\begin{Bmatrix} P_{xA} \\ P_{yA} \\ M_A \\ P_{xB} \\ P_{yB} \\ M_B \end{Bmatrix}_i = \begin{bmatrix} -\underline{T} & \frac{R}{L} & \frac{R}{L} \\ 0 & 1 & 0 \\ \underline{T} & -\frac{R}{L} & -\frac{R}{L} \\ 0 & 0 & 1 \end{bmatrix}_i \cdot \begin{Bmatrix} N \\ M'_A \\ M'_B \end{Bmatrix}_i . \qquad (4.22)$$

4.7 Internal Force-Deformation Relationship

Defining the axial strain in the deformed position as

$$\epsilon_i = \frac{L_i^2 - L_o^2}{2L_o^2}, \qquad (4.23)$$

then the second-order strain-displacement relationship is still given by equation 1.21, viz.

$$\epsilon_{i+1} = \frac{L_i^2 - L_o^2}{2L_o^2} + \frac{L_i \, \underline{T}_i^t \, \underline{\delta}}{L_o^2} + \frac{\underline{\delta}^t \, \underline{\delta}}{2L_o^2} \qquad (4.24)$$

So as to relate the internal deformations $\underline{e}$ to the internal forces $\underline{F}$, where

$$\underline{e}_i = \begin{Bmatrix} \Delta L \\ \theta'_A \\ \theta'_B \end{Bmatrix}_i \quad \text{and} \quad \underline{F}_i = \begin{Bmatrix} N \\ M'_A \\ M'_B \end{Bmatrix} ,$$

it is convenient to define the vector $\{\bar{e}\}$ as

$$\{\bar{e}\} = \begin{Bmatrix} \epsilon \\ \theta'_A \\ \theta'_B \end{Bmatrix}_i , \qquad (4.25)$$

that is

$$\{\bar{e}\}_i = \begin{Bmatrix} \dfrac{L_i^2 - L_o^2}{2L_o^2} \\ \theta'_{A_i} \\ \theta'_{B_i} \end{Bmatrix}, \tag{4.26}$$

and

$$\{\bar{e}\}_{i+1} = \begin{Bmatrix} \dfrac{L_i^2 - L_o^2}{2L_o^2} + \dfrac{L_i \underline{T}_i^t \underline{\delta}}{L_o^2} + \dfrac{\underline{\delta}^t \underline{\delta}}{2L_o^2} \\ \theta'_{A_i} + d\theta_A - d\alpha \\ \theta'_{B_i} + d\theta_B - d\alpha \end{Bmatrix} . \tag{4.27}$$

The relationship between the internal deformations and forces may now be expressed by the member stiffness matrix $[S]$ as follows:

$$\{F\}_i = [S]_i \{\bar{e}\}_i , \tag{4.28}$$

where

$$[S]_i = \begin{bmatrix} EA & 0 & 0 \\ 0 & S_{AA_i} & S_{AB_i} \\ 0 & S_{BA_i} & S_{BB_i} \end{bmatrix} . \tag{4.29}$$

Note that the axial stiffness of the member in tension or compression is based on the original cross-sectional area A and the original length L_o, whereas the flexural stiffness coefficients S_{AA}, S_{AB}, S_{BA} and S_{BB} depend on the magnitude and sign of the current value of axial force, and current chord length; as will be shown in the following section.

4.8 Stiffness Coefficients in Flexure[38]

In linear analysis the bending moment at any point on the elastic

line is considered to be unaffected by the axial forces, resulting in the flexural stiffness for the member AB of a plane frame:

$$S_{AA} = S_{BB} = \frac{4EI}{L}, \qquad \text{and} \quad S_{AB} = S_{BA} = \frac{2EI}{L}. \tag{4.30}$$

However, in second-order analysis, relatively large forces and displacements are involved, and it is necessary to determine the equation of the elastic curve on the basis of a more exact bending moment expression including the effect of axial forces.

The derivation of the following flexural stiffness coefficients is given in Appendix A. Defining the quantity

$$\phi_i = L_i \sqrt{\frac{|N_i|}{EI}}, \tag{4.31}$$

then for N_i positive, that is tensile,

$$S_{AA_i} = S_{BB_i} = \frac{\phi_i^2 \cosh \phi_i - \phi_i \sinh \phi_i}{2 - 2\cosh \phi_i + \phi_i \sinh \phi_i} \frac{EI}{L_i}, \qquad \text{and} \quad S_{AB_i} = S_{BA_i} = \frac{\phi_i \sinh \phi_i - \phi_i^2}{2 - 2\cosh \phi_i + \phi_i \sinh \phi_i} \frac{EI}{L_i}; \tag{4.32a}$$

and for N_i negative (compressive),

$$S_{AA_i} = S_{BB_i} = \frac{\phi_i \sin \phi_i - \phi_i^2 \cos \phi_i}{2 - 2\cos \phi_i - \phi_i \sin \phi_i} \frac{EI}{L_i}, \qquad \text{and} \quad S_{AB_i} = S_{BA_i} = \frac{\phi_i \sin \phi_i - \phi_i^2 \cos \phi_i}{2 - 2\cos \phi_i - \phi_i \sin \phi_i} \frac{EI}{L_i}. \tag{4.32b}$$

Curves of S_{AA} and S_{AB} vs ϕ for N tensile and compressive are given in Fig. 4.4. Note that, in comparison with the case in which the flexural stiffness is considered unaffected by axial force, a flexural member is stiffer with axial tension, but more flexible with axial compression.

Equations 4.32 are undefined if $N_i = 0$, in which case equations 4.30 are applicable.

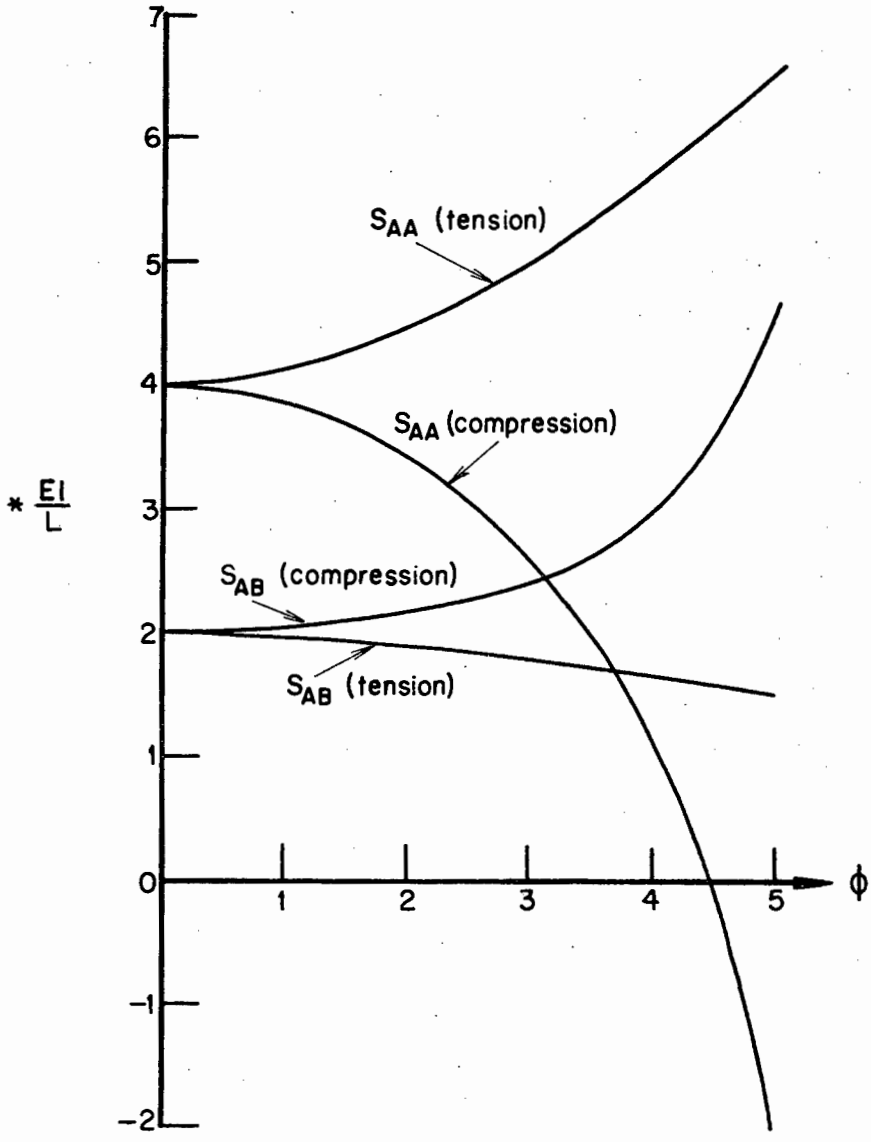

Fig. 4.4: Stiffness coefficients in flexure

4.9 Incremental Force-Displacement Equations

Recalling equations 4.20 and 4.28 viz.

$$\{P\} = [A]\{F\},$$

and $$\{F\} = [S]\{\bar{e}\};$$

and substituting equation 4.28 into equation 4.20 yields

$$\begin{Bmatrix} P_{xA} \\ P_{yA} \\ M_A \\ P_{xB} \\ P_{yB} \\ M_B \end{Bmatrix} = \begin{bmatrix} -EA\underline{T} & (S_{AA} + S_{AB})\frac{R}{L} & (S_{AA} + S_{AB})\frac{R}{L} \\ 0 & S_{AA} & S_{AB} \\ EA\underline{T} & -(S_{AA} + S_{AB})\frac{R}{L} & -(S_{AA} + S_{AB})\frac{R}{L} \\ 0 & S_{AB} & S_{BB} \end{bmatrix} \begin{Bmatrix} \epsilon \\ \theta'_A \\ \theta'_B \end{Bmatrix}. \quad (4.33)$$

Now,

$$d\{P\} = \{P\}_{i+1} - \{P\}_i ,$$

therefore, from equation 4.33,

$$d\begin{Bmatrix} P_{xA} \\ P_{yA} \end{Bmatrix} = -EA\{\underline{T}_{i+1}\,\epsilon_{i+1} - \underline{T}_i\,\epsilon_i\} + \{(S_{AA} + S_{AB})_{i+1}\frac{R_{i+1}}{L_{i+1}}(\theta'_A + \theta'_B)_{i+1} - (S_{AA} + S_{AB})_i\frac{R_i}{L_i}(\theta'_A + \theta'_B)_i\}.$$

From equations 4.26 and 4.27 this becomes

$$d\begin{Bmatrix} P_{xA} \\ P_{yA} \end{Bmatrix} = -EA\left\{\underline{T}_{i+1}\left(\frac{L_i^2 - L_o^2}{2L_o^2} + \frac{L_i\,\underline{T}_i^{\,t}\underline{\delta}}{L_o^2} + \frac{\underline{\delta}^t\underline{\delta}}{2L_o^2}\right) - \underline{T}_i\left(\frac{L_i^2 - L_o^2}{2L_o^2}\right)\right\} + \left\{(S_{AA} + S_{AB})_{i+1}\frac{R_{i+1}}{L_{i+1}}(\theta'_{A_i} + \theta'_{B_i} + d\theta_A + d\theta_B - 2d\alpha) - (S_{AA} + S_{AB})_i\frac{R_i}{L_i}(\theta'_{A_i} + \theta'_{B_i})\right\}. \quad (4.34)$$

Recall from section 4.8 that $S_{AA_{i+1}}$ and $S_{AB_{i+1}}$ are functions of $\sqrt{N_{i+1}}$

and L_{i+1}. Since the value of N_{i+1} is still to be determined, the approximation is made that the flexural stiffness coefficients in the i^{th} and $(i+1)^{th}$ positions are the same, that is

$$(S_{AA} + S_{AB})_{i+1} \doteq (S_{AA} + S_{AB})_i.$$

Now, in equation 4.34, substituting the expansions for $\underline{T}_{i+1}$, $d\alpha$ and $\frac{\underline{R}_{i+1}}{L_{i+1}}$, viz. equations 4.15, 4.17 and 4.19, noting that

$$EA\left(\frac{L_i^2 - L_o^2}{2L_o^2}\right) = N_i \quad \text{and} \quad (S_{AA} + S_{AB})_i(\theta'_A + \theta'_B)_i = (M'_A + M'_B)_i,$$

and neglecting terms of third and higher order, leads to

$$\begin{aligned} d\begin{Bmatrix} P_{xA} \\ P_{yA} \end{Bmatrix} = & -\left[(K'L_i - \frac{N_i}{L_i})[\bar{T}_i] + \frac{N_i}{L_i}[I] + \frac{M'_i}{L_i^2}\left[2[H_i] - [\bar{I}]\right] + 2\frac{S_i}{L_i}[\bar{R}_i]\right]\underline{\delta} \\ & + S_i\,\underline{R}_i(d\theta_A + d\theta_B) \\ & - \left[(K' - \frac{N_i}{L_i^2})\left[[B_i] + \tfrac{1}{2}[B_i]^t\right] - (K' - \frac{3}{2}\frac{N_i}{L_i^2})C_i[\bar{T}_i]\right. \\ & - \frac{S_i}{L_i^2}\left[6\,C_i[\bar{R}_i] - 2\,G_i[\bar{I}]\right] \\ & \left. - \frac{M'_i}{L_i^3}\left[4\,C_i[H_i] - 2\,C_i[\bar{I}] - [Q_i]\right]\right]\underline{\delta} \\ & + \frac{S_i}{L_i}\left\{[\bar{I}]\,\underline{\delta} - 2\,C_i\,\underline{R}_i\right\}(d\theta_A + d\theta_B), \end{aligned} \tag{4.35}$$

where

$$K' = \frac{EA}{L_o^2}, \qquad M' = M'_{A_i} + M'_{B_i},$$

$$[I] = \begin{bmatrix} 1 & 0 \\ 0 & 1 \end{bmatrix}, \qquad [\bar{I}] = \begin{bmatrix} 0 & -1 \\ 1 & 0 \end{bmatrix},$$

$$S_i = \frac{(S_{AA} + S_{AB})_i}{L_i}, \qquad [\bar{T}_i] = \underline{T}_i\,\underline{T}_i^t,$$

$$[\bar{R}_i] = \underline{R}_i\,\underline{R}_i^t, \qquad [H_i] = \underline{R}_i\,\underline{T}_i^t,$$

$$[Q_i] = \underline{R}_i\,\underline{\delta}^t \qquad [B_i] = \underline{\delta}\,\underline{T}_i^t,$$

$C_i = \underline{T}_i^t\,\underline{\delta} = \underline{\delta}^t\,\underline{T}_i$, a scalar, and $G_i = \underline{R}_i^t\,\underline{\delta} = \underline{\delta}^t\underline{R}_i$, a scalar.

The increment in bending moment at end A is

$$d M_A = M_{A_{i+1}} - M_{A_i}.$$

From equations 4.33, 4.26 and 4.27 this becomes

$$d M_A = S_{AA_{i+1}} (\theta'_{A_i} + d\theta_A - d\alpha) + S_{AB_{i+1}} (\theta'_{B_i} + d\theta_B - d\alpha)$$

$$- S_{AA_i} \theta'_{A_i} - S_{AB_i} \theta'_{A_i}. \qquad (4.36)$$

Substituting the expansion for $d\alpha$, viz. equation 4.17, and using the approximation

$S_{AA_{i+1}} \doteq S_{AA_i}$ and $S_{AB_{i+1}} \doteq S_{AB_i}$, equation 4.36 becomes

$$dM_A = S_{AA_i} d\theta_A + S_{AB_i} d\theta_B - S_i \underline{R}_i^t \underline{\delta} + \frac{S_i}{L_i} C_i \underline{R}_i^t \underline{\delta}. \qquad (4.37)$$

Similarly.

$$dM_B = S_{AB_i} d\theta_A + S_{AA_i} d\theta_B - S_i \underline{R}_i^t \underline{\delta} + \frac{S_i}{L_i} C_i \underline{R}_i^t \underline{\delta}. \qquad (4.38)$$

4.10 Incremental Member Stiffness Matrix

From equation 4.33

$$d \begin{Bmatrix} P_{xB} \\ P_{yB} \end{Bmatrix} = - d \begin{Bmatrix} P_{xA} \\ P_{yA} \end{Bmatrix}, \qquad (4.39)$$

and, since

$$\underline{\delta} = \begin{Bmatrix} du_{Bx} - du_{Ax} \\ du_{By} - du_{Ay} \end{Bmatrix}, \qquad (4.40)$$

equations 4.35, 4.37 and 4.38 may be assembled to give the incremental member stiffness matrix [K] relating the increments in external forces and external displacements:

$$d\underline{P} = [K]\, d\underline{u} \qquad (4.41)$$

As for the case of a space truss [K] may be written

$$[K] = [K^L] + [K^{NL}], \tag{4.42}$$

where $[K^L]$ is the linear portion of $[K]$, i.e. $[K^L]$ is independent of the increments in displacements $\underline{du}$; and $[K^{NL}]$ is the non-linear portion of $[K]$.

The thirty-six elements of $[K^L]$ and of $[K^{NL}]$ are given in Appendix B. Note that by setting $S_{AA} = S_{AB} = 0$ this stiffness matrix reduces to the two dimensional equivalent of the incremental non-linear stiffness matrix for a space truss derived in Chapter 1, as is expected.

The incremental member stiffness matrices for all the members of a plane frame are assembled to form the incremental structure stiffness matrix $[K^*]$, and the solution procedure described in section 1.8 is employed to solve for the increments in deflections.

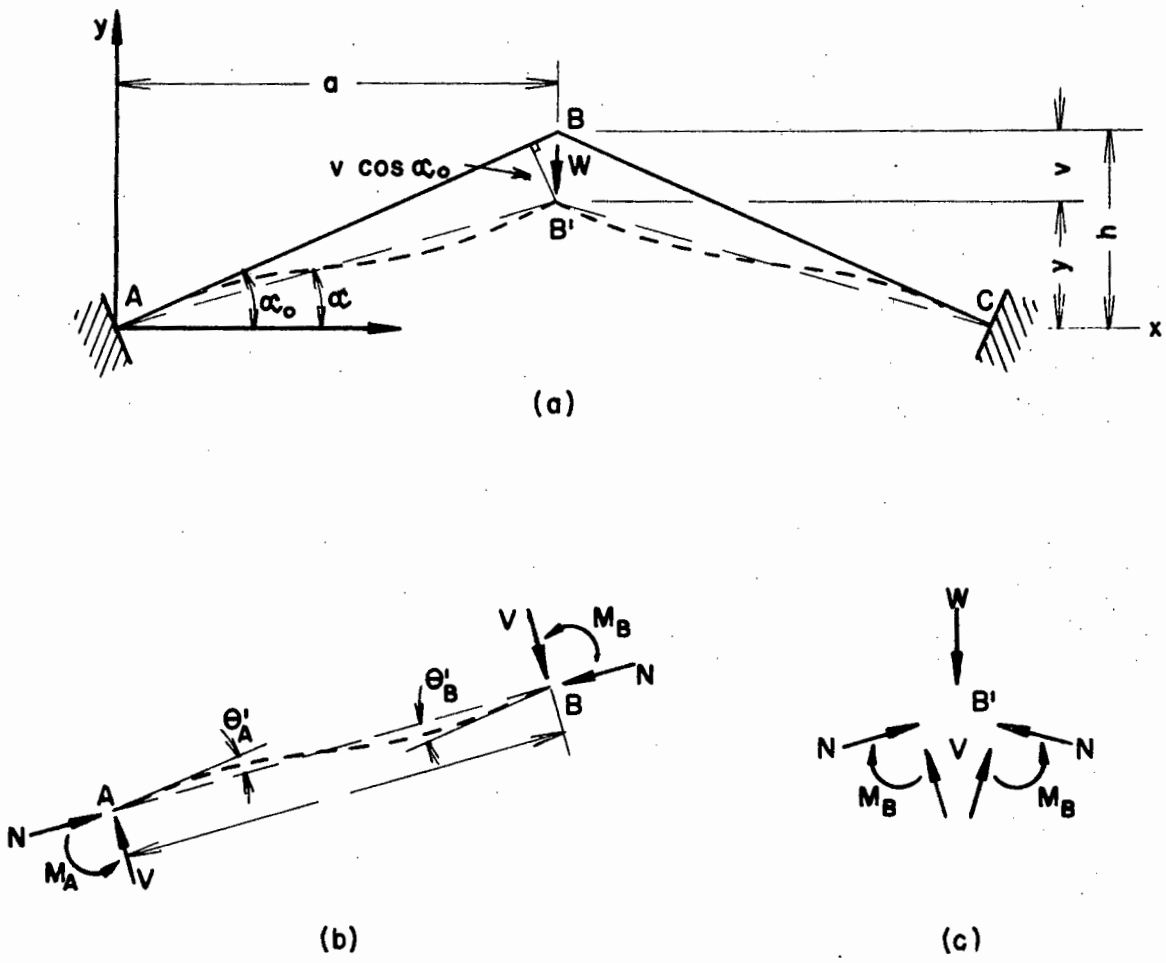

Fig. 5.1: William's toggle, Example 5.1

under axial compression as derived in Appendix A.

Now,

$$\theta'_A = \theta'_B = \sin^{-1}\left(\frac{v \cos \alpha_o}{L}\right), \tag{5.6}$$

and since

$$M_B = \frac{VL}{2}$$

then

$$V = \frac{2}{L}\left(S_{BB} + S_{BA}\right) \sin^{-1}\left(\frac{v \cos \alpha_o}{L}\right) \tag{5.7}$$

Thus equation 5.1 becomes

$$W = 2N \sin \alpha + \frac{4}{L}\left(S_{BB} + S_{BA}\right) \sin^{-1}\left(\frac{v \cos \alpha_o}{L}\right) \cos \alpha$$

and therefore

$$W = 2N\frac{(h - v)}{L} + \frac{4a}{L^2}\left(S_{AA} + S_{AB}\right) \sin^{-1}\left(\frac{v \cos \alpha_o}{L}\right) \tag{5.8}$$

Thus for a chosen value of v, the magnitude of the axial force N may be found from equations 5.2, 5.3 and 5.4; hence the flexural stiffness coefficients S_{AA} and S_{AB} may be evaluated from equations 4.32; and hence the value of load W corresponding to the chosen value of v may be found from equation 5.8.

The dimensions and properties of the aluminium toggle analysed and tested by Williams and analysed by Jennings are:-

$a = 12{,}9361$ in,
$h = 0{,}3196$ in,
$EA = 1{,}885 \times 10^6$ lb,
and $EI = 9{,}274 \times 10^3$ lb/in^2.

Using these data in equation 5.8 produced a curve of vertical load W vs. vertical deflection v, which is labelled curve (f) in Fig. 5.2. This

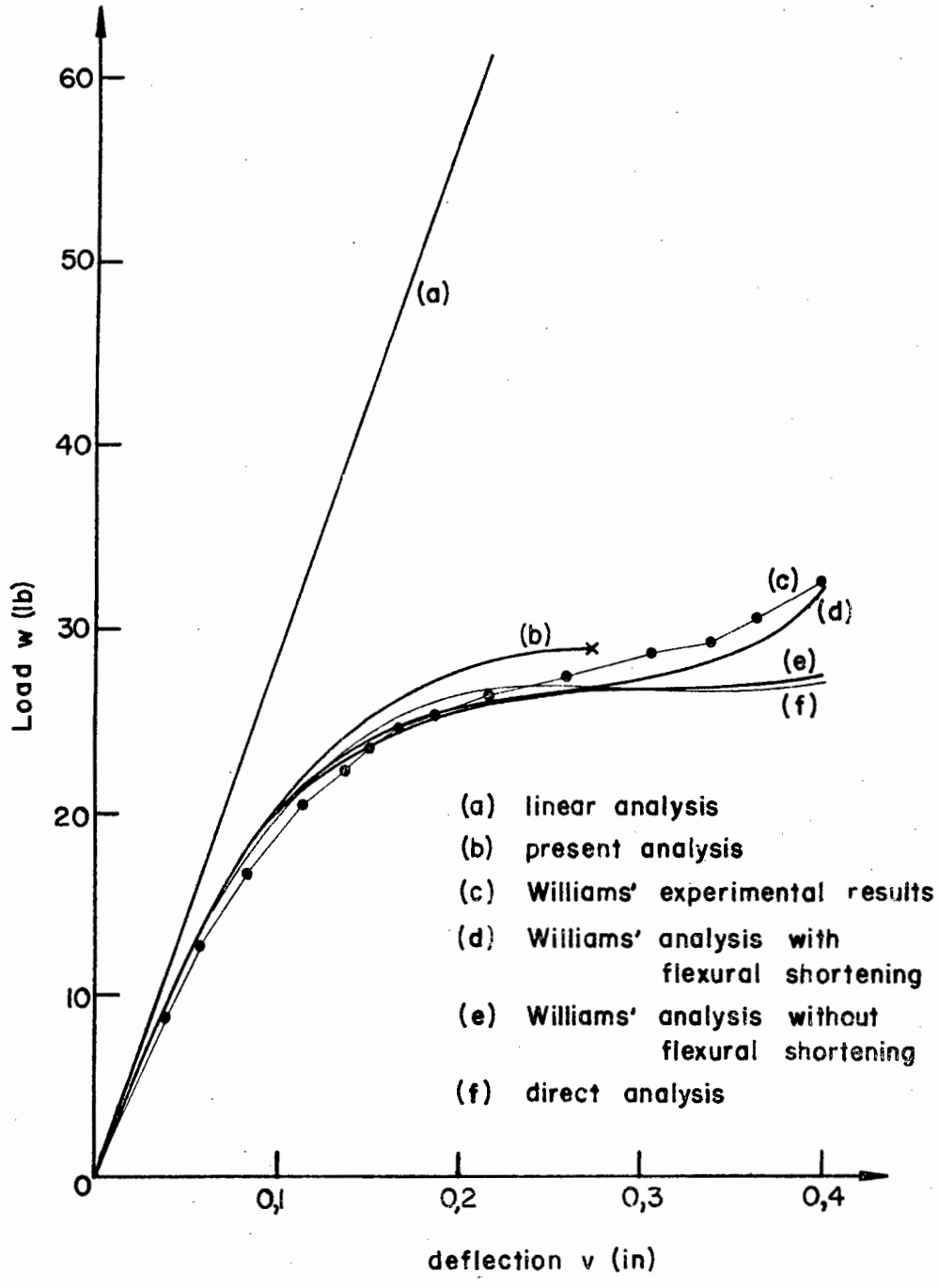

Fig. 5.2: Load-deflection characteristics of William's toggle

curve has a local maximum value of $W = 27{,}01$ lb when $v = 0{,}250$ in, and thus elastic instability should occur.

From experimental work Williams gives the stress at the limit of proportionality of the aluminium alloy in compression as 48 000 lb/in^2. In the loading range considered, the compressive stress remains well below this elastic limit.

Curve (a) in Fig. 5.2 was obtained from simple linear elastic theory while curve (c) summarizes the results obtained experimentally by Williams. This curve exhibits no 'snap-through' characteristic as predicted by the direct analytical approach which did, however, ignore the effect of flexural shortening. A theoretical analysis assumes a rigid joint of zero length at the apex of the toggle, that the ends of the members were perfectly encastré, that the material behaviour was not appreciably altered in the region of the rigid joint and the encastré ends of the members, and that the vertical load W was applied as a line-load at the apex of the toggle. As Williams states, these conditions were clearly not fully attained in his experimental work.

Curves (d) and (e) in Fig. 5.2 were obtained by Williams by using an iterative (but not incremental) approach. Curve (e) represents the results of an analysis which allows for the effects of large deflections and rotations at the ends of the member, while curve (d) in addition to these, allows for the effect of flexural shortening. The difference between curve (d) and curve (e) is thus a measure of the effect of flexural shortening of the members on the behaviour of the toggle.

Jennings' non-linear analysis takes account of flexural shortening and the effect of axial load on flexural stiffness by assuming that the elastic line of a deformed member follows a cubic curve. His more accurate results, using several sub-members per member, agree closely with Williams' solution

Curve (b) in Fig. 5.2 was obtained from the results of an incremental non-linear displacement method analysis as outlined in Chapter 4. The determinant of the structure stiffness matrix became zero at a load of $W = 29{,}00$ lb corresponding to a vertical deflection of $v = 0{,}274$ in. This load is 7 per cent higher than the critical load of the direct analytical solution, i.e. curve (f), while Williams' results do not predict any point of elastic instability at all.

Example 5.2:

For the rigid frame shown in Fig. 5.3, Wang[38] gives the numerical values of a non-linear analysis which takes account of finite displacements and the effect of axial force on flexural stiffness, for the case

$l = 60$ in,
$W = 5000$ lb
$E = 30 \times 10^6$ lb/in^2,
$A = 3{,}0682$ in^2,
and $I = 6{,}9919$ in^4.

Wang assumes no elastic limit. Analysing this toggle by means of the incremental non-linear displacement method of the preceeding chapter produced results in good agreement with those of Wang.

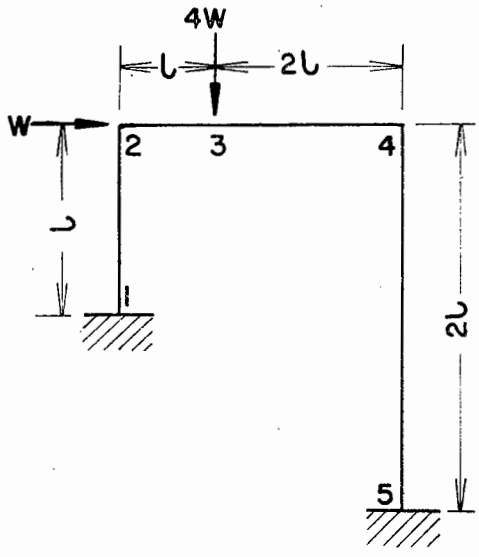

Fig. 5.3: Wang's rigid frame

An indication of the order of magnitude of the inherent error in a linear analysis of this structure and loading case is summarised in Table 5.1. The linear analysis required 0,448 sec CPU time, while the particulars of the non-linear analysis of Table 5.1 are listed under Analysis I in Table 5.2. The percentage errors listed in the last column of Table 5.1 gives the difference in magnitude of the linear and non-linear deflection or force as a percentage of the non-linear value listed in column 4 of the table. A positive percentage error implies that the magnitude of the non-linear value is greater than that of the linear.

		Linear Analysis	Non-Linear Analysis	% Error*
Node 2	u_x ≠	8,96313	10,6532	16
	u_y	- 0,01535	- 0,48822	97
	θ	- 0,12170	- 0,13618	11
Node 3	u_x	8,96145	10,3230	13
	u_y	- 5,87550	- 6,76634	13
	θ	- 0,03995	- 0,04023	1
Node 4	u_x	8,95808	10,1426	12
	u_y	- 0,02144	- 0,23684	91
	θ	0,04344	0,04777	9
Member 12	N_{12}	- 11778	- 11010	7
	V_{12}	2420	3614	33
	M_1	357914	447228	20
	M_2	- 67538	- 13634	- 396
Member 23	N_{23}	- 2580	- 1253	- 106
	V_{23}	11778	11620	- 1
	M_2	67538	13561	- 398
	M_3	639112	683625	7
Member 34	N_{34}	- 2580	- 1981	- 30
	V_{34}	- 8223	- 8847	7
	M_3	- 639112	- 683672	7
	M_4	- 347589	- 377920	8
Member 45	N_{45}	- 8223	- 8593	4
	V_{45}	2580	2836	9
	M_4	347589	377922	8
	M_5	271660	302581	10

≠ units: u_x, u_y in
θ rad.
N, V lb
M lb in

* % Error is calculated as the difference in magnitude of the linear and non-linear deflection or force as a percentage of the non-linear value.

Table 5.1: Linear and non-linear analyses of Example 5.2

Since this rigid frame has nine degrees of freedom, there are nine statics checks, these being the three conditions of equilibrium at each of the nodes 2, 3 and 4. Recalling that the directions of the axial and shear forces of the deformed structure are those associated with the directions of the straight lines joining the displaced ends of the members, resolving these nodal forces in the directions of the global axes will give some indication of the consistency of the solution. Details of the arithmetic will not be shown but the final results are given in Table 5.3, where the particulars of Analyses I, II, III and IV may be obtained from Table 5.2.

	Analysis I	Analysis II	Analysis III	Analysis IV
Number of equal load increments to final load W = 5000 lb.	20	50	20	50
Summed iteration deflection convergence tolerance	$1,0 * 10^{-2}$	$1,0 * 10^{-2}$	$1,0 * 10^{-6}$	$1,0 * 10^{-6}$
Total number of iterations required	60	100	100	200
CPU time (sec)	1,931	3,219	2,852	5,606

Table 5.2: Non-linear analyses of Example 5.2

As can be seen from Table 5.3 the accuracy of the incremental non-linear displacement method solution is best improved by decreasing the size of the load increments rather than by decreasing the summed iteration deflection convergence tolerance - for example, Analyses II and III both required the same total number of iterations, but Analysis II, with a greater number of load increments, produced a more consistent solution. Comparing the percentage errors of Analyses I and II with those of Analyses III and IV respectively, it may be seen that for the same number of load increments, some percentage errors increase when the summed iteration deflection convergence tolerance is decreases from 10^{-2} to 10^{-6}. This is probably due to accumulative computational errors after the larger number of iterations required.

		Analysis I		Analysis II		Analysis III		Analysis IV	
Node	Force‡	Value	% * Error	Value	% Error	Value	% Error	Value	% Error
2	ΣP_x	+ 5978 - 6062	1,39	+ 5970 - 5962	0,14	+ 5978 - 6068	1,49	+ 5973 - 5987	0,23
	ΣP_y	+ 11418 - 11556	1,20	+ 11442 - 11498	0,49	+ 11428 - 11556	1,11	+ 11478 - 11498	0,17
	ΣM	+ 13634 - 13561	0,53	+ 15211 - 15204	0,05	+ 13614 - 13541	0,54	+ 15144 - 15131	0,09
3	ΣP_x	+ 2462 - 2460	0,09	+ 2426 - 2440	0,57	+ 2468 - 2462	0,26	+ 2450 - 2449	0,04
	ΣP_y	+ 20239 - 20390	0,74	+ 20260 - 20234	0,13	+ 20390 - 20240	0,74	+ 20261 - 20237	0,12
	ΣM	+ 683672 - 683625	0,01	+ 678433 - 678429	0,00	+ 683695 - 683647	0,01	+ 678513 - 678505	0,00
4	ΣP_x	+ 2823 - 2833	0,37	+ 2797 - 2807	0,36	+ 2825 - 2833	0,29	+ 2806 - 2807	0,05
	ΣP_y	+ 8813 - 8834	0,23	+ 8752 - 8761	0,11	+ 8815 - 8834	0,21	+ 8760 - 8763	0,03
	ΣM	+ 377920 - 377922	0,00	+ 374440 - 374440	0,00	+ 377937 - 377939	0,00	+ 374500 - 374500	0,00

‡ units: P_x, P_y lb
M lb in

* % Error is calculated as the difference in magnitude of the positive and negative values as a percentage of their mean magnitude.

Table 5.3: Statics checks for non-linear analyses of Example 5.2

Example 5.3:

The analysis of the rigid frame shown in Fig. 5.4 reduces to an eigenvalue problem when $H = 0$. However, by giving H a small non-zero value (of the order of 0,1 % of W), the antisymmetric buckling mode will be induced. For this case Timoshenko and Gere[35] give the critical load as

$$W_c = 7{,}38 \frac{EI}{l^2} \tag{5.9}$$

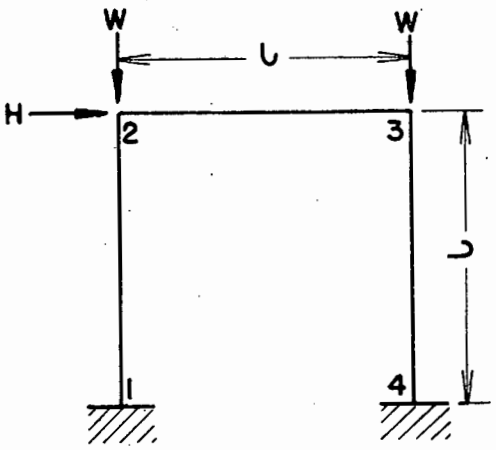

Fig. 5.4: Rigid frame

For the configuration of Fig. 5.4, with

$l = 120$ in,
$E = 30 \times 10^6$ lb/in^2,
$EA = 353{,}1 \times 10^6$ lb,
and $EI = 9303{,}0 \times 10^6$ lb in^2,

evaluation of equation 5.9 gives

$$W_c = 4{,}77 \times 10^6 \text{ lb.}$$

Using the incremental non-linear displacement method of Chapter 4, and setting $H = W/1000$, the critical value of W was found to be

$$W = 4{,}83 \times 10^6 \text{ lb,}$$

which is within 1,25 % of the value given by Timoshenko and Gere. A curve of horizontal deflection vs. W is given in Fig. 5.5. This non-linear solution was obtained by using six load increments of $0,5 \times 10^6$ lb, then four increments of $0,25 \times 10^6$ lb, and then load increments of $0,1 \times 10^6$ lb up to the point of elastic instability at $W = 4,83 \times 10^6$; the solution requiring a total of 101 iterations for a summed iteration deflection convergence tolerance of 0,05, and taking 3,015 sec. CPU time.

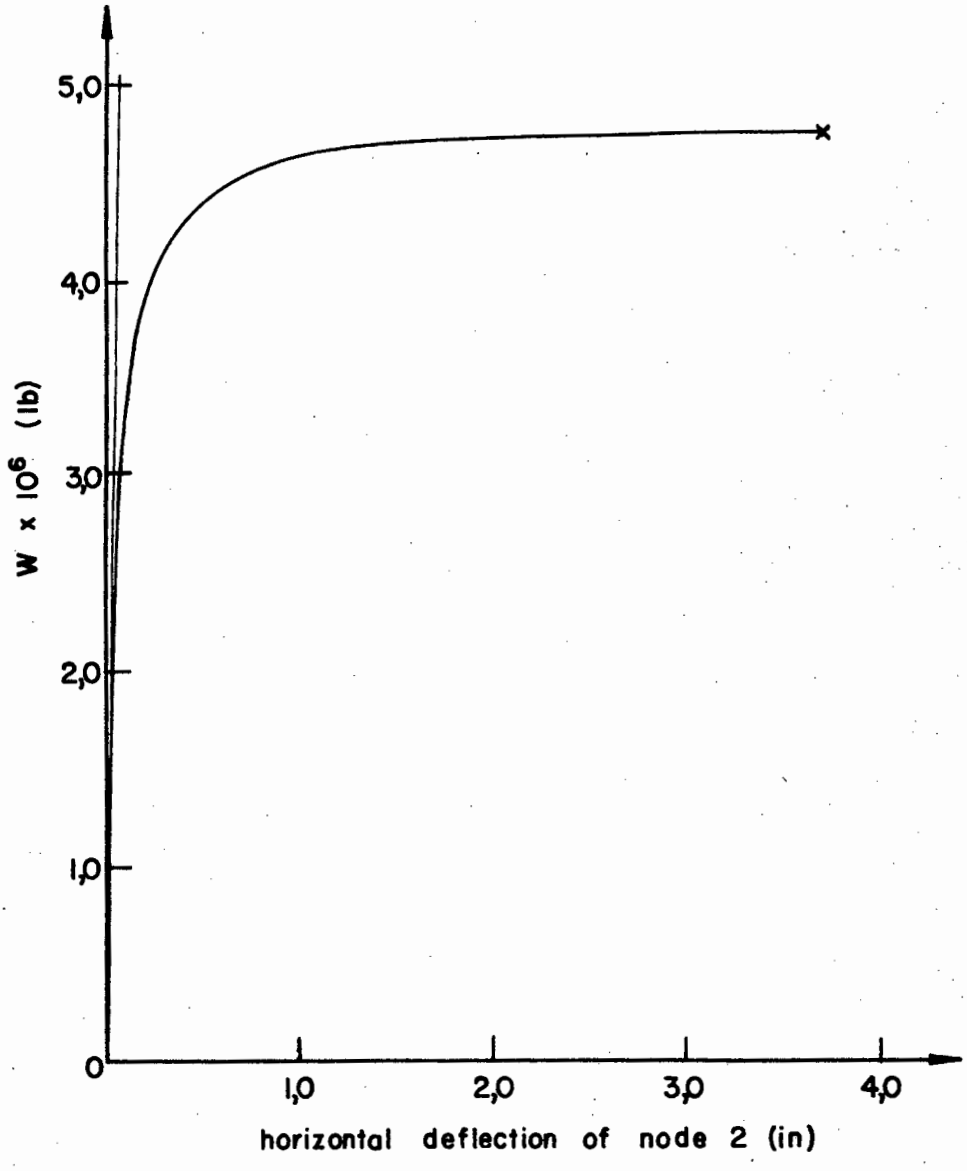

Fig. 5.5: Load-deflection characteristics of Example 5.3

Example 5.4:

An example of a circular arch of radius R, with a concentrated load W acting at the crescent is shown in Fig. 5.6. Tezcan and Ovunc[34], using ten sub-members as shown, give numerical results for the case

$R = 10$ ft,
$E = 30 \times 10^6$ lb/in^2,
$A = 1{,}0$ in^2,
and $I = 0{,}08333$ in^4.

In the incremental non-linear displacement method analysis, symmetry was made use of, and in Table 5.4 deflections and moments obtained from the present analysis (using equal load increments of 5 lb and a summed iteration deflection convergence tolerance of 0,01), are compared with values obtained by Tezcan and Ovunc, for the load case W = 940 lb.

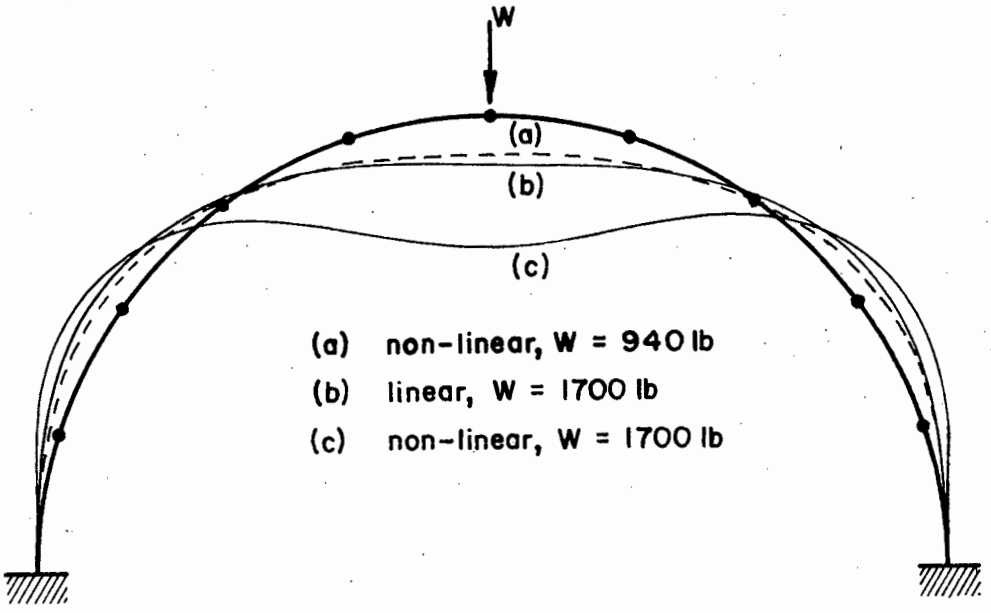

Fig. 5.6: Circular arch

Figure 5.6 shows the deflected shape of the arch. Curve (a) represents the non-linear analysis of Table 5.4, i.e. W = 940 lb, while curves (b) and (c) represent the results of linear and non-linear analyses respectively, for the load case W = 1700 lb.

Node ≠		Linear	Tezcan and Ovunc	Present Analysis
1	u_x	0	0	0
	u_y	0	0	0
	θ	0	0	0
	M	- 11905	- 14244	- 14371
3	u_x	- 3,8676	- 4,6824	- 4,7041
	u_y	1,2366	1,3128	1,3215
	θ	0,0110	0,0050	0,0055
	M	7762	10404	10581
4	u_x	- 2,6820	- 2,8728	- 2,9004
	u_y	0,0498	- 0,6240	- 0,6154
	θ	- 0,0978	- 0,1412	- 0,1417
	M	6741	8472	8697
6	u_x	0	0	0
	u_y	- 7,4342	-10,8996	-10,9500
	θ	0	0	0
	M	16520	- 20184	- 20400

≠ units: u_x, u_y in
θ rad.
M lb in

Table 5.4: Results for circular arch, W = 940 lb

Tezcan and Ovunc, whose analysis takes account of flexural shortening as well as finite displacements, give the critical value of W which causes the arch to buckle as W_{cr} = 956 lb; however, in the incremental non-linear displacement method analysis the determinant was found to become zero at a load of W = 1740 lb.

It was found that increasing the number of sub-members did not alter the value of this critical load significantly.

Example 5.5:

The 10-storey, 2-bay frame of Heyman[14] consists of 33 nodes and 50 members, as shown in Fig. 5.7(a). Taking the loading as uniform and identical on all floors; if the total vertical load per unit area is w, then, for frames spaced L apart, the distributed load of Fig. 5.7(b) is wL. The loads H in Fig. 5.7(b) represent the effect of wind loading and are taken to act at beam level. The horizontal load acting on node 1 is thus $\frac{1}{2}$ H, and if the unit of wind pressure is p, then

$$H = phL.$$

The steel sections of Heyman's frame are given in Table 5.5. The numerical calculations for the working load were carried out with the following values:

w = 5 kPa,
p = 1,5 kPa,
l = 9 m,
h = 3,65 m,
and L = 6 m

Storey	Beam Section	Internal Column	External Columns
10	409 × 179 UB 67	260 × 254 UC 89	260 × 256 UC 89
9	"	"	"
8	457 × 190 UB 74	"	"
7	"	"	"
6	"	314 × 307 UC 117	"
5	"	"	"
4	460 × 191 UB 82	321 × 309 UC 137	"
3	"	327 × 311 UC 158	"
2	464 × 192 UB 89	368 × 372 UC 177	267 × 258 UC 107
1	"	"	"

Table 5.5: Steel sections of Heyman's 10-storey, 2-bay frame

A linear analysis required 4,257 sec. CPU time while an incremental, non-linear displacement method analysis (using 10 equal load increments and a summed iteration deflection convergence tolerance of 0,01) required a total of 20 iterations resulting in 26,271 sec. CPU time.

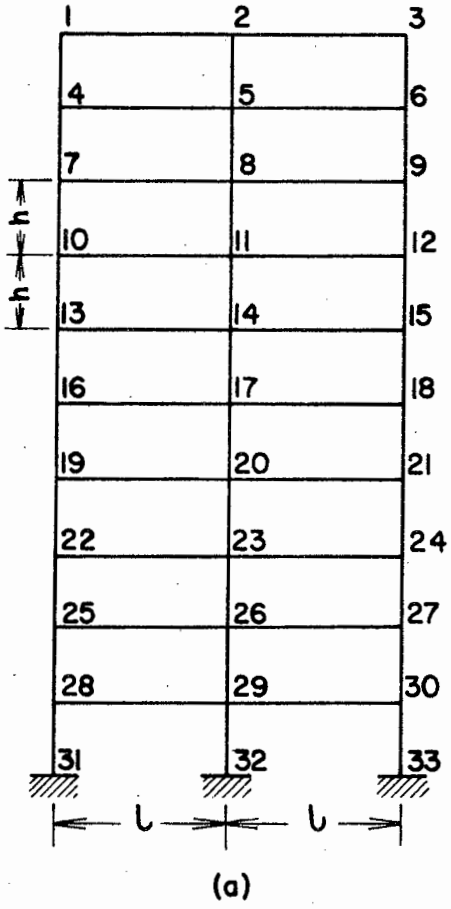

Fig. 5.7: Heyman's 10-storey, 2-bay frame. Example 5.5

The deflections at each storey level are shown in Fig. 5.8 where it is observed that the non-linear analysis increases the maximum deflection at the top storey by approximately 10 per cent.

The member end bending moments of both the linear and non-linear analyses are shown in Table 5.6, the percentage differences listed in the table being calculated as the differences between the linear and non-linear values as percentages of the latter. From Table 5.6 it should be noted that, in most cases, the magnitudes of the bending moments are increased by performing a non-linear analysis.

By using load increments of 10 % of the working load and a summed iteration deflection convergence tolerance of 0,05, the elastic critical load of the frame was found to be 8,9 times the working load. At this load, however, many of the members of the frame are strained far past the elastic limit of steel, e.g. member 30 33: compressive axial strain = 0,008
flexural strain = 0,018,
and thus the results of this elastic analysis are invalid. The 89 load increments required a total of 295 iterations which took 7 mins 8 sec. CPU time.

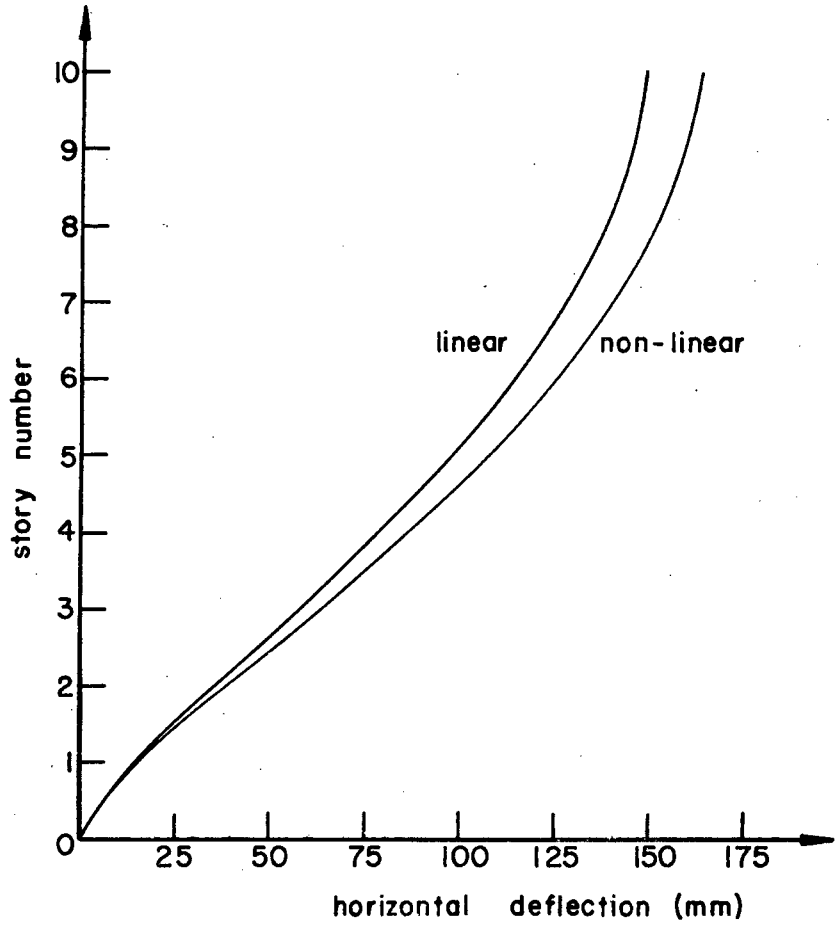

Fig. 5.8: Deflection of Example 5.5

Member		M_A (kNm)			M_B (kNm)		
A	B	linear	non-linear	% diff.	linear	non-linear	% diff.
1	2	-73.6	-74.0	.5	-30.5	-31.0	1.5
2	3	10.2	9.9	-3.0	50.1	49.6	-1.0
4	5	-45.7	-47.1	2.9	-25.6	-26.8	4.6
5	6	-30.9	-32.1	4.0	-15.9	-17.3	8.0
7	8	-94.9	-98.6	3.7	-59.6	-62.9	5.2
8	9	-54.9	-58.2	5.6	-34.8	-38.5	9.4
10	11	-127.9	-134.9	5.2	-88.0	-93.9	6.4
11	12	-77.9	-83.8	7.1	-64.1	-71.1	9.8
13	14	-159.1	-169.7	6.2	-127.1	-137.2	7.4
14	15	-108.8	-118.9	8.5	-88.4	-98.8	10.6
16	17	-186.2	-200.5	7.1	-160.0	-174.3	8.2
17	18	-135.6	-149.8	9.5	-109.6	-123.8	11.4
19	20	-224.9	-244.4	8.0	-198.4	-217.9	9.0
20	21	-165.5	-185.0	10.5	-137.1	-156.3	12.3
22	23	-251.1	-274.4	8.5	-229.8	-253.9	9.5
23	24	-190.0	-213.9	11.2	-155.7	-178.8	12.9
25	26	-275.4	-300.9	8.5	-261.2	-288.1	9.3
26	27	-221.3	-248.1	10.8	-182.9	-208.2	12.2
28	29	-267.9	-288.3	7.1	-253.3	-275.1	7.9
29	30	-202.3	-223.9	9.6	-159.1	-179.1	11.2
1	4	-128.9	-128.5	-.3	-103.8	-103.8	.1
2	5	20.3	21.1	3.7	12.1	12.5	3.4
3	6	152.4	152.9	.3	107.9	107.9	.0
4	7	-53.0	-51.6	-2.7	-66.2	-65.5	-1.1
5	8	44.4	46.5	4.5	39.3	41.0	4.2
6	9	110.5	111.9	1.2	105.0	105.6	.7
7	10	-41.4	-38.4	-7.7	-53.3	-51.7	-3.2
8	11	75.3	80.0	6.0	68.2	72.4	5.8
9	12	132.4	135.3	2.2	118.6	120.3	1.4
10	13	-21.3	-16.0	-33.4	-27.8	-23.4	-18.5
11	14	97.7	105.4	7.3	82.9	89.3	7.2
12	15	148.0	153.2	3.4	140.2	144.6	3.0
13	16	-15.6	-9.4	-66.2	-21.8	-16.6	-31.0
14	17	153.0	166.8	8.2	129.2	140.2	7.8
15	18	150.6	156.8	3.9	144.1	149.2	3.4
16	19	5.4	14.6	62.7	2.2	10.3	78.7
17	20	166.4	183.8	9.5	155.4	170.7	9.0
18	21	168.0	177.0	5.1	162.0	170.0	4.7
19	22	20.2	31.5	35.8	15.0	25.4	40.9
20	23	208.5	232.1	10.2	185.1	205.4	9.9
21	24	177.6	188.8	5.9	172.9	183.2	5.6
22	25	33.6	46.5	27.8	38.1	51.2	25.7
23	26	234.7	262.4	10.6	225.3	252.6	10.8
24	27	185.3	198.1	6.4	182.3	195.3	6.7
25	28	34.8	47.2	26.1	39.1	53.2	26.5
26	29	257.2	283.5	9.3	272.1	304.5	10.6
27	30	203.1	215.4	5.7	212.8	226.8	6.2
28	31	26.3	32.6	19.3	127.5	139.1	8.3
29	32	183.5	194.3	5.6	464.0	497.9	6.8
30	33	148.7	154.7	3.9	189.1	200.6	5.7

Table 5.6: Bending Moments of Example 5.5

CONCLUSIONS

An incremental non-linear displacement method for the elastic analysis of space trusses and plane frames has been presented. Fortran V computer programmes were developed to apply the analytical method to numerical examples. The results of these numerical examples show the capabilities and limitations of the method, and where comparisons could be made, the results were in good agreement with those in the literature, which were obtained by other methods. Further development of the method to analyse rigid-jointed space frames can be accomplished without difficulty.

Using an approximate method, non-linearity due to material behaviour can be included in the incremental analysis. By approximating the stress-strain characteristics of the material of construction with a suitable equation, after each load increment the instantaneous stress-strain relationship can be determined by evaluating the slope of the stress-strain curve at the current value of stress existing in each member of the structure. The further approximation must then be made that these instantaneous stress-strain relationships remain constant for the increase in stress due to the next load increment.

Chord shortening of a truss compression member which has an initial imperfection in straightness was accounted for by suitable adjustment to the axial stiffness term. As Williams' [40] and Saafan's [27] numerical examples show, chord shortening of flexural members due to member-end rotations (neglected in the present analysis), can be of numerical significance and should be included in a non-linear analysis. Saafan takes account of flexural shortening by approximating the shape of the elastic line of a deformed member with a cubic curve. A further point is that while modification of member flexural stiffness due to axial load is included, the modification of axial stiffness due to bowing of flexural members is neglected.

In the application of the present analysis care must be taken to ensure that magnitudes of load increments do not cause third- and higher-order terms (neglected in the development of the method) to become of numerical significance, and thus cause the load-deflection characteristics of the structure to wander from the true relationship.

As with any displacement method analysis the system stiffness matrix is banded, the band width depending on nodal numbering. The linear portion of the system stiffness matrix is evaluated once for each load increment. As this portion is symmetric only the non-zero values on and above the leading diagonal need by calculated and stored. The non-linear portion (which is evaluated for each iteration of a load increment) is not symmetric due to the choice of second-order terms retained in the development of the analysis, and thus the full band of non-zero values must be calculated and stored.

It is likely that non-linear elastic solutions to frame analysis problems will be required by designers more frequently in future because of the development of high strength steels which are economically viable. Frames made of such materials will be more flexible and linear solutions could well involve errors of significant magnitude. In addition, the estimation of maximum frame strength as frames are more closely designed to economise on material will require more accurate methods of analysis.

References:

1. AZAR, J.J., Matrix Structural Analysis, Pergamon Press, 1972.

2. BARON, F. and VENKATESAN, M.S., Nonlinear Analysis of Cable and Truss Structures, J. Str. Div., ASCE, vol. 97, ST2, Feb., 1971.

3. BLASZKOWIAK, S. and KACZKOWSKI, Z., Iterative Methods in Structural Analysis, Polish Scientific Publishers, Warsaw, 1966.

4. CHAJES, A., Principles of Structural Stability Theory, Prentice-Hall, 1974.

5. CONNER, J.J., LOGCHER, R.D. and SHING-CHING CHAN, Nonlinear Analysis of Elastic Framed Structures, J. Str. Div., ASCE, vol. 94, ST6, June, 1968.

6. CONWAY, H.D., The Nonlinear Bending of Thin Circular Rods, ASME, vol. 78, 1956.

7. EPSTEIN, M. and TENE, Y., Nonlinear Analysis of Pin-jointed Space Structures, J. Str. Div., ASCE, vol. 97, ST9, Sept., 1971.

8. GALLAGHER, R.H. and PADLOG, J., Discrete Element Approach to Structural Instability, AIAA Journal 1(6), 1963.

9. GERE, J.M. and WEAVER, W., Analysis of Framed Structures, Van Nostrand, New York, 1965.

10. GOLDBERG, J.E. and RICHARD, R.M., Analysis of Nonlinear Structures, J. Str. Div., ASCE, vol. 89, ST4, Aug., 1963.

11. HARRISON, H.B., The Analysis of Triangulated Plane and Space Structures Accounting for Temperature and Geometric Changes, in: Space Structures, R.M. Davies, editor, University of Surrey, Sept. 1966.

12. HARTZ, B.J., Matrix Formulation of Structural Stability Problems, J. Str. Div., ASCE, vol. 91, ST6, Dec. 1965.

13. HENSLEY, R.C. and AZAR, J.J., Computer Analysis of Nonlinear Truss Structures, J. St. Div., ASCE, vol. 94, ST6, June, 1968.

14. HEYMAN, J., An Approach to the Design of Tall Steel Buildings, Proc. Int. Civ. Engrs., vol. 17, 1960.

15. HORNE, M.R., The Effect of Finite Deformations in the Elastic Stability of Plane Frames, Proc. Roy. Soc. A, 266 (1324), 1962.

16. JENNINGS, A., Frame Analysis Including Change of Geometry, J. Str. Div., ASCE, vol. 94, ST3, March, 1968.

17. JOHNSON, D. and BROTTON, D.M., A Finite Deflection Analysis for Space Structures, in: Space Structures, R.M. Davies, editor, University of Surrey, Sept., 1966.

18. LIVESLEY, R.K., The Application of an Electronic Digital Computer to Some Problems of Structural Analysis, Str. Engr., 34(1), 1956.

19. MAJID, K.I., Non-Linear Structures, Butterworth, 1972.

20. MARTIN, H.C., On the Derivation of Stiffness Matrices for the Analysis of Large Deflection and Stability Problems, Proc. 1st Conf. Matrix Methods, Ohio, Wright-Patterson Air Force Base, 1966.

21. MEEK, J.L., Matrix Structural Analysis, McGraw-Hill, 1971.

22. NOOR, A.K., Nonlinear Analysis of Space Trusses, J. Str. Div., ASCE, vol. 100, ST3, March, 1974.

23. NOVOZHILOV, V.V., Foundations of the Nonlinear Theory of Elasticity, Grayloch Press, Rochester, N.Y., 1953.

24. POSKITT, T.J., Numerical Solution of Nonlinear Structures, J. Str. Div., ASCE, vol. 93, ST4, Aug., 1967.

25. PRASAD, H.S.S., TEZCAN, S.S. and MAHAPATRA, B.C., Discussion of paper cited in 5. above, J. Str. Div., ASCE, vol. 95, ST3, March, 1969.

26. RENTON, J.D., Stability of Space Frames by Computer Analysis, J. Str., Div., ASCE, vol. 88, ST4, Aug., 1962.

27. SAAFAN, S.A., Nonlinear Behaviour of Structural Plane Frames, J. Str. Div., ASCE, vol. 89, ST4, Aug., 1963.

28. SALEM, A.H., Buckling of Rigidly Jointed Plane Trusses, J. Str. Div., ASCE, vol. 95, ST6, June, 1969.

29. SHAW, F.S., Virtual Displacements and Analysis of Structures, Prentice-Hall, 1972.

30. SPIEGAL, M.R., Mathematical Handbook, McGraw-Hill, 1968.

31. TAKABEYA, F., Multi-Storey Frames, Wilhelm Ernst and Sohn, Berlin, 1965.

32. TEZCAN, S.S., Computer Analysis of Plane and Space Frames, J. Str. Div. ASCE, vol. 92, ST2, April, 1966.

33. TEZCAN, S.S. and MAHAPATRA, B.C., Tangent Stiffness Matrix for Space Frame Members, J. Str. Div., ASCE, vol. 95, ST6, June, 1969.

34. TEZCAN, S.S. and OVUNC, B., An Iteration Method for the Nonlinear Buckling of Framed Structures, in: Space Structures, R.M. Davies, editor, University of Surrey, Sept., 1966.

35. TIMOSHENKO, S.P. and GERE, J.M., Theory of Elastic Stability, McGraw-Hill, 1961.

36. TURNER, M.J., CLOUGH, R.W., MARTIN, H.C. and TOPP, L.J., Stiffness and Deflection Analysis of Complex Structures, J. Aero. Sciences, vol. 23, No. 9, Sept., 1956.

37. TURNER, M.J., DILL, E.H., MARTIN, H.C. and MELOSH, R.J., Large Deflections of Structures Subjected to Heating and External Loads, J. Aero. Sciences, vol. 27, Feb., 1960.

38. WANG, C., Computer Methods in Advanced Structural Analysis, Intext Press, New York, 1973.

39. WHITE, R.N., GERGELY, P. and SEXSMITH, R.G., Structural Engineering, vol. 2, Indeterminate Structures, John Wiley and Sons, 1972.

40. WILLIAMS, F.W. An Approach to the Nonlinear Behaviour of the Members of a Rigid Jointed Plane Framework with Finite Deflections, Quart. J. Mech and App. Maths., vol. 17, Nov., 1964.

41. WISEMANN, J.W., Nonlinear Structural Analysis, Proc. 1st Conf. Matrix Methods, Ohio, Wright-Patterson Air Force Base, 1966.

42. YOSHIZAWA, N., Numerical Analysis of Nonlinear Problems of Pin-Jointed Trusses, Trans. Japan Soc. Engrs., vol. 2, part 2, 1970.

43. ZIEGLER, H., Principles of Structural Stability, Blaisdell Publishing Co., Waltham, Mass., 1968.

APPENDIX A : Stiffness Coefficients in Flexure[38]

Consider first the case in which the axial force N of Fig. A.1 is tensile.

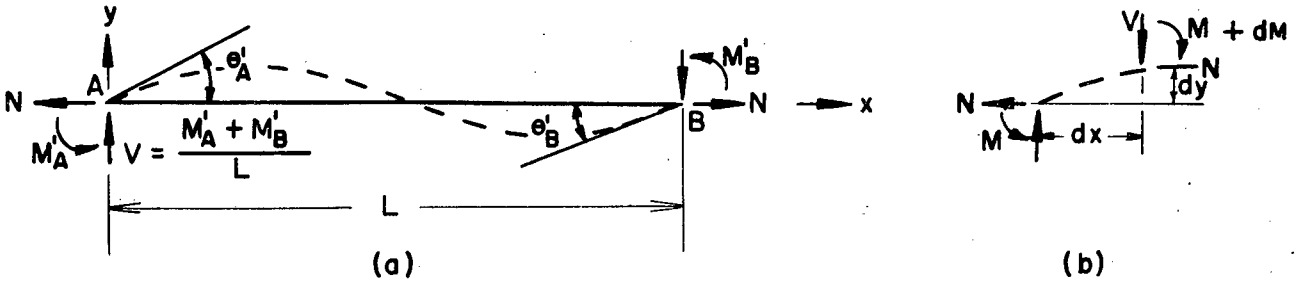

Fig. A.1: A flexural member under axial tension

For moment equilibrium of an infinitesimal segment dx in Fig. A.1b,

$$(M + dM) + Vdx + Ndy = M$$

therefore

$$\frac{dM}{dx} = -N\frac{dy}{dx} - V,$$

and differentiating with respect to x yields

$$\frac{d^2M}{dx^2} = -N\frac{d^2y}{dx^2} - \frac{dV}{dx}, \qquad \text{A.2}$$

but, without transverse load on the segment, $\frac{dV}{dx} = 0$.
Using the usual beam bending theory, the curvature of the elastic line is

$$\frac{d^2y}{dx^2} = -\frac{M}{EI}. \qquad \text{A.3}$$

Hence, equation A.2 becomes

$$\frac{d^4y}{dx^4} = \frac{N}{EI}\frac{d^2y}{dx^2},$$

or, writing $\phi = L\sqrt{\frac{N}{EI}}$,

$$\frac{d^4y}{dx^4} - \frac{\phi^2}{L^2}\frac{d^2y}{dx^2} = 0, \qquad \text{A.4}$$

which has the complete solution given by

$$y = A \sinh \frac{\phi}{L} x + B \cosh \frac{\phi}{L} x + Cx + D. \qquad \text{A.5}$$

Applying the four boundary conditions

$$y = 0 \quad \text{when} \quad x = 0,$$
$$y = 0 \quad \text{when} \quad x = L,$$
$$\frac{dy}{dx} = \theta'_A \quad \text{when} \quad x = 0,$$
$$\text{and} \quad \frac{dy}{dx} = \theta'_B \quad \text{when} \quad x = L,$$

results in four simultaneous linear equations which may be solved to give:

$$\frac{A}{L} = \frac{(1 - \cosh \phi + \phi \sinh \phi)\ \theta'_A + (\cosh \phi - 1)\ \theta'_B}{\phi(2 - 2 \cosh \phi + \phi \sinh \phi)} \qquad \text{A.6a}$$

$$\frac{B}{L} = \frac{(\sinh \phi - \phi \cosh \phi)\ \theta'_A + (\phi - \sinh \phi)\ \theta_B}{\phi(2 - 2 \cosh \phi + \phi \sinh \phi)}, \qquad \text{A.6b}$$

$$C = \frac{(1 - \cosh \phi)\ \theta'_A + (1 - \cosh \phi)\ \theta'_B}{(2 - 2 \cosh \phi + \phi \sinh \phi)}, \qquad \text{A.6c}$$

$$\text{and} \quad \frac{D}{L} = \frac{(\phi \cosh \phi - \sinh \phi)\ \theta'_A + (\sinh \phi - \phi)\ \theta'_B}{\phi(2 - 2 \cosh \phi + \phi \sinh \phi)}. \qquad \text{A.6d}$$

Differentiating equation A.5 yields

$$\frac{d^2y}{dx^2} = A \frac{\phi^2}{L^2} \sinh \frac{\phi}{L} x + B \frac{\phi^2}{L^2} \cosh \frac{\phi}{L} x,$$

and from equation A.3 we therefore have

$$M_x = - EI \frac{\phi^2}{L^2} (A \sinh \frac{\phi}{L} + B \cosh \frac{\phi}{L} x).$$

When $x = 0$, $M_x = M'_A$,

therefore

$$M'_A = - EI \frac{\phi^2}{L^2} B; \qquad \text{A.7a}$$

and when $x = L$, $M_x = - M'_B$,

therefore $M'_B = EI \frac{\phi^2}{L^2} (A \sinh \phi + B \cosh \phi)$. A.7b

Substituting equations A.6 into equations A.7 yields

$$\begin{Bmatrix} M'_A \\ M'_B \end{Bmatrix} = \begin{bmatrix} \frac{\phi^2 \cosh \phi - \phi \sinh \phi}{2 - 2 \cosh \phi + \phi \sinh \phi} \frac{EI}{L} & \frac{\phi \sinh \phi - \phi^2}{2 - 2 \cosh \phi + \phi \sinh \phi} \frac{EI}{L} \\ \frac{\phi \sinh \phi - \phi^2}{2 - 2 \cosh \phi + \phi \sinh \phi} \frac{EI}{L} & \frac{\phi^2 \cosh \phi - \phi \sinh \phi}{2 - 2 \cosh \phi + \phi \sinh \phi} \frac{EI}{L} \end{bmatrix} \begin{Bmatrix} \theta'_A \\ \theta'_B \end{Bmatrix}. \quad \text{A.8}$$

If N is a compressive force, the differential equation of the elastic line (equation A.4) becomes

$$\frac{d^4y}{dx^4} + \frac{\phi^2}{L^2} \frac{d^2y}{dx^2} = 0;$$

the general solution of which is given by

$$y = A \sin \frac{\phi}{L} x + B \cos \frac{\phi}{L} x + Cx + D; \quad \text{A.9}$$

and applying the boundary conditions as before yields

$$\frac{A}{L} = \frac{(1 - \cos \phi - \phi \sin \phi) \theta'_A + (\cos \phi - 1) \theta'_B}{\phi(2 - 2 \cos \phi - \phi \sin \phi)}, \quad \text{A.10a}$$

$$\frac{B}{L} = \frac{(\sin \phi - \phi \cos \phi) \theta'_A + (\phi - \sin \phi) \theta'_B}{\phi(2 - 2 \cos \phi - \phi \sin \phi)}, \quad \text{A.10b}$$

$$C = \frac{(1 - \cos \phi) \theta'_A + (1 - \cos \phi) \theta'_B}{(2 - 2 \cos \phi - \phi \sin \phi)},$$

and $$\frac{D}{L} = \frac{(\phi \cos \phi - \sin \phi) \theta'_A + (\sin \phi - \phi) \theta'_B}{\phi(2 - 2 \cos \phi - \phi \sin \phi)}.$$

Differentiating equation A.9 and substituting into equation A.3 yields

$$M_x = EI \frac{\phi^2}{L^2} (A \sin \frac{\phi}{L} x + B \cos \frac{\phi}{L} x).$$

Again, when $x = 0$, $M_x = M'_A$,

therefore,

$$M'_A = EI \frac{\phi^2}{L^2} B; \quad \text{A.11a}$$

and when $x = L$, $M_x = - M'_B$,

therefore,

$$M'_B = - EI \frac{\phi^2}{L^2} (A \sin \phi + B \cos \phi). \qquad \text{A.11b}$$

Substituting equations A.10 into equations A.11 yields

$$\begin{Bmatrix} M'_A \\ M'_B \end{Bmatrix} = \begin{bmatrix} \frac{\phi \sin \phi - \phi^2 \cos \phi}{2 - 2 \cos \phi - \phi \sin \phi} \frac{EI}{L} & \frac{\phi^2 - \phi \sin \phi}{2 - 2 \cos \phi - \phi \sin \phi} \frac{EI}{L} \\ \frac{\phi^2 - \phi \sin \phi}{2 - 2 \cos \phi - \phi \sin \phi} \frac{EI}{L} & \frac{\phi \sin \phi - \phi^2 \cos \phi}{2 - 2 \cos \phi - \phi \sin \phi} \frac{EI}{L} \end{bmatrix} \begin{Bmatrix} \theta'_A \\ \theta'_B \end{Bmatrix}. \qquad \text{A.12}$$

Equations A.8 and A.12 may be written in the form

$$\begin{Bmatrix} M'_A \\ M'_B \end{Bmatrix} = \begin{bmatrix} S_{AA} & S_{AB} \\ S_{BA} & S_{BB} \end{bmatrix} \begin{Bmatrix} \theta'_A \\ \theta'_B \end{Bmatrix}$$

where $S_{AA} = S_{BB}$,

and $S_{AB} = S_{BA}$.

Equations A.8 and A.12 are undefined if $\phi = 0$ (i.e. if $N = 0$), in which case equations 4.30 are applicable.

Curves of S_{AA} and S_{AB} vs N for N tensile and compressive are given in Fig. 4.4.

APPENDIX B : The Incremental Non-Linear Member Stiffness Matrix for a Member of a Plane Frame

The relationship between the increments in external forces and external displacements is

$$d\underline{P} = [K]\, d\underline{u}$$

or

$$d\begin{Bmatrix} P_{xa} \\ P_{ya} \\ M_A \\ P_{xB} \\ P_{yB} \\ M_B \end{Bmatrix} = \begin{bmatrix} k_{11} & k_{12} & k_{13} & k_{14} & k_{15} & k_{16} \\ k_{21} & k_{22} & k_{23} & k_{24} & k_{25} & k_{26} \\ k_{31} & k_{32} & k_{33} & k_{34} & k_{35} & k_{36} \\ k_{41} & k_{42} & k_{43} & k_{44} & k_{45} & k_{46} \\ k_{51} & k_{52} & k_{53} & k_{54} & k_{55} & k_{56} \\ k_{61} & k_{62} & k_{63} & k_{64} & k_{65} & k_{66} \end{bmatrix} d\begin{Bmatrix} u_{Ax} \\ u_{Ay} \\ \theta_A \\ u_{Bx} \\ u_{By} \\ \theta_B \end{Bmatrix}.$$

The incremental member stiffness matrix $[K]$ may be written

$$[K] = [K^L] + [K^{NL}],$$

where $[K^L]$ is the linear portion of $[K]$, i.e. $[K^L]$ is independent of the increments in displacements $d\underline{u}$; and $[K^{NL}]$ is the non-linear portion of $[K]$.

From equations 4.35, 4.37, 4.38, 4.39 and 4.40,

$$\begin{bmatrix} k_{11} & k_{12} \\ k_{21} & k_{22} \end{bmatrix}^L = \left[(K' L_i - \frac{N_i}{L_i})[\bar{T}_i] + \frac{N_i}{L_i}[I] + \frac{M'_i}{L_i^2}\left[2[H_i] - [\bar{I}]\right] + 2\frac{S_i}{L_i}[\bar{R}] \right],$$

$$\begin{bmatrix} k_{11} & k_{12} \\ k_{21} & k_{22} \end{bmatrix}^{NL} = \left[(K' - \frac{N_i}{L_i^2})\left[[B_i] + \tfrac{1}{2}[B_i]^t\right] - (K' - \frac{3}{2}\frac{N_i}{L_i^2})\, C_i\, [\bar{T}_i] \right.$$

$$\left. - \frac{S_i}{L_i^2}\left[6\, C_i[\bar{R}_i] - 2\, G_i[\bar{I}]\right] - \frac{M'_i}{L_i^3}\left[4\, C_i[H_i] - 2\, C_i[\bar{I}] - [Q_i]\right] \right],$$

$$\begin{bmatrix} k_{44} & k_{45} \\ k_{54} & k_{55} \end{bmatrix} = \begin{bmatrix} k_{11} & k_{12} \\ k_{21} & k_{22} \end{bmatrix}, \quad \begin{bmatrix} k_{14} & k_{15} \\ k_{24} & k_{25} \end{bmatrix} = \begin{bmatrix} k_{41} & k_{42} \\ k_{51} & k_{52} \end{bmatrix} = -\begin{bmatrix} k_{11} & k_{12} \\ k_{21} & k_{22} \end{bmatrix},$$

$$\begin{bmatrix} k_{13} \\ k_{23} \end{bmatrix}^{L} = S_i \, \underline{R}_i,$$

$$\begin{bmatrix} k_{13} \\ k_{23} \end{bmatrix}^{NL} = \frac{S_i}{L_i} \left\{ [\bar{I}] \, \underline{\delta} - 2 \, C_i \, \underline{R}_i \right\},$$

$$\begin{bmatrix} k_{16} \\ k_{26} \end{bmatrix} = \begin{bmatrix} k_{13} \\ k_{23} \end{bmatrix}, \quad \begin{bmatrix} k_{43} \\ k_{53} \end{bmatrix} = \begin{bmatrix} k_{46} \\ k_{56} \end{bmatrix} = - \begin{bmatrix} k_{13} \\ k_{23} \end{bmatrix},$$

$$\begin{bmatrix} k_{33} \end{bmatrix} = \begin{bmatrix} k_{66} \end{bmatrix} = S_{AA_i},$$

$$\begin{bmatrix} k_{36} \end{bmatrix} = \begin{bmatrix} k_{63} \end{bmatrix} = S_{AB_i},$$

$$\begin{bmatrix} k_{31} & k_{32} \end{bmatrix}^{L} = S_i \, \underline{R}_i^t,$$

$$\begin{bmatrix} k_{31} & k_{32} \end{bmatrix}^{NL} = - \frac{S_i}{L_i} \, C_i \, \underline{R}_i^t,$$

$$\begin{bmatrix} k_{61} & k_{62} \end{bmatrix} = \begin{bmatrix} k_{31} & k_{32} \end{bmatrix}, \quad \begin{bmatrix} k_{34} & k_{35} \end{bmatrix} = \begin{bmatrix} k_{64} & k_{65} \end{bmatrix} = - \begin{bmatrix} k_{31} & k_{32} \end{bmatrix},$$

where

$$N_i = EA \left(\frac{L_i^2 - L_o^2}{2L_o^2} \right), \qquad M'_i = M'_{A_i} + M'_{B_i} = (S_{AA} + S_{AB})_i (\theta'_A + \theta'_B)_i,$$

$$K' = \frac{EA}{L_o^2}, \qquad \underline{T}_i = \begin{Bmatrix} \cos \alpha_i \\ \sin \alpha_i \end{Bmatrix},$$

$$\underline{R}_i = \begin{Bmatrix} - \sin \alpha_i \\ \cos \alpha_i \end{Bmatrix}, \qquad \underline{\delta} = \begin{Bmatrix} dx \\ dy \end{Bmatrix} = \begin{Bmatrix} du_{xB} - du_{xA} \\ du_{yB} - du_{yA} \end{Bmatrix},$$

$$S_i = \frac{(S_{AA} + S_{AB})_i}{L_i}, \qquad [\bar{T}_i] = \underline{T}_i \, \underline{T}_i^t,$$

$$[I] = \begin{bmatrix} 1 & 0 \\ 0 & 1 \end{bmatrix}, \qquad [\bar{I}] = \begin{bmatrix} 0 & -1 \\ 1 & 0 \end{bmatrix},$$

$$[B_i] = \underline{\delta} \, \underline{T}_i^t, \qquad [\bar{R}_i] = \underline{R}_i \, \underline{R}_i^t,$$

$$[Q_i] = \underline{R}_i \, \underline{\delta}^t, \qquad [H_i] = \underline{R}_i \, \underline{T}_i^t,$$

$$C_i = \underline{T}_i^t \, \underline{\delta} = \underline{\delta}^t \underline{T}_i, \text{ a scalar;} \qquad G_i = \underline{R}_i^t \, \delta = \delta^t \underline{R}_i. \text{ a scalar.}$$

APPENDIX C: Computer Programme NLST for Non-Linear Space Truss Analysis

```
NLST,MAIN
 1              COMPILER (XM=1)
 2              PARAMETER NI=34,MI=60
 3              PARAMETER M=3*NI,MJ=M+1
 4              COMMON SS,SK
 5              INTEGER CON(NI,3),TITLE(12),BOW
 6              DIMENSION ME(MI,2),IC(3)
 7              DOUBLE PRECISION SS(105,105),SK(105,105),EA(MI),KD(MI),OL(MI),
 8             1NC(MI),OC(NI,3),C(NI,3),PP(M),P(M),DELP(M),U(M),DELU(M),T(MI,3),
 9             2TB(MI,3,3),EN(MI),DET,INDEX,N80
10              DOUBLE PRECISION PL(3),PIS,FINC(200),F,E,A,INERT
11              READ(8,101) (TITLE(I),I=1,12)
12          101 FORMAT(12A6)
13              WRITE(5,203) (TITLE(I),I=1,12)
14          203 FORMAT(1H1,12A6)
15          100 FORMAT()
16              READ(8,100) NN,NM
17              N=3*NN
18              NP=N+1
19              DO 1 I=1,NN
20            1 READ(8,100) (OC(I,J),J=1,3)
21              PIS=3.86960440108359
22              READ(8,102) INE
23              IF(INE.EQ.'C') READ(8,100) E
24              DO 2 I=1,NM
25              IF(INE.EQ.'C') READ(8,100) ME(I,1),ME(I,2),A,INERT
26              IF(INE.EQ.'V') READ(8,100) ME(I,1),ME(I,2),A,INERT,E
27              EA(I)=E*A
28              IE=ME(I,1)
29              JE=ME(I,2)
30              DO 9 J=1,3
31            9 PL(J)=OC(JE,J)-OC(IE,J)
32              OL(I)=DSQRT(PL(1)**2+PL(2)**2+PL(3)**2)
33              KD(I)=EA(I)/OL(I)**2
34            2 NC(I)=E*INERT*PIS/OL(I)**2
35              DO 3 I=1,NN
36              DO 3 J=1,3
37            3 CON(I,J)=1
38            6 READ(8,100) NODE1,NODE2
39              IF(NODE1.LE.0) GO TO 4
40              READ(8,100) (IC(J),J=1,3)
41              DO 15 I=NODE1,NODE2
42              DO 13 J=1,3
43           13 CON(I,J)=IC(J)
44              GO TO 6
45            4 DO 7 I=1,N
46            7 PP(I)=0
47           14 READ(8,100) NODE
48              IF(NODE.LE.0) GO TO 12
49              J=3*(NODE-1)
50              READ(8,100) (PP(I+J),I=1,3)
51              GO TO 14
52           12 READ(8,102) NAL
53          102 FORMAT(A1)
54              IF(NAL.EQ.'N') GO TO 5
55              READ(8,100) FINC(1)
56              MINC=1
```

```
      NOUT=1
      GO TO 10
    5 READ(8,100) ERROR
      READ(8,102) BOW
      IF(BOW.EQ.'B') READ(8,100) INDEX,NBO
      MINC=0
      J=0
   17 READ(8,100) I,F
      IF(I.LE.0) GO TO 19
      MINC=MINC+I
      DO 18 II=1,I
      J=J+1
   18 FINC(J)=F
      GO TO 17
   19 READ(8,100) NOUT
   10 DO 20 I=1,NM
   20 EN(I)=0
      DO 26 I=1,NN
      DO 26 J=1,3
   26 C(I,J)=OC(I,J)
      DO 24 I=1,N
      U(I)=0
   24 P(I)=0
      KOUNT=0
      INST2=0
   23 INST=0
      DO 15 I=1,MINC
      DO 16 J=1,N
   16 DELP(J)=PP(J)*FINC(I)
      KOUNT=KOUNT+1
      IF(I.EQ.1.AND.INST2.EQ.1) KOUNT=KOUNT-1
      CALL STIFF (NI,MI,M,MJ,NN,NM,N,NP,ME,CON,EA,KD,OL,NC,
     1OC,C,PF,P,DELP,U,DELU,T,TS,EN,DET,KOUNT,NOUT,INST,KOUNT2,
     2NAL,BOW,INDEX,NBO,ERROR)
      IF(INST.EQ.0) GO TO 15
      IF(INST.EQ.1.AND.INST2.EQ.0) GO TO 21
      PRINT 201
  201 FORMAT(1HO,'POINT OF INSTABILITY WAS PASSED DURING THE LAST LOAD I
     1NCREMENT')
      DO 8 IJK=1,N
      IF(P(IJK)) 11,8,11
    8 CONTINUE
   11 FACT=P(IJK)/PP(IJK)
      WRITE(5,202) FACT
  202 FORMAT(1H0,'ELASTIC CRITICAL LOAD FACTOR =',E11.6)
      WRITE(5,204) KOUNT2
  204 FORMAT(1H0,'TOTAL NO. OF ITERATIONS',I5)
      GO TO 22
   21 DO 25 J=1,20
   25 FINC(J)=FINC(I)/10
      INST2=1
      NOUT=2000
      GO TO 23
   15 CONTINUE
      IF(NAL.EQ.'L') GO TO 22
      PRINT 200
  200 FORMAT(1H0,'POINT OF INSTABILITY HAS NOT BEEN REACHED')
```

```
114          22 CONTINUE
115             END


NLS1.STIFF
  1             COMPILER (XM=1)
  2             SUBROUTINE STIFF (NI,MI,M,MJ,NN,NM,N,NP,ME,CON,EA,KD,OL,NC,
  3            1OC,C,PP,P,DELP,U,DELU,T,TB,EN,DET,KOUNT,NOUT,IAST,KOUNT2,
  4            2NAL,BOW,INDEX,NBO,ERROR)
  5             COMMON SS,SK
  6             INTEGER CON(NI,3),BOW
  7             DIMENSION ME(MI,2)
  8             DOUBLE PRECISION SS(105,105),SK(105,105),EA(MI),KD(MI),CL(MI),
  9            1NC(MI),OC(NI,3),C(NI,3),PP(M),P(M),DELP(M),U(M),DELL(M),T(MI,3),
 10            2TB(MI,3,3),EN(MI),DET,INDEX,NBO
 11             DOUBLE PRECISION PL(3),CL,CI,DEL,K(3,3),PASUM,PRSUM,B(3,3),STRAIN,
 12            1PREV,DUM1,DUM2,AX
 13             DO 1 I=1,N
 14             DO 1 J=1,N
 15           1 SK(I,J)=0
 16             DO 2 II=1,NM
 17             IE=ME(II,1)
 18             JE=ME(II,2)
 19             DO 3 J=1,3
 20           3 PL(J)=C(JE,J)-C(IE,J)
 21             CL=DSQRT(PL(1)**2+PL(2)**2+PL(3)**2)
 22             DO 4 I=1,3
 23           4 T(II,I)=PL(I)/CL
 24             IF(EN(II).GE.0.0.OR.BOW.EQ.'N') GO TO 27
 25             DUM1=DABS(INDEX*0.002/EN(II)*(EN(II)/NBO/NC(II))**INDEX)
 26             KD(II)=EA(II)/(CL(II)**2+EA(II)*OL(II)**2*DUM1)
 27          27 DO 5 I=1,3
 28             DO 5 J=1,3
 29           5 TB(II,I,J)=T(II,I)*T(II,J)
 30             DUM1=KD(II)-EN(II)/CL**2
 31             DUM2=KD(II)-1.5*EN(II)/CL**2
 32             DO 6 I=1,3
 33             DO 6 J=1,3
 34           6 K(I,J)=CL*DUM1*TB(II,I,J)
 35             DO 7 I=1,3
 36           7 K(I,I)=K(I,I)+EN(II)/CL
 37             NR=3*(IE-1)
 38             NRR=3*(JE-1)
 39             ICH=0
 40           2 CALL ADD (M,MJ,ICH,K,NR,NRR)
 41             DO 10 I=1,N
 42          10 DELU(I)=0
 43             PASUM=0
 44             MITER=200
 45             IF(NAL.EQ.'L') MITER=1
 46             DO 11 JJ=1,MITER
 47             DO 12 I=1,N
 48             DO 12 J=1,N
 49          12 SS(I,J)=SK(I,J)
 50             IF(JJ.EQ.1) GO TO 13
 51             DO 14 II=1,NM
```

```
      NR=3*(ME(II,1)-1)
      NRR=3*(ME(II,2)-1)
      CI=0
      DO 16 I=1,3
      DEL=DELU(NRR+I)-DELU(NR+I)
      CI=CI+DEL*T(II,I)
      DO 16 J=1,3
   16 B(I,J)=DEL*T(II,J)
      DO 17 I=1,3
      DO 17 J=1,3
   17 K(I,J)=DUM1*(B(I,J)+B(J,I)/2)-DUM2*CI*TB(II,I,J)
      ICH=1
   14 CALL ADD (M,MJ,ICH,K,NR,NRR)
   13 DO 19 I=1,N
   19 SS(I,NP)=DELP(I)
      L=0
      DO 20 I=1,NN
      DO 20 J=1,3
      L=L+1
      IF(CON(I,J).NE.0) GO TO 20
      DO 21 IJ=1,N
      SS(IJ,L)=0
   21 SS(L,IJ)=0
      SS(L,NP)=0
      SS(L,L)=1
   20 CONTINUE
      CALL SOLVE (M,MJ,N,NP,PRSUM,DET)
      DO 22 I=1,N
   22 DELU(I)=SS(I,NP)
      IF(DABS(PASUM/PRSUM-1).LE.ERROR) GO TO 23
   11 PASUM=PRSUM
   23 IF(DET.LE.0) GO TO 26
      KOUNT2=KOUNT2+JJ
      DO 24 I=1,N
      P(I)=P(I)+DELP(I)
   24 U(I)=U(I)+DELU(I)
      DO 25 I=1,NN
      DO 25 J=1,3
      IJ=3*(I-1)+J
   25 C(I,J)=OC(I,J)+U(IJ)
      DO 30 I=1,NM
      IE=ME(I,1)
      JE=ME(I,2)
      IF(NAL.EQ.'N') GO TO 18
      NR=3*(IE-1)
      NRR=3*(JE-1)
      DEL=0
      DO 8 J=1,3
    8 DEL=DEL+T(I,J)*(U(NRR+J)-U(NR+J))
      EN(I)=EA(I)*DEL/OL(I)
      GO TO 30
   18 DO 31 J=1,3
   31 PL(J)=C(JE,J)-C(IE,J)
      CL=DSQRT(PL(1)**2+PL(2)**2+PL(3)**2)
      STRAIN=(CL**2/OL(I)**2-1)/2
      EN(I)=EA(I)*STRAIN
      IF(EN(I).GE.0.0.OR.BOW.EQ.'N') GO TO 30
```

```
109             AX=-EN(I)
110             STRAIN=-STRAIN
111             PREV=AX
112             DO 32 J=1,50
113             DUM1=0.002*(AX/(NBC*NC(I)))**INDEX
114             AX=AX-(AX/EA(I)+DUM1-STRAIN)/(1/EA(I)+INDEX*DUM1/AX)
115             IF(DABS(AX-PREV).LE..5E-04) GO TO 33
116          32 PREV=AX
117          33 EN(I)=-AX
118          30 CONTINUE
119             IF(KOUNT.LT.NOUT) GO TO 34
120             CALL OUTPUT (NI,MI,M,NN,NM,N,ME,OC,C,P,U,EN,KOUNT,KOUNT2,JJ,NAL)
121             IF(NAL.EQ.'L') GO TO 34
122             WRITE(5,200) DET
123         200 FORMAT(1H0,'DETERMINANT OF STIFFNESS MATRIX = ',D12.6)
124             GO TO 34
125          26 INST=1
126          34 CONTINUE
127             RETURN
128             END
```

```
NLST.ADD
  1             COMPILER (XM=1)
  2             SUBROUTINE ADD (M,MJ,ICH,K,II,JJ)
  3             COMMON SS,SK
  4             DOUBLE PRECISION SS(105,105),SK(105,105),K(3,3)
  5             IF(ICH.EQ.0) GO TO 2
  6             DO 1 I=1,3
  7             DO 1 J=1,3
  8             SS(II+I,II+J)=SS(II+I,II+J)+K(I,J)
  9             SS(JJ+I,JJ+J)=SS(JJ+I,JJ+J)+K(I,J)
 10             SS(II+I,JJ+J)=SS(II+I,JJ+J)-K(I,J)
 11           1 SS(JJ+I,II+J)=SS(JJ+I,II+J)-K(I,J)
 12             GO TO 3
 13           2 DO 4 I=1,3
 14             DO 4 J=1,3
 15             SK(II+I,II+J)=SK(II+I,II+J)+K(I,J)
 16             SK(JJ+I,JJ+J)=SK(JJ+I,JJ+J)+K(I,J)
 17             SK(II+I,JJ+J)=SK(II+I,JJ+J)-K(I,J)
 18           4 SK(JJ+I,II+J)=SK(JJ+I,II+J)-K(I,J)
 19           3 CONTINUE
 20             RETURN
 21             END
```

NLST.SOLVE

```
 1              COMPILER (XM=1)
 2              SUBROUTINE SOLVE (M,MJ,N,NP,PRSUM,DET)
 3              DOUBLE PRECISION SS(105,105),SK(105,105),CONST,PRSUM,DET
 4              COMMON SS,SK
 5              IK=N-1
 6              DO 1 I=1,IK
 7              II=I+1
 8              DO 1 L=II,N
 9              IF(SS(L,I)) 4,1,4
10            4 CONST=SS(L,I)/SS(I,I)
11              DO 5 IJ=II,NP
12              IF(SS(I,IJ)) 6,5,6
13            6 SS(L,IJ)=SS(L,IJ)-CONST*SS(I,IJ)
14            5 CONTINUE
15            1 CONTINUE
16              DO 2 I=N,2,-1
17              SS(I,NP)=SS(I,NP)/SS(I,I)
18              J=I-1
19              DO 2 L=1,J
20              IF(SS(L,I)) 7,2,7
21            7 SS(L,NP)=SS(L,NP)-SS(L,I)*SS(I,NP)
22            2 CONTINUE
23              SS(1,NP)=SS(1,NP)/SS(1,1)
24              PRSUM=0
25              DET=1
26              DO 3 I=1,N
27              DET=DET*SS(I,I)
28            3 PRSUM=PRSUM+DABS(SS(I,NP))
29              RETURN
30              END
```

NLST.OUTPUT

```
 1              COMPILER (XM=1)
 2              SUBROUTINE OUTPUT (NI,MI,M,NN,NM,N,ME,OC,C,P,U,EN,KOUNT,KOUNT2,
 3             1KOUNT3,NAL)
 4              COMMON SS,SK
 5              DOUBLE PRECISION SS(105,105),SK(105,105)
 6              DOUBLE PRECISION P(M),OC(NI,3),C(NI,3),U(M),EN(MI)
 7              DIMENSION ME(MI,2)
 8              IF(NAL.EQ.'N') GO TO 3
 9              PRINT 106
10        106 FORMAT(1H0,/1H ,'LINEAR ANALYSIS',/,1H ,15('-'))
11              GO TO 4
12            3 WRITE(5,101) KOUNT,KOUNT3,KOUNT2
13        101 FORMAT(1H0,/,1H ,'RESULTS AFTER',I3,2X,'LOAD INCREMENTS',//,
14             11H ,'INCREMENT IN DEFLECTION ITERATED',I3,2X,'TIMES',
15             2//,1H ,'TOTAL NUMBER OF ITERATIONS',I9)
16            4 PRINT 102
17        102 FORMAT(1H0,/,1H ,'NODE',5X,'APPLIED LOADS',3X,
18             1'ORIG. COORD',4X,'FINAL COORD',5X,'DEFLECTION',/,1H ,4('-'),5X,
19             213('-'),3X,11('-'),4X,11('-'),5X,10('-'))
20              DO 1 I=1,NN
21              J=3*(I-1)
22            1 WRITE(5,103) I,(P(J+JJ),OC(I,JJ),C(I,JJ),U(J+JJ),JJ=1,3)
23        103 FORMAT(1H0,I2,2X,'X',1X,4(4X,E11.6),/,1H ,4X,'Y',1X,4(4X,E11.6),
24             1/,1H ,4X,'Z',1X,4(4X,E11.6))
25              PRINT 104
26        104 FORMAT(1H0,/,1H ,'AXIAL FORCES - (TENSION POSITIVE)',/,1H ,33('-'
27             1),//,1H ,'MEMBER',7X,'FORCE')
28              DO 2 I=1,NM
29            2 WRITE(5,105) ME(I,1),ME(I,2),EN(I)
30        105 FORMAT(1H0,2I3,4X,E11.6)
31              RETURN
32              END
```

Example of data input and computer printout for example 3.1, programme NLST

Data Input:

```
 1:  2-BAR TRUSS EX POSKITT, ASCE J.S.D. AUG. 1967
 2:  3,2
 3:  0., 0., 0.
 4:  1., 0.577350, 0.
 5:  2., 0., 0.
 6:  C E
 7:  1.0
 8:  1, 2, 1., 1.
 9:  1, 3, 1., 1.
10:  1,3
11:  0, 0, 0
12:  2,2
13:  1, 1, 0
14:  -1. -1
15:  2
16:  0., 1., 0.
17:  -1
```

(a)

```
18:  L
19:  -0.05
```

(b)

```
18:  NL
19:  0.05
20:  NO
21:  4, -0.010
22:  1, -0.005
23:  2, -0.0025
```

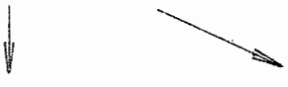

```
24:  -1, -1.
25:  7
```

(c)

```
24:  5, -0.001
25:  -1, -1.
26:  12
```

Explanation of data input:

line	1	: title of example
line	2	: number of nodes, number of members
lines	3 to 5	: cartesian co-ordinates x, y, z of each node
line	6	: 'Constant E'; Young's modulus same for all members
line	7	: value of Young's modulus for all members
lines	8 to 9	: member end nodes, cross-sectional area, moment of inertia against bowing (enter any value if there are no initial imperfections in the members).

Should the value of Young's modulus not be the same for every member:

line	6	: V E for Variable E
line	7	: omit
lines	8 to 9	: member end nodes, cross-sectional area, moment of inertia against bowing (enter any value if there are no initial imperfections in the members), Young's modulus
line	10	: constraints: nodes 1 to 3 inclusive
line	11	: constrained in x, y, z, directions
line	12	: constraints, nodes 2 to 2
line	13	: constrained in z direction
line	14	: signifies end of constraints
line	15	: external nodal forces: node
line	16	: forces in x, y, z directions
line	17	: signifies end of external nodal forces

(a)

line	18	: Linear analysis
line	19	: load factor

(b)

line	18	: Non-Linear analysis
line	19	: summed interation deflection convergence tolerance
line	20	: NO bowing

Should bowing of compression members having initial imperfections in straightness be included:

line 20 : BOW

insert additional line giving values of bowing parameters n and $\bar{N}_o$

eg : 7., 0.95

lines 21 to 23 : number of load increments, magnitude of load factor

line 24 : signifies end of load increments

line 25 : first printout after 7 load increments

(c)

lines 21 to 24 : number of load increments, magnitude of load factor

line 25 : signifies end of load increments

line 26 : first printout after 12 load increments

The results of analyses (a), (b) and (c) listed above follow on the next pages.

(a)

2-BAR TRUSS EX POSKITT, ASCE J.S.D. AUG. 1967

LINEAR ANALYSIS

NODE		APPLIED LOADS	ORIG. COORD	FINAL COORD	DEFLECTION
1	X	.000000	.000000	.000000	.000000
	Y	.000000	.000000	.000000	.000000
	Z	.000000	.000000	.000000	.000000
2	X	.000000	.100000+01	.100000+01	.000000
	Y	-.500000-01	.577350+00	.461880+00	-.115470+00
	Z	.000000	.000000	.000000	.000000
3	X	.000000	.200000+01	.200000+01	.000000
	Y	.000000	.000000	.000000	.000000
	Z	.000000	.000000	.000000	.000000

AXIAL FORCES - (TENSION POSITIVE)

MEMBER		FORCE
1	2	-.500000-01
2	3	-.500000-01

(b)

```
2-BAR TRUSS EX POSKITT, ASCE J.S.D. AUG. 1967

RESULTS AFTER  7  LOAD INCREMENTS

INCREMENT IN DEFLECTION ITERATED  3  TIMES

TOTAL NUMBER OF ITERATIONS       21

NODE      APPLIED LOADS   ORIG. COORD    FINAL COORD     DEFLECTION
----      -------------   -----------    -----------     ----------
 1  X       .000000         .000000        .000000        .000000
    Y       .000000         .000000        .000000        .000000
    Z       .000000         .000000        .000000        .000000
 2  X       .000000         .100000+01     .100000+01     .000000
    Y      -.500000-01      .577350+00     .383905+00    -.193445+00
    Z       .000000         .000000        .000000        .000000
 3  X       .000000         .200000+01     .200000+01     .000000
    Y       .000000         .000000        .000000        .000000
    Z       .000000         .000000        .000000        .000000

AXIAL FORCES - (TENSION POSITIVE)
---------------------------------

MEMBER       FORCE

  1  2     -.697314-01

  2  3     -.697314-01

DETERMINANT OF STIFFNESS MATRIX =  .133333+000

POINT OF INSTABILITY HAS NOT BEEN REACHED
```

(c)

```
2-BAR TRUSS EX POSKITT, ASCE J.S.D. AUG. 1967

POINT OF INSTABILITY WAS PASSED DURING THE LAST LOAD INCREMENT

ELASTIC CRITICAL LOAD FACTOR =-.528000-01

TOTAL NO. OF ITERATIONS   48
```

APPENDIX D: Computer Programme NLPF for Non-Linear Plane Frame Analysis

```
NLPF.MAIN
 1              PARAMETER NI=33,MI=50
 2              PARAMETER M=3*NI,MJ=M+1
 3              INTEGER CON(NI,3),TITLE(12)
 4              DIMENSION ME(MI,2),IC(3)
 5              DOUBLE PRECISION SS(M,MJ),SK(M,MJ),EI(MI),EA(MI),KD(MI),OL(MI),
 6             1OALPH(MI),PRALPH(MI),OC(NI,2),C(NI,2),PP(M),P(M),DELP(M),U(M),
 7             2DELU(M),T(MI,2),TB(MI,2,2),R(MI,2),RB(MI,2,2),H(MI,2,2),EN(MI),
 8             3EM(MI,2),V(MI),SAA(MI),SAB(MI),ENDD(MI),EMDD(MI),SD(MI),SDD(MI),
 9             4DET
10              DOUBLE PRECISION A,E,INERT,PL(2),PI,FINC(1000),F
11              READ(8,101) (TITLE(I),I=1,12)
12            101 FORMAT(12A6)
13              WRITE(5,203) (TITLE(I),I=1,12)
14            203 FORMAT(1H1,12A6)
15              PRINT 204
16            204 FORMAT(1H0,,'N  - AXIAL FORCE  (TENSION +VE)',/,1H ,
17               1'V  - SHEAR FORCE  (CAUSING A CLOCKWISE MOMENT ON A-B POSITIVE)',
18               2/,1H ,'MOMENTS  (ANTI-CLOCKWISE POSITIVE)',/,1H ,
19               3'MA - MOMENT AT END  A  OF MEMBER A-B',/,1H ,'MB - MOMENT AT END
20               4B  OF MEMBER A-B')
21            100 FORMAT()
22              READ(8,100) NN,NM
23              N=3*NN
24              NP=N+1
25              DO 1 I=1,NN
26             1 READ(8,100) (OC(I,J),J=1,2)
27              PI=3.141592653589793
28              READ(8,102) INE
29              IF(INE.EQ.'C') READ(8,100) E
30              DO 2 I=1,NM
31              IF(INE.EQ.'C') READ(8,100) ME(I,1),ME(I,2),A,INERT
32              IF(INE.EQ.'V') READ(8,100) ME(I,1),ME(I,2),A,INERT,E
33              EA(I)=E*A
34              EI(I)=E*INERT
35              IE=ME(I,1)
36              JE=ME(I,2)
37              DO 9 J=1,2
38             9 PL(J)=OC(JE,J)-OC(IE,J)
39              OL(I)=DSQRT(PL(1)**2+PL(2)**2)
40              KD(I)=EA(I)/OL(I)**2
41              IF(PL(1).GE.0..AND.PL(2).GE.0.) OALPH(I)=DASIN(PL(2)/OL(I))
42              IF(PL(1).LT.0..AND.PL(2).GE.0.) OALPH(I)=PI-DASIN(PL(2)/OL(I))
43              IF(PL(1).LT.0..AND.PL(2).LT.0.) OALPH(I)=PI+DATAN(PL(2)/PL(1))
44              IF(PL(1).GE.0..AND.PL(2).LT.0.) OALPH(I)=2*PI-DACOS(PL(1)/OL(I))
45             2 IF(OALPH(I).GT.PI) OALPH(I)=OALPH(I)-2*PI
46              DO 3 I=1,NN
47              DO 3 J=1,3
48             3 CON(I,J)=1
49             6 READ(8,100) NODE1,NODE2
50              IF(NODE1.LE.0) GO TO 4
51              READ(8,100) (IC(J),J=1,3)
52              DO 13 I=NODE1,NODE2
53              DO 13 J=1,3
54            13 CON(I,J)=IC(J)
55              GO TO 6
56             4 DO 7 I=1,N
```

```
      7 PP(I)=0
     14 READ(8,100) NODE
        IF(NODE.LE.0) GO TO 12
        J=3*(NODE-1)
        READ(8,100) (PP(I+J),I=1,3)
        GO TO 14
     12 READ(8,102) NAL
    102 FORMAT(A1)
        IF(NAL.EQ.'N') GO TO 5
        READ(8,100) FINC(1)
        MINC=1
        NOUT=1
        GO TO 10
      5 READ(8,100) ERROR
        MINC=0
        J=0
     17 READ(8,100) I,F
        IF(I.LE.0) GO TO 19
        MINC=MINC+I
        DO 18 II=1,I
        J=J+1
     18 FINC(J)=F
        GO TO 17
     19 READ(8,100) NOUT
     10 DO 20 I=1,NM
        EN(I)=0
        PRALPH(I)=OALPH(I)
        DO 20 J=1,2
     20 EM(I,J)=0
        DO 26 I=1,NN
        DO 26 J=1,2
     26 C(I,J)=OC(I,J)
        DO 24 I=1,N
        U(I)=0
     24 P(I)=0
        KOUNT=0
        INST2=0
     23 INST=0
        DO 15 I=1,MINC
        DO 16 J=1,N
     16 DELP(J)=PP(J)*FINC(I)
        KOUNT=KOUNT+1
        IF(I.EQ.1.AND.INST2.EQ.1) KOUNT=KOUNT-1
        CALL STIFF (NI,MI,M,MJ,NN,NM,N,NP,ME,CON,SS,SK,EI,EA,KD,OL,
       1OALPH,PRALPH,OC,C,PP,P,DELP,U,DELU,T,TB,R,RB,H,EN,EM,V,SAA,
       2SAB,ENDD,EMDD,SD,SDD,GET,KOUNT,NOUT,INST,NAL,KOUNT2,ERROR)
        IF(INST.EQ.0) GO TO 15
        IF(INST.EQ.1.AND.INST2.EQ.0) GO TO 21
        PRINT 201
    201 FORMAT(1H0,'POINT OF INSTABILITY WAS PASSED DURING THE LAST LOAD I
       1NCREMENT')
        DO 8 IJK=1,N
        IF(P(IJK)) 11,8,11
      8 CONTINUE
     11 FACT=P(IJK)/PP(IJK)
        WRITE(5,205) FACT
    205 FORMAT(1H0,'ELASTIC CRITICAL LOAD FACTOR =',E11.6)
```

```
      WRITE(5,206) KOUNT2
  206 FORMAT(1HO,'TOTAL NO. OF ITERATIONS',I5)
      GO TO 22
   21 DO 25 J=1,20
   25 FINC(J)=FINC(I)/10
      INST2=1
      NOUT=2000
      GO TO 23
   15 CONTINUE
      IF(NAL.EQ.'L') GO TO 22
      PRINT 200
  200 FORMAT(1HO,'POINT OF INSTABILITY HAS NOT BEEN REACHED')
   22 CONTINUE
      END
```

NLPF.ADD

```
      SUBROUTINE ADD (M,MJ,MI,S,K,SAA,SAB,ICH,II,JJ,L)
      DOUBLE PRECISION S(M,MJ),K(3,3),SAA(MI),SAB(MI)
      DO 1 I=1,2
      S(II+I,II+3)=S(II+I,II+3)+K(I,3)
      S(II+I,JJ+3)=S(II+I,JJ+3)+K(I,3)
      S(JJ+I,II+3)=S(JJ+I,II+3)-K(I,3)
      S(JJ+I,JJ+3)=S(JJ+I,JJ+3)-K(I,3)
      S(II+3,II+I)=S(II+3,II+I)+K(I,3)
      S(JJ+3,II+I)=S(JJ+3,II+I)+K(I,3)
      S(II+3,JJ+I)=S(II+3,JJ+I)-K(I,3)
      S(JJ+3,JJ+I)=S(JJ+3,JJ+I)-K(I,3)
      DO 1 J=1,2
      S(II+I,II+J)=S(II+I,II+J)+K(I,J)
      S(JJ+I,JJ+J)=S(JJ+I,JJ+J)+K(I,J)
      S(II+I,JJ+J)=S(II+I,JJ+J)-K(I,J)
    1 S(JJ+I,II+J)=S(JJ+I,II+J)-K(I,J)
      IF(ICH.EQ.2) GO TO 2
      S(II+3,II+3)=S(II+3,II+3)+SAA(L)
      S(JJ+3,JJ+3)=S(JJ+3,JJ+3)+SAA(L)
      S(II+3,JJ+3)=S(II+3,JJ+3)+SAB(L)
      S(JJ+3,II+3)=S(JJ+3,II+3)+SAB(L)
    2 CONTINUE
      RETURN
      END
```

```
      K(I,3)=S*R(II,I)
      DO 6 J=1,2
      K(I,J)=DUM1*TB(II,I,J)+EMD*(2*H(II,I,J)-BARI(I,J))+2*S/CL*
     1RB(II,I,J)
    6 IF(I.EQ.J) K(I,J)=K(I,J)+END
      NR=3*(IE-1)
      NRR=3*(JE-1)
      ICH=1
      CALL ADD (M,MJ,MI,SK,K,SAA,SAB,ICH,NR,NRR,II)
      END(II)=END/CL
      EMD(II)=EMD/CL
      SD(II)=S/CL
    2 SDD(II)=SD(II)/CL
      DO 10 I=1,N
   10 DELU(I)=0
      PASUM=0
      MITER=50
      IF(NAL.EQ.'L') MITER=1
      DO 11 JJ=1,MITER
      DO 12 I=1,N
      DO 12 J=1,N
   12 SS(I,J)=SK(I,J)
      IF(JJ.EQ.1) GO TO 13
      DO 14 II=1,NM
      NR=3*(ME(II,1)-1)
      NRR=3*(ME(II,2)-1)
      DO 8 I=1,2
    8 DEL(I)=DELU(NRR+I)-DELU(NR+I)
      CI=0
      GI=0
      DO 9 I=1,2
      CI=CI+T(II,I)*DEL(I)
      GI=GI+R(II,I)*DEL(I)
      DO 9 J=1,2
      B(I,J)=DEL(I)*T(II,J)
    9 Q(I,J)=R(II,I)*DEL(J)
      DUM1=KD(II)-END(II)
      DUM2=KD(II)-1.5*END(II)
      DO 17 I=1,2
      K(I,3)=-2*CI*R(II,I)
      DO 17 J=1,2
   17 K(I,J)=DUM1*(B(I,J)+0.5*B(J,I))-DUM2*CI*TB(II,I,J)-SDD(II)*
     1(6*CI*RB(II,I,J)-2*GI*BARI(I,J))-EMDD(II)*(4*CI*H(II,I,J)-2*CI*
     2BARI(I,J)-Q(I,J))
      K(1,3)=SD(II)*(K(1,3)-DEL(2))
      K(2,3)=SD(II)*(K(2,3)+DEL(1))
      ICH=2
   14 CALL ADD (M,MJ,MI,SS,K,SAA,SAB,ICH,NR,NRR,II)
   13 DO 19 I=1,N
   19 SS(I,NP)=DELP(I)
      L=0
      DO 20 I=1,NN
      DO 20 J=1,3
      L=L+1
      IF(CON(I,J).NE.0) GO TO 20
      DO 21 IJ=1,N
      SS(IJ,L)=0
```

```
      21 SS(L,IJ)=0
         SS(L,NP)=0
         SS(L,L)=1
      20 CONTINUE
      42 CONTINUE
         CALL SOLVE (M,MJ,N,NP,SS,PRSUM,DET)
         DO 22 I=1,N
      22 DELU(I)=SS(I,NP)
         IF(DABS(PASUM/PRSUM-1).LE.ERROR) GO TO 23
      11 PASUM=PRSUM
      23 IF(DET.LE.0.) GO TO 26
         KOUNT2=KOUNT2+JJ
         DO 24 I=1,N
         P(I)=P(I)+DELP(I)
      24 U(I)=U(I)+DELU(I)
         DO 25 I=1,NN
         DO 25 J=1,2
         IJ=3*(I-1)+J
      25 C(I,J)=OC(I,J)+U(IJ)
         PI=3.141592653589793
         DO 30 I=1,NM
         IE=ME(I,1)
         JE=ME(I,2)
         IF(NAL.EQ.'N') GO TO 44
         CALL LINEAR (IE,JE,OALPH(I),KU(I),EI(I),OL(I),SAA(I),SAB(I),U,M,
        1EN(I),EM(I,1),EM(I,2),V(I))
         GO TO 30
      44 DO 31 J=1,2
      31 PL(J)=C(JE,J)-C(IE,J)
         CL=DSQRT(PL(1)**2+PL(2)**2)
         EN(I)=0.5*EA(I)*((CL/OL(I))**2-1)
         IF(PL(1).GE.0..AND.PL(2).GE.0.) ALPH=DASIN(PL(2)/CL)
         IF(PL(1).LT.0..AND.PL(2).GE.0.) ALPH=PI-DASIN(PL(2)/CL)
         IF(PL(1).LT.0..AND.PL(2).LT.0.) ALPH=PI+DATAN(PL(2)/PL(1))
         IF(PL(1).GE.0..AND.PL(2).LT.0.) ALPH=2*PI-DACOS(PL(1)/CL)
         IF(ALPH.GT.PI) ALPH=ALPH-2*PI
         DUM1=ALPH-PRALPH(I)
         DEL(1)=DELU(3*IE)-DUM1
         DEL(2)=DELU(3*JE)-DUM1
         EM(I,1)=EM(I,1)+SAA(I)*DEL(1)+SAB(I)*DEL(2)
         EM(I,2)=EM(I,2)+SAA(I)*DEL(2)+SAB(I)*DEL(1)
         V(I)=(EM(I,1)+EM(I,2))/CL
         PRALPH(I)=ALPH
      30 CONTINUE
         IF(KOUNT.LT.NOUT) GO TO 34
         CALL OUTPUT (NI,MI,M,NN,NM,ME,OC,C,P,U,EN,EM,V,KOUNT,KOUNT2,JJ,
        1NAL)
         IF(NAL.EQ.'L') GO TO 34
         WRITE(5,200) DET
     200 FORMAT(1H0,//,1H ,'DETERMINANT OF STIFFNESS MATRIX = ',D12.6)
         GO TO 34
      26 INST=1
      34 CONTINUE
         RETURN
         END
```

NLPF.SOLVE

```
 1            SUBROUTINE SOLVE (M,MJ,N,NP,SS,PRSUM,DET)
 2            DOUBLE PRECISION SS(M,MJ),CONST,PRSUM,DET
 3            IK=N-1
 4            DO 1 I=1,IK
 5            II=I+1
 6            DO 1 L=II,N
 7            IF(SS(L,I)) 4,1,4
 8          4 CONST=SS(L,I)/SS(I,I)
 9            DO 5 IJ=II,NP
10            IF(SS(I,IJ)) 6,5,6
11          6 SS(L,IJ)=SS(L,IJ)-CONST*SS(I,IJ)
12          5 CONTINUE
13          1 CONTINUE
14            DO 2 I=N,2,-1
15            SS(I,NP)=SS(I,NP)/SS(I,I)
16            J=I-1
17            DO 2 L=1,J
18            IF(SS(L,I)) 7,2,7
19          7 SS(L,NP)=SS(L,NP)-SS(L,I)*SS(I,NP)
20          2 CONTINUE
21            SS(1,NP)=SS(1,NP)/SS(1,1)
22            PRSUM=0
23            DET=1
24            DO 3 I=1,N
25            DET=DET*SS(I,I)
26          3 PRSUM=PRSUM+DABS(SS(I,NP))
27            RETURN
28            END
```

NLPF.OUTPUT

```
 1             SUBROUTINE OUTPUT (NI,MI,M,NN,NM,ME,OC,C,P,U,EN,EM,V,KOUNT,
 2            1KOUNT2,KOUNT3,NAL)
 3             DIMENSION ME(MI,2)
 4             DOUBLE PRECISION OC(NI,2),C(NI,2),P(M),U(M),EN(MI),EM(MI,2),V(MI)
 5             IF(NAL.EQ.'N') GO TO 3
 6             PRINT 106
 7           106 FORMAT(1H1,'LINEAR ANALYSIS',/,1H ,15('-'))
 8             GO TO 4
 9           3 WRITE(5,101) KOUNT,KOUNT3,KOUNT2
10           101 FORMAT(1H0,//,1H ,'RESULTS AFTER',I3,2X,'LOAD INCREMENTS',//,
11              1H ,'INCREMENT IN DEFLECTION ITERATED',I5,2X,'TIMES',
12              2//,1H ,'TOTAL NUMBER OF ITERATIONS',I9)
13            4 PRINT 102
14           102 FORMAT(1H0,//,1H ,'NODE',5X,'APPLIED LOADS',3X,
15              1'ORIG. COORD',4X,'FINAL COORD',5X,'DEFLECTION',//,1H ,4('-'),5X,
16              213('-'),3X,11('-'),4X,11('-'),5X,10('-'))
17             DO 1 I=1,NN
18             J=3*(I-1)
19           1 WRITE(5,103) I,(P(J+JJ),OC(I,JJ),C(I,JJ),U(J+JJ),JJ=1,2),P(J+3),
20              U(J+3)
21           103 FORMAT(1HC,I2,2X,'X',1X,4(4X,E11.6),/,1H ,4X,'Y',1X,4(4X,E11.6),
22              1/,1H ,4X,'-',/,1H+,4X,'0',5X,E11.6,34X,E11.6)
23             PRINT 104
24           104 FORMAT(1H0,//,1H ,'MEMBER A-B',6X,'N',14X,'V',14X,'MA',13X'MB',
25              1/,1H ,10('-'),6X,'-',14X,'-',14X,'--',13X,'--')
26             DO 2 I=1,NM
27           2 WRITE(5,105) ME(I,1),ME(I,2),EN(I),V(I),EM(I,1),EM(I,2)
28           105 FORMAT(1H0,2I3,4(4X,E11.6))
29             RETURN
30             END
```

```
NLPF.LINEAR
 1              SUBROUTINE LINEAR (IE,JE,ALPH,KD,EI,OL,SAA,SAB,U,M,EN,EM1,
 2             1EM2,V)
 3              DOUBLE PRECISION ALPH,KD,EI,OL,SAA,SAB,U(M),EN,EM(2),V,
 4             1AT(3,4),X(4),S,C,DUM,EM1,EM2
 5              S=DSIN(ALPH)
 6              C=DCOS(ALPH)
 7              DUM=6*EI/OL**2
 8              KD=KD*OL
 9              AT(1,1)=KD*C
10              AT(1,2)=KD*S
11              AT(2,1)=DUM*S
12              AT(2,2)=-DUM*C
13              AT(2,3)=SAA
14              AT(2,4)=SAB
15              AT(3,1)=AT(2,1)
16              AT(3,2)=AT(2,2)
17              AT(3,3)=SAB
18              AT(3,4)=SAA
19              II=3*(IE-1)
20              JJ=3*(JE-1)
21              DO 1 I=1,2
22            1 X(I)=U(JJ+I)-U(II+I)
23              X(3)=U(3*IE)
24              X(4)=U(3*JE)
25              EN=AT(1,1)*X(1)+AT(1,2)*X(2)
26              DO 2 I=1,2
27              EM(I)=0
28              DO 2 J=1,4
29            2 EM(I)=EM(I)+AT(I+1,J)*X(J)
30              EM1=EM(1)
31              EM2=EM(2)
32              V=(EM(1)+EM(2))/OL
33              RETURN
34              END
```

Example of data input and computer printout for example 5.2, programme NLPF

Data Input:

```
 1:  EXAMPLE EX WANG, 'COMP. METHS. ADV. STR. ANAL'., P. 156
 2:  5,4
 3:  0., 120.
 4:  0., 240.
 5:  60., 240.
 6:  180., 240.
 7:  180., 0.
 8:  C E
 9:  30E+06
10:  1, 2, 3.0682, 6.9919
11:  2, 3, 3.0682, 6.9919
12:  3, 4, 3.0682, 6.9919
13:  4, 5, 3.0682, 6.9919
14:  1, 1
15:  0, 0, 0
16:  5, 5
17:  0, 0, 0
18:  -1, -1
19:  2
20:  1., 0., 0.
21:  3
22:  0., -4., 0.
23:  -1
```

(a)

```
24:  L
25:  5000
```

(b)

```
24:  NL
25:  0.01
26:  20, 250
27:  -1, -1.
28:  20
```

Explanation of data input:

line 1 : title of example
line 2 : number of nodes, number of members
lines 3 to 7 : cartesian co-ordinates x, y of each node
line 8 : 'Constant E', Young's modulus same for all members
line 9 : value of Young's modulus
lines 10 to 13: member end nodes, cross-sectional area, moment of inertia in x-y plane

Should the value of Young's modulus not be the same for every member:

line 8 : V E for Variable E
line 9 : omit
lines 10 to 13: member end nodes, cross-sectional area, moment of inertia in x - y plane, Young's modulus
line 14 : constraints, nodes 1 to 1
line 15 : constrained in x and y directions and constrained against rotation
line 16 : constraints, nodes 5 to 5
line 17 : constrained in x and y directions and constrained against rotation
line 18 : signifies end of constraints
line 19 : external nodal forces: node
line 20 : forces in x and y directions, anti-clockwise moment
line 21 : external nodal forces: node
line 22 : forces in x and y directions, anti-clockwise moment
line 23 : signifies end of external nodal forces

(a)
line 24 : Linear analysis
line 25 : load factor

(b)
line 24 : Non-Linear analysis
line 25 : summed iteration deflection convergence tolerance

line 26 : number of load increments, magnitude of load factor

line 27 : signifies end of load increments

line 28 : first printout after 20 load increments

The results of analyses (a) and (b) listed above follow on the next pages.

(a)

EXAMPLE EX WANG, 'COMP. METHS. ADV. STR. ANAL.', P. 156

N - AXIAL FORCE (TENSION +VE)
V - SHEAR FORCE (CAUSING A CLOCKWISE MOMENT ON A-B POSITIVE)
MOMENTS (ANTI-CLOCKWISE POSITIVE)
MA - MOMENT AT END A OF MEMBER A-B
MB - MOMENT AT END B OF MEMBER A-B

LINEAR ANALYSIS

NODE		APPLIED LOADS	ORIG. COORD	FINAL COORD	DEFLECTION
1	X	.000000	.000000	.000000	.000000
	Y	.000000	.120000+03	.120000+03	.000000
	B	.000000			.000000
2	X	.500000+04	.000000	.896313+01	.896313+01
	Y	.000000	.240000+03	.239985+03	-.153843-01
	B	.000000			-.121699+00
3	X	.000000	.800000+02	.899614+02	.896145+01
	Y	-.200000+05	.240000+03	.234124+03	-.587550+01
	B	.000000			-.399507-01
4	X	.000000	.160000+03	.150958+03	.895808+01
	Y	.000000	.240000+03	.239979+03	-.214391-01
	B	.000000			.414381-01
5	X	.000000	.180000+03	.180000+03	.000000
	Y	.000000	.000000	.000000	.000000
	B	.000000			.000000

MEMBER A-B		N	V	MA	MB
1	2	-.117775+05	.241980+04	.357914+06	-.875383+05
2	3	-.258020+04	.117775+05	.875383+05	.639112+06
3	4	-.258020+04	-.822250+04	-.639112+06	-.347599+06
4	5	-.822250+04	.258020+04	.347599+06	.271680+06

(b)

EXAMPLE EX WANG, 'COMP. METHS. ADV. STR. ANAL.', P. 156

N - AXIAL FORCE (TENSION +VE)
V - SHEAR FORCE (CAUSING A CLOCKWISE MOMENT ON A-B POSITIVE)
MOMENTS (ANTI-CLOCKWISE POSITIVE)
MA - MOMENT AT END A OF MEMBER A-B
MB - MOMENT AT END B OF MEMBER A-B

RESULTS AFTER 20 LOAD INCREMENTS

INCREMENT IN DEFLECTION ITERATED 3 TIMES

TOTAL NUMBER OF ITERATIONS 60

NODE		APPLIED LOADS	ORIG. COORD	FINAL COORD	DEFLECTION
1	X	.000000	.000000	.000000	.000000
	Y	.000000	.120000+03	.120000+03	.000000
	B	.000000			.000000
2	X	.500000+04	.000000	.100332+02	.100332+02
	Y	.000000	.240000+03	.239512+03	-.488222+00
	B	.000000			-.136181+00
3	X	.000000	.600000+02	.703230+02	.103230+02
	Y	-.200000+05	.240000+03	.233234+03	-.676634+01
	B	.000000			-.402304-01
4	X	.000000	.180000+03	.190143+03	.101426+02
	Y	.000000	.240000+03	.239763+03	-.236841+00
	B	.000000			.477667-01
5	X	.000000	.180000+03	.180000+03	.000000
	Y	.000000	.000000	.000000	.000000
	B	.000000			.000000

MEMBER A-B		N	V	MA	MB
1	2	-.110096+05	.361372+04	.447228+06	-.136336+05
2	3	-.125306+04	.116199+05	.135618+05	.683625+06
3	4	-.198121+04	-.384679+04	-.683672+06	-.377920+06
4	5	-.859308+04	.283569+04	.377922+06	.382581+06

DETERMINANT OF STIFFNESS MATRIX = .491952+052

POINT OF INSTABILITY HAS NOT BEEN REACHED